Multi-Site Application of the Geomechanical Approach for Natural Fracture Exploration

Final Report

Reporting period: October 1, 1999 to March 31, 2006

Prepared by:

R. L. Billingsley

V. Kuuskraa

March 2006

DOE Award No. DE-RA26-99FT40720

Submitting Organization:

Advanced Resources International, Inc.
4501 Fairfax Drive, Suite 910
Arlington, Virginia 22203-1661

In Association with:
Union Pacific Resources
Barrett Resources
Burlington Resources
Colorado School of Mines

Disclaimer

This report was prepared as an account of work sponsored by an agency of the United States Government. Neither the United States Government nor any agency thereof, nor any of their employees, makes any warranty, express or implied, or assumes any legal liability or responsibility for the accuracy, completeness, or usefulness of any information, apparatus, product, or process disclosed, or represents that its use would not infringe privately owned rights. Reference herein to any specific commercial product, process, or service by trade name, trademark, manufacturer, or otherwise does not necessarily constitute or imply its endorsement, recommendation, or favoring by the United States Government or any agency thereof. The views and opinions of authors expressed herein do not necessarily state or reflect those of the participating companies. The views and opinions of authors expressed herein do not necessarily state or reflect those of the United States Government or any agency thereof.

Abstract

In order to predict the nature and distribution of natural fracturing, Advanced Resources Inc. (ARI) incorporated concepts of rock mechanics, geologic history, and local geology. into a geomechanical approach for natural fracture prediction within mildly deformed, tight (low-permeability) gas reservoirs. Under the auspices of this project, ARI utilized and refined this approach in tight gas reservoir characterization and exploratory activities in three basins: the Piceance, Wind River and the Anadarko. The primary focus of this report is the knowledge gained on natural fractural prediction along with practical applications for enhancing gas recovery and commerciality.

Of importance to tight formation gas production are two broad categories of natural fractures: (1) *shear related natural fractures* and (2) *extensional (opening mode) natural fractures*. While arising from different origins this natural fracture type differentiation based on morphology is sometimes inter related. Predicting fracture distribution successfully is largely a function of collecting and understanding the available relevant data in conjunction with a methodology appropriate to the fracture origin.

Initially ARI envisioned the geomechanical approach to natural fracture prediction as the use of elastic rock mechanics methods to project the nature and distribution of natural fracturing within mildly deformed, tight (low permeability) gas reservoirs. Technical issues and inconsistencies during the project prompted re-evaluation of these initial assumptions. ARI's philosophy for the geomechanical tools was one of *heuristic* development through field site testing and iterative enhancements to make it a better tool.

The technology and underlying concepts were refined considerably during the course of the project. As with any new tool, there was a substantial learning curve. Through a heuristic approach, addressing these discoveries with additional software and concepts resulted in a stronger set of geomechanical tools. Thus, the outcome of this project is a set of predictive tools with broad applicability across low permeability gas basins where natural fractures play an important role in reservoir permeability.

Potential uses for these learnings and tools range from rank exploration to field-development portfolio management. Early incorporation of the permeability development concepts presented here can improve basin assessment and direct focus to the high potential areas within basins. Insight into production variability inherent in tight naturally fractured reservoirs leads to improved wellbore evaluation and reduces the incidence of premature exits from high potential plays.

A significant conclusion of this project is that natural fractures, while often an important, overlooked aspect of reservoir geology, represent only one aspect of the overall reservoir fabric. A balanced perspective encompassing all aspects of reservoir geology will have the greatest impact on exploration and development in the low permeability gas setting.

TABLE OF CONTENTS

Disclaimer i
Abstract ii
List of Graphical Materials vii
Acknowledgements x
INTRODUCTION 1
A. Background, Goals and Objectives 1
B. Rationale for Project Consortium & Test Basin Selection 1
C. Scope, Technology and Methodology 3
1. Work Scope 3
2. Technology 4
3. Methodology 5
Task 1: Site Selection and Site Characterization 5
Task 2: Geomechanical Analysis for Prospect Delineation 5
Task 3: Post-Appraisal and Impact Assessment 6
EXECUTIVE SUMMARY 7
TECHNOLOGY DEVELOPMENT DISCUSSION 9
A. The Problem 9
B. Frames of Reference 10
Natural Fracture Terminology 10
Natural Fracture Characterization 12
Drilling Induced vs. Natural Fractures 13
Shear vs. Extensional Natural Fractures 13
Shear Natural Fractures 13
Extensional Natural Fractures 15
Joints 16
Extensional Fractures 16
B. Demonstration Models and Processes 18
1. Models 19
Geomechanical Modeling 19
Visco-Elastic Modeling 19
Failure Criterion and Tectonic Stress Estimation Modeling 20
Boundary Element Modeling 20
2. Geomechanical Work Flow Process 22
C. Field Test Experience 22

Bullfrog 22
Elk City 23
Piceance 23
D. Implications 23
1. Importance of Unloading 24
2. Material Behavior 25
Griffith Material Model 25
3. The Role of Temperature 27
4. Tectonic Influence 32
5. Uplift Model Validation 33
5. Prospect Generation 38
E. Resources 39
RESULTS AND DISCUSSION 40
I. Study Area #1: Waltman/Cave Gulch 40
A. Overview 40
B. Purpose 40
C. Site Selection 40
Discovery and Development History 42
D. Regional Geologic and Tectonic Setting 43
Frontier Stratigraphy 46
Structural Setting 48
Reservoir Properties 49
E. Site Characterization 50
Reservoir Overview 50
Data Collection 51
Petrophysics 53
Natural Fractures 53
Fracture Porosity 54
Bullfrog 5-12 Core Interpretation 54
Bullfrog 5-12 Log Analysis 55
F. Prospect Generation 62
G. Well Drilling and Testing 63
Results 63
Subsequent Actions 64
Impact Assessment 65

II. Study Area #2: Anadarko 67
A. Overview 67
B. Purpose 67
C. Site Selection 67
D. Regional Geologic and Tectonic Setting 69
Wichita Fault System 72
Miscellaneous Structures 73
Hydrocarbon Production 73
E. Site Characterization 74
Fractures and Stress 74
Key Well 80
Summary 84
F. Prospect Generation 85
Seismic Interpretation 86
Boundary Element Modeling 88
FracGen Modeling 92
Calibration and Prospect Generation 95
Proposed Locations 98
G. Well Drilling and Testing 99
H. Key Learnings 99
Summary 100
III. Study Area #3: RCP Consortium Williams/Piceance Basin 101
A. Overview 101
B. Purpose 104
C. Site Selection 104
D. Regional Geologic and Tectonic Setting 104
MWX Fractures and Stresses 108
E. Site Characterization 111
F. Post-Simulation Appraisal and Impact Assessment 120
Geomechanical Simulation Results 120
A. Original Project Premise 124
B. Changes to Original Project Premise 124
C. Key Learnings 126
D. Thoughts for the Future 127
REFERENCES 128

ACRONYMS AND ABBREVIATIONS **132**
APPENDICES **135**
A. Bullfrog 5-12 Core Report **135**
B. Natural Fracture Supporting Documentation **135**

List of Graphical Materials

Figures

Fig. O-1. Fractured Frontier Fm. Barrett Bullfrog #5-12 14
Fig. O-2. Natural fracture characterization 15
Fig. O-3. Atoka (Steffes Fm) fault related natural fractures 18
Fig. O-4. Boundary element modeling 21
Fig. O-5. Geomechanical workflow process 22
Fig. O-6 Schematic representation of the Griffith material model 26
Fig. O-7. Almond unloading fracture 27
Fig. O-8. Thermo-elastic expansion of a spherical quartz grain 28
Fig. O-9. Coefficients of thermal expansion of common constituents 29
Fig. O-10. Generation of grain bounding microfractures through cooling 29
Fig. O-11. Cycle of thermal expansion generates internal stresses 30
Fig. O-12a & O-12b. Permeability impact of cooling & composition 31
Fig. O-13. Strain and pressure solution 33
Fig. O-14. Vr (% Ro) maximum burial depth calibration 35
Fig. O-15. Projected uplift vs. normalized permeability 36
Fig. O-16. Prospect generation via geomechanical modeling 38
Fig. I-1. Barrett Resources test site – Wind River basin 41
Fig. I-2. Structure Map, top of Frontier Fm, Wind River basin 45
Fig. I-3. Generalized stratigraphic column, Rocky Mtn. area 46
Fig. I-4. Isolith map of total Frontier Sandstone in central Rocky Mtn. area 47
Fig. I-5. Gross Sandstone Isopach, Frontier Fm, Wind River basin 49
Fig. I-6. Frontier Fm pay zone in the Cave Gulch #16 51
Fig. I-7. Fractured Frontier Fm. Barrett Bullfrog #5-12 52
Fig. I-8. Bullfrog 5-12 dipmeter segment 55
Fig. I-9. Bullfrog 5-12 FMI summary 57
Fig. I-10. N-S Diagrammatic cross-section of the Bullfrog/Waltman area 58
Fig. I-11. Perspective view of the Bullfrog fault system 59
Fig. I-12. Basemap of the Bullfrog/Cave Gulch project area 60
Fig. I-13. Generalized structure contour map on the Frontier Fm horizon 60
Fig. I-14. Generalized Frontier structure map and simulated displacement 62
Fig. I-15. Distribution of Coulomb stress 63
Fig. I-16. Final prospecting map for the Bullfrog field demonstration site 64

Fig. II-1. Anadarko basin field demonstration project area 68
Fig. II-2. Basement structure, Anadarko basin & adjacent basins & uplifts 69
Fig. II-3. Deep Anadarko basin (stipple): basement depth > 15,000' 70
Fig. II-4. South (left) to north (right) cross-section of Deep Anadarko 71
Fig. II-5. Frontal faults of the Wichita uplift, Slick Hills region 72
Fig. II-6. Fracture trends and strain orientations in the Slick Hills area 75
Fig. II-7. Wellbore enlargements in eastern Anadarko basin 76
Fig. II-8. Schematic illustration of wellbore breakout vs. fracture enlargement 77
Fig. II-9. Locations of borehole breakout studies conducted by Dart (1990) 78
Fig. II-10. Atoka natural fractures 80
Fig. II-11. Marie Walters 1-14 location 80
Fig. II-12. Marie Walters seismic transect 81
Fig. II-13. Marie Walters 1-14 FMS 82
Fig. II-14.Marie Walters 1-14 type curve pressure and derivative 83
Fig. II-15. Marie Walters' mudlog 84
Fig. II-16. Anadarko-Pennsylvanian structure with exaggeration 85
Fig. II-17. Faulting timeslice 86
Fig. II-18. Vertical section 87
Fig. II-19. Atoka Steffes reservoir large calcite-filled fractures 88
Fig. II-20. Anastomosing, interpenetrating faults within the structural core of the anticline. 89
Fig. II-21. Reservoir horizon and faults in depth. 90
Fig. II-22. Simulated Vertical displacement of an area of the Elk City structure. ... 91
Fig. II-23. Coulomb stress 91
Fig. II-24. Max shear 92
Fig. II-25. FracGen model-Coulomb stress example. 93
Fig. II-26. FracGen model realization 94
Fig. II-27. Discrete Fracture Network (DNF) permeability from Poly3D and FracGen simulations 95
Fig. II-28. Phih from logs vs. EUR 96
Fig. II-29. Pseudo Perm vs. EUR 97
Fig. II-30. Final kPhih vs. EUR correlation 98
Fig. III-1. Piceance Basin regional structure contour and index map 102
Fig. III-2. Regional cross section 103
Fig. III-3. Rulison stratigraphic column section 105

Fig. III-4. Generalized tectonic features of the Piceance basin 106
Fig. III-5. Partial Ant Tracker time slice of Seitel regional survey, Piceance basin area 107
Fig. III-6. MWX fracture “logs” section 109
Fig. III-7. MWX fracture types and pressure gradients section 110
Fig. III-8. RCP survey location section 112
Fig. III-9. Raw “patch” volume as received from K. Jansen 113
Fig. III-10. Faults with GT 130 patches 114
Fig. III-11. Poly3D model fault cluster 115
Fig. III-12. Base well control 116
Fig. III-13. Perspective view northwest along the major fault trend 116
Fig. III-14. EW section Poly3D model 117
Fig. III-15. NS cross section Poly3D model 117
Fig. III-16. 3D view greatest strain 118
Fig. III-17. Geomechanical model results 119
Fig. III-18. Future activity 122

Tables

Table O-1. Undeveloped recoverable tight gas resources in priority basins 2
Table O-2. Porosity, permeability, & Vr data from cores in Almond Fm, SW Wyoming 34
Table. I-1 Reservoir characteristics— Waltman/Cave Gulch field 50
Table I-2. Production characteristics— Waltman/Cave Gulch field 50
Table II-1. Core and Image Log Observation Summary 79
Table III-1. Rulison Reservoir Properties 103
Table III-2. Well productivity in high enhanced perm areas 121
Table III-3. Well productivity in low/no enhanced perm areas 121
Table III-4. Comparative economics provide additional insights on the value of the geomechanical technology 122

Acknowledgements

Advanced Resources International, Inc. would like to acknowledge the National Energy Technology Laboratory (NETL), Morgantown, WV, for their role as lead funding agency together with the following companies and other governmental groups who contributed data, sampling opportunities or discussion: Bill Barrett Corp., Burlington Resources Corp., Reservoir Characterization Project, Colorado School of Mines, Staff and students of the Rock Fracture Project, Stanford University. NETL Project Managers Gary Covatch and Kelly Rose were helpful and supportive throughout the project.

We would also like to thank the following individuals for their interpretive efforts or insightful discussion and comments, George Koperna, Dr. Tom Davis, Ms. Tanya Inks, and Kjetl Jansen. For their tireless efforts, Diane Suchomel, data collection, and Dianne Finch-Smith, technical editing, deserve special recognition.

INTRODUCTION

A. Background, Goals and Objectives

The future of natural gas development increasingly needs to draw on the 349-tcf of natural gas resources that exist in low permeability (tight) formations. A host of sophisticated exploration and production (E&P) technologies are required to economically produce these resources. Near the top of the list are technologies that enable operators to find the naturally fractured ”sweet spots” in these otherwise “tombstone tight” formations.

In 1999, Advanced Resources International Inc. (ARI), with support from the U.S. Department of Energy (DOE), convened this research program (DE-RA26-99FT40720) to support the efficient development of low-permeability resources. The DOE Federal Energy Technology Center (FETC) Low Permeability Natural Gas Supply Research and Development (R&D) Program set a goal to demonstrate emerging natural fracture detection technology to accelerate its commercial use. Realizing this goal depended on achieving three objectives.

1) Providing successful demonstrations of the geomechanical approach to natural fracture detection and predictions in an exploration mode.
2) Performing these demonstrations in a number of geologic/basin settings.
3) Promoting widespread industry acceptance and commercial use of the geomechanical model through technology transfer.

B. Rationale for Project Consortium & Test Basin Selection

DOE/FETC’s low-permeability natural R&D program has supported the development and optimization of a valuable set of technologies for delineating naturally fractured areas in low permeability natural gas plays. This technology was first field tested in the Mesaverde formation (Fm), Rulison field, Piceance basin, followed by testing in the Frontier Fm Table Rock field (Greater Green River basin). However, the industry was slow to explore new sweet spots using this geomechanically-based technology for three reasons:

- There were no field demonstrations of this technology in a true exploration (predictive) mode before drilling.
- The field demonstrations were limited to only a few areas and geological settings, resulting in a statistically small set of performance data.
- Outside the Rocky Mountain region little was known about this technology.

DOE/FETC's Program Research and Development Announcement (PRDA) addressed these issues and set a goal of rapidly commercializing the geomechanical approach to natural fracture detection technology. To best meet the DOE/FETC objectives for extrapolating and commercializing natural fracture detection technology, ARI envisioned a multi-company consortium across multiple basins. This strategy encompassed these critical success factors:

1. **Building a record of successful results.** For commercial acceptance by the industry, the geomechanical technology and to show a repeatable, quantifiable, track record of success. One or two successful efforts are often viewed as "luck," particularly in a complex problem such as exploring for natural fractures. Thus, a key aspect of this program was the project organization—a consortium involving multiple field sites and industry partners.

   ARI assembled a consortium of leading tight gas developers—Barrett Resources, Burlington Resources, and the Reservoir Characterization Project (RCP) at the Colorado School of Mines (CSM) in conjunction with the Williams Companies. The ARI consortium-style approach added four critical performance data points to the commercial evaluation of the natural fracture detection technology.

2. **Testing results in priority basins and alternative settings.** The industry believes that each basin has unique characteristics requiring adaptation of the technology to the geologic and structural setting of the basin. For this reason, the consortium considered six priority basins (Table O-1) as test sites.

Table O-1. Undeveloped recoverable tight gas resources in priority basins

Basin	Old Plays (tcf)	New Plays (tcf)	Total (tcf)
1. Green River	**25.3***	**87.3**	**112.6**
2. Piceance	**8.7***	**29.9**	**38.6**
3. Anadarko	**12.6**	**16.0**	**28.6**
4. Wind River	**3.7***	**12.8**	**16.5**
5. Uinta	**1.9***	**6.7**	**8.6**
6. San Juan	**1.9**	**0**	**1.9**

Source: NPC 1992 (Advanced Technology) *Allocated from Rocky Mountain foreland basins

Ultimately we tested integrated geomechanical technology for natural fracture detection in three distinct tight gas basins—(1) the Piceance, (2) the Wind River (WRB) and (3) a basin outside the Rockies, the Anadarko. Originally, we targeted the GGRB as one of the pure test sites, but we modified this to adapt to changes in the industry climate. Thus, we used the Greater Green River basin (GGRB) field as a software development area instead of using it as a pure test site.

We also considered the San Jan basin, but eliminated it because there was no exploration setting left in that basin. Similarly, we excluded the Uinta basin because of its relatively small tight gas potential in only one formation (Wasatch).

3. **Involving active, technologically innovative companies.** By involving Barrett Resources, Burlington Resources, the Reservoir Characterization Project, and the Williams Companies in demonstrations of the technology, ARI anticipated accelerating its commercial acceptance. If these active tight gas drillers endorsed the technology, then it would influence other technically sophisticated companies to buy into it as well.
4. **Rigorous technical and peer review.** We envisioned a consortium to share technical information and accomplish rigorous critique of the technology. However, rapid, unforeseen changes in the industry climate negated this particular strategy.
5. **Cost efficiencies.** By combining multiple field demonstrations under the umbrella of one project, we reduced costs while at the same time increasing the efficiency of commercialization.
6. **Heuristic process.** ARI's philosophy for the geomechanical tools was one of heuristic development through field site testing and iterative enhancements to make it a better tool. For example, at the onset of the program ARI envisioned the geomechanical approach to natural fracture prediction as the use of elastic rock mechanics methods to project the nature and distribution of natural fracturing within mildly deformed, tight (low permeability) gas reservoirs. Technical issues and inconsistencies during the project prompted re-evaluation of these initial assumptions.

   Thus, the technology and underlying concepts were refined considerably during the course of the project. As with any new tool, there was a substantial learning curve. Through a heuristic approach, addressing these discoveries with additional software and concepts resulted in a stronger set of geomechanical tools

C. Scope, Technology and Methodology

1. Work Scope

The scope of the project went beyond a single application of a technology, in a single field area. ARI, in conjunction with Barrett Resources, Burlington Resources, the Reservoir Characterization Project (RCP), and the Williams Companies demonstrated geomechanical technology for natural fracture exploration in a variety of geologic settings and basins.

The project consisted of three separate field test sites. The first field was located in the WRB. The target reservoir was the deep Frontier Fm. The third field site was the Anadarko basin, a high priority basin located outside the Rocky Mountain region. The final site was the Reservoir Characterization Project field test site at Rulison in the Southern Piceance basin. The target reservoirs were the Williams Fork (Mesaverde) sands. Originally, the Frontier formation, in the Wamsutter Arch area of the GGRB was a targeted reservoir. Instead, in order to respond to changes in the industry climate, ARI used the GGRB field site as a software development area.

2. Technology

The objective of the "Multi-site Application of the Geomechanical Approach for Natural Fracture Exploration" project was to demonstrate geomechanical technology in a variety of field exploration settings. The project grew out of DOE efforts to exploit the reservoir characterization research performed at the multi-well experiment (MWX) site in Rulison field, Colorado, where natural fractures were determined to be major influence on gas permeability in tight formations. The long-term goal was to develop a "break through" exploration technology and increase gas production from other basins across the country where large noncommercial gas resources existed in similar settings.

Prior to this project, ARI spent five years identifying key technologies and methodologies for detecting natural fractures in existing fields, supported in large part by DOE/FETC's Low Permeability Program. As part of this effort, we examined seismic-based techniques of fracture detection including:

- Shear-wave splitting
- P-wave azimuthal velocity anomalies
- Natural fracture characterization using imaging logs and core
- Geomechanical methods that predict natural fracture genesis due to local structural deformation.

As a result of this work, ARI proposed a geomechanical technology that incorporated observational data and predicted the location and character of a reservoir's sweet spot. *Rather than depend on a single observation, the geomechanical technology integrated surface, borehole and seismic observations with the application of a scientifically rigorous geomechanical model.* ARI's geomechanical model integrated observational data to provide a prospective target by predicting the location and character of natural fracture clusters. This integrated geomechanical approach met with industry-wide interest and showed great potential for reducing the exploration risk of low permeability gas development.

We first tested the geomechanical approach in the Piceance basin. Based on two-dimensional (2D) seismic data and a small 3D patch, the reverse faults at Rulison and Mamm Creek fields were shown to control the occurrence of fault-related natural fracture clusters in the down-thrown side of fault systems. The geomechanical model successfully identified the high production areas of Mamm Creek and predicted the highly productive area in the south Rulison field.

ARI next used the geomechanical approach to corroborate the location and orientation of a horizontal well in the Table Rock field, for Union Pacific Railroad Corporation (UPRC) and the DOE/FETC. After examination of existing core for natural fracture characterization and 3D seismic data for fault mapping, it became apparent that the structural and tectonic nature of the area required a different application of the geomechanical approach.

Rather than determining the occurrence of extensional fractures, the area required the prediction of sheared fractures that control production. The geomechanical prediction for the well location was within the failure envelope for sheared natural fractures and that the orientation of the horizontal leg was appropriate for the predicted natural fracture orientations. This prediction was verified by the Rock Island #4-H horizontal well, a well capable of delivering 12 to 20-MMcfd gas.

3. Methodology

The geomechanical model defines the limits of expected natural fracture occurrence to delineate the prospect area, and helps select the location of the exploration well. It is dependant on two key inputs into the model: (1) observational inputs from seismic and borehole data and (2) an understanding of the geologic and tectonic framework for natural fracture genesis.

We implemented the geomechanical approach in each of the field demonstrations, as a series of three tasks. Although each of the three tasks had definite actions and deliverables, the exact details of the types of data and deliverables were slightly different for each field site. Each field project included three tasks.

Task 1: Site Selection and Site Characterization

This task provided all the appropriate geologic information of the study. The commercial-scale demonstration of the geomechanical approach was in three distinct geologic settings. The study areas were located in two Rocky Mountain priority basins identified by the National Petroleum Council (NPC) and DOE/FETC: the Wind River basin (WRB) and Piceance basins. The third site, Elk City field in the Anadarko basin, is outside the Rocky Mountain region.

Task 2: Geomechanical Analysis for Prospect Delineation

The geomechanical analysis uses a 3D boundary element numerical model to predict natural fracture occurrence due to faulting. Three primary data types are necessary: (1) image logs, (2) core and (3) either 3D or 2D seismic data. Inputs include fault geometry, displacement vectors (or orientation and magnitudes of remote stresses), and rock properties. Outputs from the geomechanical model include the location of the expected natural fracture cluster in three dimensions, the orientation(s) of the natural fractures, and a relative intensity of the cluster that correlates with natural fracture density. Integrating this information with other reservoir information produces the prospective locations for an exploration well. The analytical process follows these steps:

1. Assemble fault geometry and regional tectonic control.
2. Build and run geomechanical models.
3. Identify possible prospective areas.

Task 3: Post-Appraisal and Impact Assessment

Post-appraisal is essential to technical credibility. Our plan was to drill an exploration well on the prospect identified by the geomechanical approach. After drilling, appropriate down hole data was to be collected verifying the presence of natural fractures (potentially including core, image logs), and production tests to ascertain the economic success of the well.

Ideally, this task would have been undertaken once the operator and the DOE agreed on the drilling location. In reality, the volatile nature of the industrial competitive climate (shifting operator strategies, priorities, and consolidation) combined with unanticipated technology development needs blocked the sequential execution of the demonstrations as originally planned.

EXECUTIVE SUMMARY

Advanced Resources International Inc. (ARI), with support from the U.S. Department of Energy (DOE), conducted a field demonstration program (DE-RA26-99FT40720) to demonstrate the utility of elastic geomechanical methods for the prediction of natural fracturing in low permeability reservoirs. The purpose of the program was to improve natural gas production from recognized low permeability resources by building credibility and operator acceptance of the technology through positive field demonstrations and technology transfer. The Wind River, Anadarko and Piceance basins, where large volumes of tight gas resources remain to be exploited, where chosen for the demonstration.

An earlier project (the DOE Multiwell Experiment Project in the Piceance Basin), generated notions about the nature of natural fracturing because it was demonstrated to have a positive impact on the productivity of low permeability gas reservoirs. Within low permeability reservoirs, natural fracturing exhibited characteristics of brittle failure, consistent with principles of elastic rock mechanics. From this, it seemed likely that the nature and distribution of natural fractures within the low permeability reservoirs could be predicted by the use of continuum mechanics and software simulation. Poly3D, an emerging boundary element-modeling (BEM) program from Stanford University, was successfully employed in the Piceance Basin near the MWX site, so we selected it as the core technology to use in this project as well.

In this project, ARI implemented geomechanics technology in three separate settings (within three different basins). The results challenged the underlying assumptions about the use of geomechanics to predict the nature and distribution of natural fracturing within mildly deformed, tight (low-permeability) gas reservoirs. Limitations that emerged early on in the project included software input/output, scaling, seismic resolution, and uncertainty regarding the origin of the fractures (for predictability). As each issue was encountered, it was assessed and we made modifications to the overall technological approach.

We worked within the limitations of the Poly3D software, with exception being made when alternative approaches could be identified and implemented. The NextGen package then under development (DE-AC26-99FT40688) was refined to address input/output issues. We supplemented Poly3D and NextGen with additional software packages as the need arose. The genesis and role of natural fractures in low permeability (sand) gas reservoirs underwent a heuristic process, and our view was revised to integrate our original concepts with our practical experience.

The quantitative relationship originally envisioned between regional stress or local fault strain and bulk production permeability at the wellbore was not established. Barriers to developing the desired quantitative relationship between the geological elements simulated and highly variable wellbore productivity included seismic resolution, time varying rock properties, and viscoelastic behavior of the reservoir sediments. The demonstrations revealed that both direct

and indirect relationships exist between individual types of natural fractures and reservoir history and structural fabric.

A significant conclusion of this project is that natural fractures, while often an important, overlooked aspect of reservoir geology, represent only one aspect of the overall reservoir fabric. Thus, a balanced focus and perspective encompassing all aspects of reservoir geology will have the greatest impact on exploration and development in the low permeability gas setting.

TECHNOLOGY DEVELOPMENT DISCUSSION

A. The Problem

Natural fractures play several roles in low-permeability gas reservoir geology and production. Their exact roles and performance are difficult to describe or quantify, primarily because of their scale with respect to the overall system. No single tool or method directly detects volumetric distribution of natural fractures at the reservoir scale where their impact is most significant. Core, logs and certain image logs allow detection and characterization at the wellbore scale.

Seismic methods generally attempt detection by indirect means, using attribute analysis calibrated to production or electric logs. Pressure transient testing may indicate natural fracture presence under some circumstances but delivers a non-unique solution. Analysis of long-term production data represents a greater fraction of the reservoir but also yields a non-unique solution. Geomechanical modeling methods are predictive in nature but difficult to frame geologically as addressed later in this report.

Natural fracture systems can be described statistically (LaPointe and Hudson 1985, McKoy and Sams 1997) and are known to generally follow power laws of frequency distribution (Marrett 1997). Therefore, either unconditional or conditional methods will numerically simulate their distribution. Discrete fracture networks (DFN) generated through these approaches can be simulated directly (McKoy 1996) or transformed into other formats for use in conventional reservoir simulations. Nevertheless, descriptive statistics, geographic distribution of faults, and bulk reservoir permeability "ground truth" are required to calibrate the overall process and generate a relevant reservoir description.

To further complicate matters, pressure transient analyses (PTA) may not distinguish highly fractured, low matrix permeability reservoirs from high matrix permeability reservoirs. PTA as well as similar methods depends on a contrast between fracture and matrix permeabilities (dual permeability). When two or more directions of fracturing are present (common in highly fractured settings), reservoir bulk permeability can become very large and lose its dual permeability characteristic.

The vagaries of pay determination, completion philosophy, completion effectiveness, and operating practice add to the confusion already inherent in the fractured reservoir behavior. Ultimately, the productivity of any given well in a naturally fractured tight gas reservoir is a multivariate function of many competing factors. The challenge in unraveling fractured reservoir production is that many of the key elements are not scrutinized, not understood, subject to chance, and/or are below resolution of current technologies.

Recognition and effective characterization of fractured reservoir systems typically depends on multiple indicators. Viewed individually, each indicator may yield a non-unique answer. Viewed jointly, these indicators converge for reasonable, if not determinative predictions.

B. Frames of Reference

Determining the distribution and permeability impact of natural fractures in a reservoir is a difficult task that often requires analysis from multiple approaches or views. The approach or view from which the analysis is undertaken often determines the nature and complexity of the solution. As an example, the physical organization of the solar system and the equations of planetary orbits are relatively simple when described from a solar centered perspective. They appear much more complex when described from an earth centered coordinate system, as Kepler discovered. It can be done but it is difficult and hinders the conceptual advance towards understanding the larger organization of the solar system. Much the same can be said for analysis of natural fracture systems.

Frames of reference is a term used in physics to describe the point of view from which a motion or action is observed. Here we use the term in the numerical sense to describe the coordinate system used for geomechanical modeling, and in the philosophical sense to describe a point of view in which to describe or project rock failure by fracture.

The spatial frame of reference for all geomechanical modeling performed in this study is global. Although Poly3D allows description of problems and construction of models in local coordinates, we used global coordinate systems because they reduce the potential for serious positional errors in prospect location. Thus, input data was in accordance with local geographic coordinates, producing drillable prospect locations consistent with legal land description. The result of this global modeling process was cartographic and dimensional consistency.

The philosophical frame of reference is important when defining the immediate problem and choosing the appropriate tools for its resolution. Prior to choosing which tool to employ, we must consider the nature of the fractures in question. Two frames of reference were employed in this study: (1) external forces acting inward upon the rock as a whole and (2) internal forces acting outward in response to changes in the environmental conditions through time. Poly3D, a linear elastic boundary element model developed at Stanford University (A. L. Thomas 1993) was used for the externally referenced situations and experimental viscoelastic modeling software developed at Sandia National Laboratories was used for the internally referenced situations (Warpinski 1989).

Natural Fracture Terminology

The aim of the geomechanical approach is to successfully characterize, understand, and predict natural fractures near or below the limits of seismic resolution. These natural fractures and small faults are difficult to characterize adequately or project using currently available technologies.

Ideally, geomechanics uses fundamental scientific principles of structural geology to relate the genesis of natural fractures and related deformation to the local and regional stresses of the area. N. J. Price developed the methodology for studying natural fracturing in the earth's crust in his classic, *Fault and Joint Development in Brittle and Semi-Brittle Rock* (1966). Using the concepts of brittle failure and elasticity theory, he described, idealized and then modeled faults and natural fractures. Today his underlying principles of the geomechanical approach remain unchanged, although contemporary theories of fracture mechanics have advanced and modified our understanding of fracture growth and development in rock.

Numerical models of rock deformation, based on continuum mechanics, provide an important tool for the interpretation of geologic structures for tight-gas exploration and production. ARI used the boundary element method to approximate faults as three-dimensional (3D) surfaces of displacement discontinuity in an elastic material. We computed stress fields to predict the locations and orientations of sub-seismic faults and fractures. Given the fault shape and slip geometry from seismic data and/or the loading history from tectonic analysis, we could use boundary-element modeling calculate the local stress concentrations believed to control the mechanical interaction of faults and the development of sub-seismic scale natural fractures.

Identification, description, and statistical characterization of fractures at the surface, and in the subsurface from core image logs or other data is a requisite of developing appropriate input data for geomechanical technology. The numerous references are available on this subject will not be recounted here. Pollard and Aydin (1988), Lorenz (1989), Aguilera (1995), and Nelson (2001) are all substantive on the topic of natural fracture description and characterization.

Identification is only one aspect of developing a complete fractured reservoir description and geographic prediction. The best technical strategy to achieve the most accurate naturally fractured reservoir characterization is to incorporate as many lines of evidence and data as are available. Geomechanics, the focus of this project, is a way to predict natural fracturing between control points.

Any high quality reservoir characterization, fractured or otherwise, is highly dependent on the quality and amount of data that form the basis for the interpretation. Towards that end, every effort should be made to acquire high quality pertinent data upon which to build the reservoir description.

Koepsell, Cummella and Mullen (2003) offer valuable insights to make borehole image data more useable through statistical transformations. McKoy and Sams (1997), and LaPointe and Hudson (1985) provide schemes for generating statistically valid DFN's. Wellbore based bulk permeability estimates can be described geostatistically through variograms, and distributed through conditional simulations to achieve a statistically valid geographic distribution of bulk reservoir permeability. Seismic attributes may also reflect natural fracture distribution.

Natural Fracture Characterization

Natural fracture type plays a similar role in fractured reservoir characterization as sedimentary structures do in reconstruction of depositional environments. Core and image logs of various types provide clues to the origin of natural fractures as well as reservoir impact. *Like sedimentary facies*, the types of natural fractures have been linked to corresponding conditions of failure postulated in the subsurface.

Unlike sedimentary facies and their corresponding depositional environments, rock failure is not directly observable as it occurs in the subsurface. In laboratory experiments, workers measured rock properties (by observing deformation of rock specimens under load), and generated systems of equations to project the behavior of the rock into subsurface conditions. From the geological perspective, the laboratory experiments were of short duration so they may not accurately depict the actual rock behavior at depth over geologic time.

Our inability to observe rock failure over geologic time in the subsurface is a key source of technical uncertainty in the field of rock mechanics and by extension, the geomechanical approach to natural fracture prediction. Mechanical properties of rocks can be determined with great accuracy and precision in a controlled laboratory setting. Conversely, their range of values in actual occurrence and geologic settings is nearly infinite and varies through time in response to changing conditions of confinement.

Computers can simulate rock failure behavior using mathematical models and assumptions with great precision but the results are only as accurate as the inputs or bounding concepts used to construct the model and describe the subsurface environment. Consequently, precise computer simulations of instantaneous elastic rock failure envelopes in the subsurface are often calculated. These precision simulations frequently lack accuracy in describing the true conditions and processes of rock failure over geologic time and may imbue a false sense of confidence in the resulting interpretation.

On balance, the genetic relationships observed between depositional processes and sedimentary structures in the recent are more accurate (although more difficult to simulate) when projected to the geologic past than the equivalent relationships between evolving subsurface conditions and the various types of natural fractures. Relationships between stress conditions and resulting failure types are determined through practical laboratory experiments. Projection of these relationships into the geologic past via simulation remains extremely difficult because of the complexities in accurately determining the geologic environment and rock properties at any given point in time(when the failure may have occurred). The result is often a precise answer to the wrong question.

Drilling Induced vs. Natural Fractures

The methods and procedures for analyzing core and image logs to differentiate between drilling-induced fractures and natural fractures are particularly important because of the potential insights into horizontal in situ stresses. Lorenz (1989) and Dart (1990) provide convincing evidence on this aspect of fractured reservoir interpretation. Valuable, documented examples of drilling and natural fractures are typically available upon client request to image log vendors.

Drilling induced fractures occur in core and the walls of the wellbore. During the drilling process, fractures occur as a result of perturbations in the local stress field around the core and wellbore. The rocks fail in shear or extension depending the exact conditions. The local stress conditions are inferred from the most common mode of failure observed. The orientation of drilling induced fractures reflects the orientation of the present day in situ stress field and may be important in the determination of boundary conditions for use in later modeling.

Shear vs. Extensional Natural Fractures

There are two basic types of natural fracture, classified by (1) the presence or (2) the absence of displacement across the fracture face. Rock failure in *shear mode* occurs when the shear component generated by the differential stress on the rock exceeds its shear strength (determined by it's internal coefficient of friction). *Extension fractures* occur when shear stress applied to the rock is relatively low (else there would be post rupture displacement along the fracture plane). Both types of fractures occur at a wide range of scales during reservoir development.

Shear Natural Fractures

Shear fractures in brittle reservoirs often develop at depth, are relatively insensitive to stress, and *can be attractive targets when there is a thorough grasp of the hydrocarbon distribution in the reservoir.* Shear fractures (as targeted in this project) develop in and around the mapped discontinuities where mean and differential stresses associated with displacement are high. In practice, this means the tip propagation zones around the edges of the faults. Fig. O-1 is an example of a highly permeable shear fracture recovered from great depth.

Disarticulated, bed bound natural fracture from Frontier Fm at 17,818 md in Barrett, Bullfrog #5-12. The fracture is lined with euhedral carbonate crystals 2-3mm in size. Note non-planar geometry of the fracture face.

Fig. O-1. Fractured Frontier Fm. Barrett Bullfrog #5-12

Shear fractures are common where rocks have been folded or faulted. They also occur as grains are crushed during mechanical compaction, by either burial or lateral shortening. Shear fractures are characterized by displacement of the opposing sides in the plane of the fracture surface. A shear fracture is shown diagrammatically on the right side of fig.O-2.

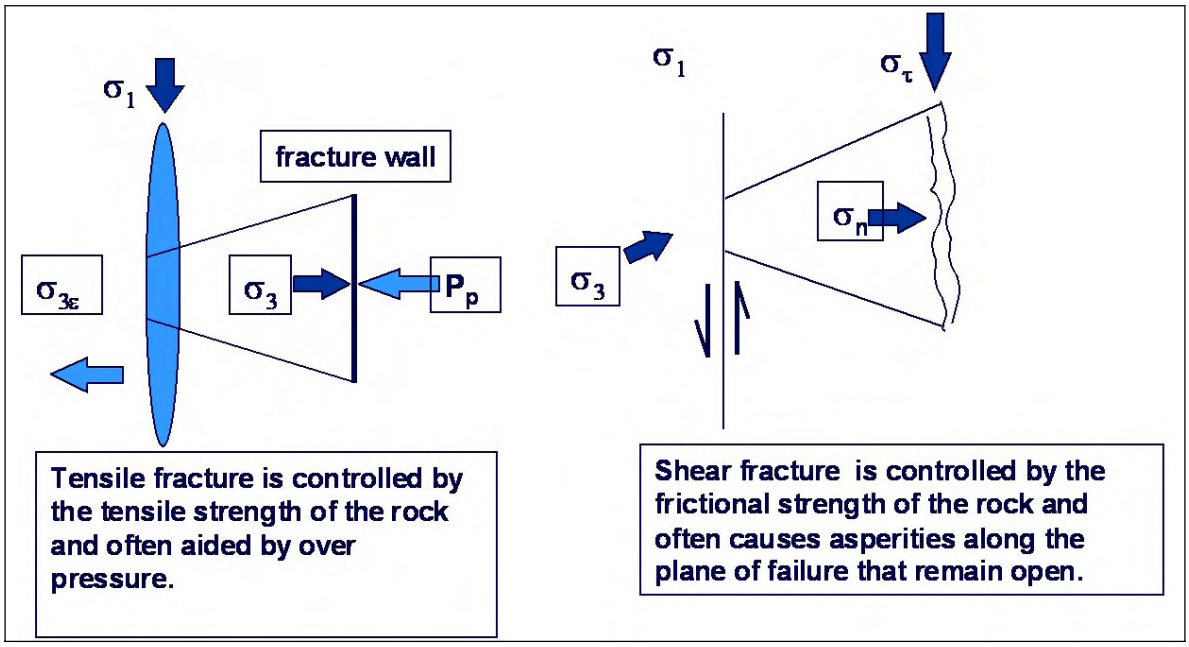

Fig. O-2. Natural fracture characterization

Open shear fractures in brittle reservoir rocks may show extremely high permeabilities and little sensitivity to stress direction or magnitude. Asperities (small irregularities) along the fracture plane in brittle rocks may act as "props" to hold the fracture open after initiation. The sense of motion along the fracture can be deduced from *slickensides*—the grinding of grains, asperities and cements during subsequent displacement, which form striated surfaces within the plane of the fracture.

> *Note:* This project did not rule out conjugate shear natural fractures. They were not targeted, as they are commonly believed to form in, around and on anticlines.

Extensional Natural Fractures

Descriptive nomenclature remains a problem within the oil industry as it grapples with the issue of naturally fractured reservoirs. In 1988, Pollard and Aydin proposed the use of classification schemes based on descriptive terminology, independent of the feature's genetic origin. They specifically cautioned against the use of the classification *extensional fracture*, which the industry had adopted into broad usage because both joints and extension fractures can be caused by contraction or extension

The nomenclature, semantics, and multiple origins have contributed confusion and misunderstanding to the origins and role extension fractures play in tight gas reservoirs. However, the term *extension fracture* has been less cumbersome to petroleum geologists operationally than the perceived seal risk associated with a direct connection between joints (at the surface) and joints (in the reservoir).

Being mindful of the value of making distinctions in the genetic origin of the feature, this discussion includes distinctions in the following classification nomenclature.

Joints

A joint is a fracture between two chunks of things, either caused by extension (net stretching) or contraction (unloading) and we believe prudent use of the term is restricting to those fractures with field evidence for dominantly open displacements.

The widespread conventional use of the term *joint* associates it with fractures exposed and studied at the surface. Thus prior to the advent of techniques for recovering oriented core, and borehole image logs in the latter part of the 20th century there was little direct information about the density, orientation, habitat, or description of joints in the deeper subsurface.

Initial studies of joints performed on broad exposures of rock that exhibited consistent patterns of fracturing resulted in numerous definitions and terms.1988, Pollard and Aydin chronicled over a century of research and thought on *jointing* to deliver an illuminating historical perspective.

While the high level of interest in research related to the importance of jointing in tight gas reservoir permeability has not waned since 1988, a single unified concept of the broad spectrum of occurrence and settings documented has yet to emerge. Even after intervening decades of study, the origin and distribution of joints in reservoirs remain enigmatic topics.

Extensional Fractures

An extensional fracture is one caused by net stretching. In this report the term *extension fracture* is used to describe a fracture where the aperture (width) is significantly less than height or length and the faces of the fracture have been displaced perpendicular to the fracture plane (left side, fig. O-2).

The genetic implication of the adjective *extension* is accepted but as Pollard and Aydin (1988) noted, extensional strain may result from externally applied far-field stresses or may be generated internally by cooling and shrinkage of the matrix.

Thus, the extension fracture commonly described in core and image logs and used as an indicator of principal stress directions has more than one potential origin and geologic implication.

Contractional Fractures

A contractional fracture is one caused by unloading. Bourne and Willemse (2001) used Poly3D modeling to demonstrate the elastic stress patterns around a small fault in Wales. Then, using modified Griffith failure criteria they demonstrated that tensile failure area from actual fault displacement is less than the shear failure area (4% vs. 5%). Later isotropic stress change is required to account for tensile-shear proportions of 85%-7%, which is more similar to the outcrop maps.

They attribute the isotropic stress change to erosion, temperature change or pore fluid pressures individually or in combination. This work indicates fault related stress and strain fields set the stage for later extensional fracturing during uplift or other unloading process.

As a result, we draw a strong distinction between fault related extensional fracturing and extensional fracturing associated with changing conditions within the reservoir matrix which we choose to call "unloading extensional fracturing" or "unloading fractures".

Early tensile fractures related to faulting may carry a significant risk of cementation or inclusion in later stages of deformation. Fig. O-3 (Steffes core) illustrates this aspect of the problem. A large extension fracture has formed, filled with calcite, and been itself deformed later. Younger unloading fractures formed during a late stage uplift phase may be more attractive as reservoir targets than the older fault related fractures.

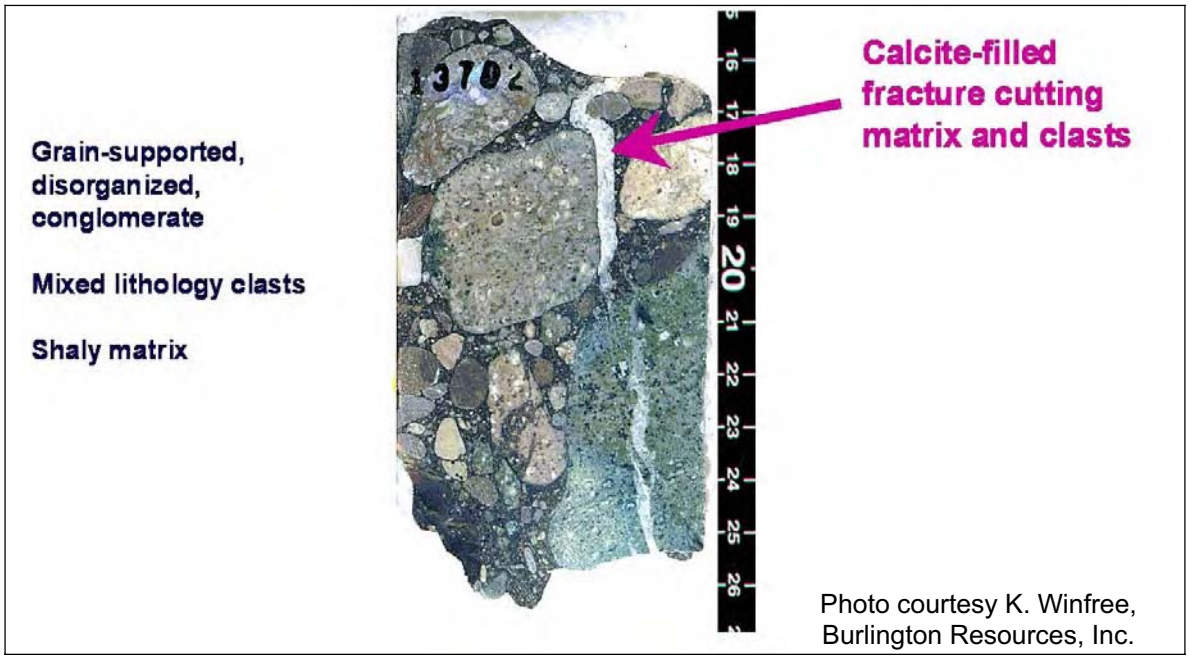

Fig. O-3. Atoka (Steffes Fm) fault related natural fractures

B. Demonstration Models and Processes

There were three major barriers to generating rigorous, time dependent stress and rock failure maps: (1) understanding the variability of rock properties through time; (2) implementation of realistic failure criteria, and (3) correct application of tectonic loading boundary conditions. Insufficient data was available in the Wind River and Anadarko basin demonstration areas to fully develop the process required to support the technology so we returned to the Piceance basin area, where the geomechanical concept originated. This work has changed the way we approach exploration for naturally fractured plays.

Tight gas reservoir development spans large amounts of geologic time and as a result, reservoir rock properties change continuously as well. In the case of the Mesaverde (Piceance basin), for example, reservoir deposition is followed by 50^{+} million years of subsidence, one or more periods of tectonic shortening and variable amounts of uplift. The reservoir is heated, pressurized, stressed (vertically and horizontally), subjected to potential or actual stress loading that may exceed its strength and then stressed again through unloading to varying degrees over the course of its development.

Porosity destruction via compaction, diagenesis or other chemical and physical changes are not elastic (recoverable) in the true sense of the term. Thermal, mechanical or chemical energy input during the process drives irreversible changes in the reservoir as they are absorbed and transformed from one form to another as they seek equilibrium. Energy input to the system remains available for later output and can generate stress of its own accord, displaced in time, in response to changing conditions (Warpinski 1989).

Rock properties measured from core reflect the nature of the rock at the surface after collection. Even when attempts to project the measured properties of in situ conditions are successful, the projection remains an instantaneous present day estimate that is only one point of many in the geologic history of the reservoir.

Rocks display true elastic behavior for very short periods of time. In geological time, rocks tend to equilibrate to relieve imposed stresses through inelastic changes in their shape, composition, or other characteristics. As a result, applied stress is converted to an inelastic strain over geologic time.

The problem of effective natural fracture prediction requires the effective prediction of the nature and conditions under which the energy, stored in the rock (visco elastically), will transform itself into a new strain in response to changing conditions. Instead of a near instantaneous determinative problem in static mechanics, the solution now requires solving a multivariate problem with dynamically changing variables.

The initial perceived barriers to determinative natural fracture prediction via boundary element modeling remain significant barriers. This arises primarily due to the difficulties in accurately back projecting the required variables in geologic time and may ultimately be insoluble. Attempts at resolving these issues during the course of the project however have given rise to alternative approaches to the problem requiring less determinative input.

1. Models

Geomechanical Modeling

Two types of modeling techniques were used in attempts during the project to correctly simulate the subsurface in situ stress and relate it to fracturing or bulk well bore permeability. A visco elastic model written by Warpinski (1989) was adapted to estimate a regional stress component generated during burial and uplift. Poly3D (citation) was used to estimate stress or strain resulting from displacements on seismically defined faults. Either or both models can be incorporated into a geomechanically driven exploration program depending on the setting.

Visco-Elastic Modeling

A visco elastic model was written at Sandia National Laboratory by Warpinski (1989). The model itself is primitive by contemporary standards but unlike Poly3D does treat the evolution of the reservoir through time. SHSTVIS software simulated reservoir stress conditions at a single point through time. It required a complete geologic history (similar to source rock maturation models) for the point being simulated as well as estimates of supporting rock properties. Multiple runs with different inputs were compiled and used to simulate an area. Please see Warpinski (1989) for a more thorough discussion.

We used Warpinski's visco elastic model to simulate representative areas of the Piceance basin and develop depth-dependent, time-variable stress maps for the study area. These maps of

model results account for time, temperature, and pressure effects of burial, maturation, diagenesis and other elements of geologic history. Once the model is built, the various inputs can be adjusted until the known present day stress is matched.

Warpinski's visco-elastic modeling identifies a major role for temperature induced stress (i.e. the burial-uplift cycle) in producing irreversible mechanical changes in the sediments. This supports the contention by Bourne and Willemse (2001) and Higgs (1993) that the majority of extensional fracturing occurs during the conditions of falling mean stress associated with uplift. Warpinski's model also supports the concept of "locked in" tectonic stresses (in sandstones) that control orientation of more recent extensional fractures around essentially dormant faults.

Failure Criterion and Tectonic Stress Estimation Modeling

For failure criteria and tectonic stress estimation methodologies, we followed techniques outlined by Bourne and Willemse (2001). This model uses a re-arrangement of classical Mohr envelope approaches to define failure as a function of the internal friction coefficient and cohesive stress of the rocks.

By applying Bourne's techniques to the areally variable, time dependent stress maps of the objective horizon, along with Poly3D modeling (Thomas 1993) we were able to establish:

1. Stress history trajectories that directly identified areas of fault related shear failure.
2. Fault related extensional halos.
3. Regional areas failing by extension during regional uplift and cooling.

Viscoelastic and discrete fracture network modeling proved important to the overall process. Because the stress-modeling program was developed in an academic setting, it required field calibration, testing, and demonstration to achieve industry acceptance and commercial use. The potential for using stress modeling to estimate in situ bulk permeability within naturally fractured reservoirs was first observed in the Rulison area of the Southern Piceance Basin. Stress modeling was an obvious and promising tool for high grading locations to increase gas recovery (on a per well basis) within a development program.

Within the context of our heuristic process, we produced a final iteration for this model, calibrated to patterns of productivity for the areas of study.

Boundary Element Modeling

The core technology under demonstration in the multi-site project is the use of geomechanical modeling incorporating a *boundary element-code* to delineate areas of potential increased natural fracturing associated with faulting at depth. Using boundary element-code, we can model the stresses distributed around a mathematically defined discontinuity (fault) in a 3D space imbued with the physical properties of the modeled reservoir. Predictions of natural fracture distribution were made by correlating mapped stresses with the styles of fracturing

known to exist in the reservoir and deducing, by analog, other unexploited areas with potential for natural fractures.

Poly3D, a software program written at Stanford University by A. L. Thomas (1993), was used for the boundary element modeling. Fig. O-4 illustrates the patterns of high stress (red) developed because of displacement around a hypothetical circular fault. We used the regional geology, core fracture characterization, and micro-resistivity imaging-log characterization information to set the boundary conditions for the geomechanical modeling.

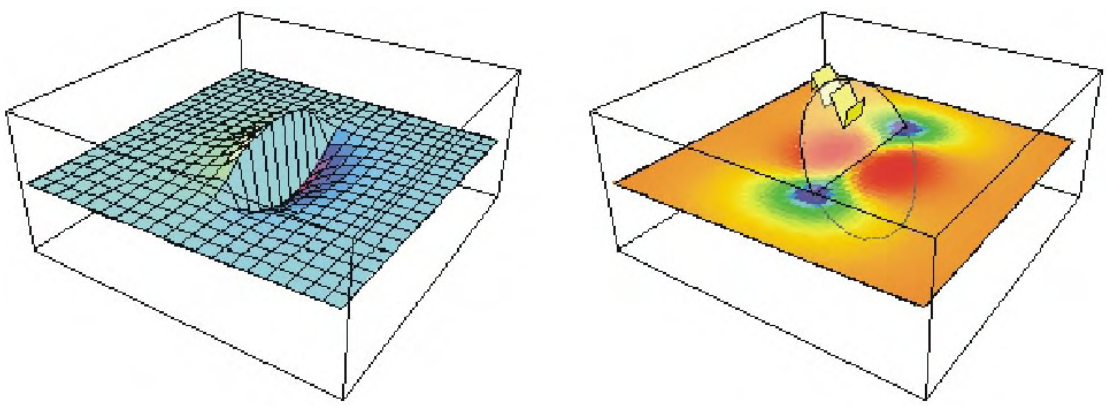

These diagrams illustrate the general concept of boundary element modeling as it relates to the mapped distribution of stress around faults. In this extensional example, the red areas on the diagram to the right indicate the extensional areas where higher concentrations of fracturing would be expected.

Fig. O-4. Boundary element modeling

The location and intensity of fault related natural fractures in the subsurface was predicted by calculating, comparing, and interpreting fault-related stresses via the modeling with a failure criteria. Since absolute stress values and failure criteria were not being calculated by Poly3D in the first study area it wasn't possible to definitively project fractured vs. unfractured rock.

Once Poly3d was implemented, the methodology for subsequent demonstrations consisted of determining the background, or average, value of the calculated stress, using existing control points from core or logs to establish a control "fractured" area, and then inferring that areas with higher mapped stress will be more "fractured". One of the constraints with this approach is that existing well control from earlier drilled wells in the area (or in analogous areas) was necessary to calibrate the mapping.

2. Geomechanical Work Flow Process

As the process flow chart in fig. O-5 indicates, we did not anticipate temperature, pressure, time-variable rock properties, or regional stresses would be required to predict natural fracturing from a simple boundary element model. Yet, in the course of heuristically demonstrating the technology first to Barrett and later to Burlington, it emerged that a credible technology had additional requirements. For example, the geomechanical approach requires detailed structure mapping and rigorous, time variable rock mechanics techniques in order to predict areas of failure that can be calibrated to production behavior and used for prospect delineation and risk management.

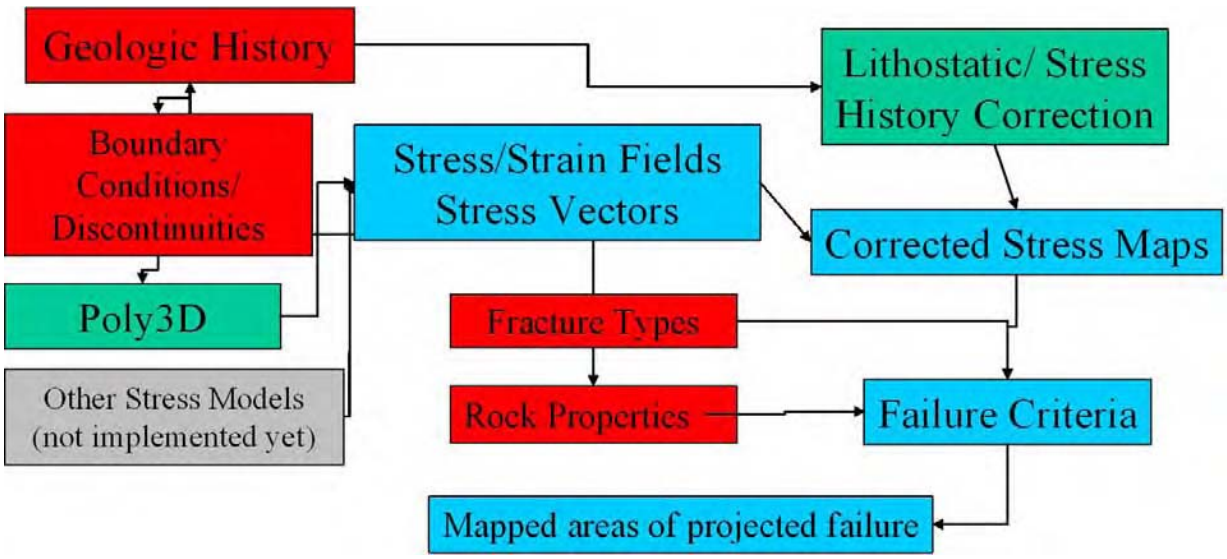

Fig. O-5. Geomechanical workflow process

C. Field Test Experience

Bullfrog

Results from the Bullfrog field demonstration indicated few, if any, effective extensional fractures at depth in the well. A fortuitous show in the Frontier Fm was cored and a large open shear fracture (fig. O-1) was recovered. The large NNW trending fracture had an undulatory surface and appeared to have been the result of a rotational displacement.

A few minor, cemented extension fractures were present as well as some centerline coring induced petal fractures. The minor extension fractures are interpreted to be fault related. The orientations of the petal fractures were subparallel to the fault related extension fractures with both sets oriented ENE to NE indicating that present day in situ stress has a similar orientation

as the paleo stress. The productive capacity of the well correlated strongly to the large observed shear fracture.

Elk City

The Elk City field demonstration site was located at depth on a strongly sheared structure. A poor quality formation micro-scanner (FMS) log on a local, highly productive well indicated a large shear fracture (similar to the Frontier Fm fracture at Bullfrog) was responsible for the excellent productivity. Analysis of long-term production data also indicated dual permeability behavior. The well drilled during the demonstration showed some fracturing (indeterminate nature) oriented consistent with a shear system.

A few fractures and one fault were observed on the poor quality FMS of the confirmation well. The fractures interpreted clustered approximately at a N70E and N110E orientation. Present day in situ stress derived from the interpreted drilling induced fractures observed on the FMS is oriented just south of east. The present day in situ stress appears to nearly bisect the acute angle between interpreted natural fracture clusters. The FMS data suggests the natural fractures interpreted from the FMS may be conjugate shears formed around an easterly principal horizontal stress that has remained stable since the deformation.

Piceance

The Rulison field (RCP, Piceance Basin) project area is centered on a gas productivity sweetspot localized in and around a positive flower structure related to strike-slip faulting. Results from the DOE MWX research program indicated a high extension fracture density localized above and around several small reverse faults. Earlier proprietary modeling work performed outside the field demonstration area suggested regional productivity patterns were related to varying amounts of uplift along the southern margin of the basin.

Present day principal horizontal stress (NW-SE) is rotated approximately 90 degrees from paleo principal stress directions inferred from regional Laramide structure (NE-SW). Taken in total, core and structural modeling results suggest the greatest extensional fracture enhancement is localized in the areas where paleo-confining stress has been the highest. These stresses may be the result of a burial uplift cycle or localization within the compressive core of structures. While there appears to be a relationship between mapped and modeled faults, it appears to be inverse in nature.

D. Implications

Results from two of the three field demonstration areas are consistent with the structural models built from the 3D seismic in conjunction with regional boundary conditions inferred from local macro structure. Shear fracture systems (when recognized) can be directly related to local and regional paleo stress directions and regimes: Even when found at great depth, these systems can be prolific reservoirs or permeability channels. Their extremely high permeability means they do carry a significant risk of unexpected water production.

Somewhat surprising was the apparent inverse relationship between high densities of extensional fractures in areas of simulated high confining stress. If the faults control the fracturing directly and the reservoir is behaving elastically, as the brittle fracture styles suggest, the highest density of extension fractures should have been in the areas of simulated tensile failure. In fact, core studies suggest the fracturing is overwhelmingly extensional when compared numerically with the number of shear fractures observed. This result contradicted the original project premise, dictating further study before extensive implementation of the geomechanical approach.

1. Importance of Unloading

The concept of unloading, or release of previously imposed stress, and it's conversion to strain dates to the 19th century (Pollard and Aydin 1988). Other terms applied to this phenomenon are *locked in stress* (Lorenz, pers. comm.) and *residual stress* (Lajtai and Allison 1979). In the late 20th century, Warpinski (1989) articulated a viscoelastic approach to stress calculations that incorporated time varying rock properties and quantified time dependent differences in stress-strain behavior between rigid sands and more viscous shales.

Warpinski argued that present day in situ stresses in basins were, in fact, the cumulative result of past geologic stress history. By any name, the underlying concept is that stress, accumulated in a rock as strain, released later in time in a different form as the local conditions of confinement change, breaks the direct stress-strain relationship inherent in elastic approaches to rock mechanics.

Even though they are frequently approximated using *elastic approaches* (strict conservation of energy in the stress-strain relationship), many of the processes and transformations rocks undergo during a burial uplift cycle are inherently *inelastic*. Examples of this inelasticity are grain crushing; pressure solution; and redistribution of the resulting mass as cements and overgrowths. The rock undergoes fundamental changes during burial diagenesis that can never be simply reversed on uplift.

Mechanical elasticity exists in rocks for short periods. Over longer periods (tens to hundreds of million years) the rocks change shape in response to externally applied stresses and equilibrate to the new confinement conditions. This effectively transforms the applied stress energy into thermal or chemical strain. Long after the original event, later events such as uplift can release manifestations of previously applied stresses. Rock bursts in quarries are one example.

Lajtai and Allison (1979) performed practical laboratory experiments demonstrating the residual stress phenomenon. They placed wet mixtures of sand and cement in uniaxial confined compression until solidified. During release they observed weaker planes of micro-fractures forming perpendicular to the previous principal stress. In cases of higher confining stress they observed formation of a smaller population of load parallel micro-fractures.

They hypothesized the load parallel micro-fractures accommodated the shortening and extension associated with the cyclic loading process. In a practical sense, they simulated a rectilinear joint system similar to many observed on the outcrop and in well bores today. The broader implication of their work, however, was to attribute a 90-degree shift in principal stress to the unloading process rather than any external tectonic rearrangement.

Engelder and Fischer (1996) used the Griffith energy-balance concept to create a *fixed grips* scenario for the development of joints by subsurface thermoelastic stress release. Under this scenario the basin margins remain *fixed* and the basin fill accommodates the release of thermal load by internal contraction; the basin fill appearing to develop extensional strain because the matrix shrinks creating void space. Such matrix shrinkage across existing planes of weakness gives the impression of stress reorientation when compared to field macro structural evidence.

The general concepts of stored stress to strain transformation via unloading and viscoelastic behavior of materials have received little emphasis in the mainstream fractured reservoir community. *As key problems aren't being addressed by the pervasive elastic approaches, the time is ideal to re-evaluate some previously discarded notions and theories.*

2. Material Behavior

Griffith Material Model

Griffith pioneered work in the field of materials science and fracture mechanics in the early 20th century (Pollard 1988). Griffith's material model is of interest because it treats materials as composites of smaller particles (molecules, grains, etc.). *Specifically, the* Griffith material model explains the phenomenon of natural fracture aperture distributions in sediments following power laws (Marrett 1997), and conceptual models for material behavior accounting for this characteristic of sedimentary rocks.

Griffith envisioned a compositionally homogenous solid with microscopic cracks randomly distributed throughout its volume. Fig. O-6 is a schematic representation of the material model and its behavior under load. In the Griffith conceptual system, failure (in this case shear) involves the concentration of stress at fracture edges in conjunction with coalescence of multiple microfractures along the optimally oriented failure plane.

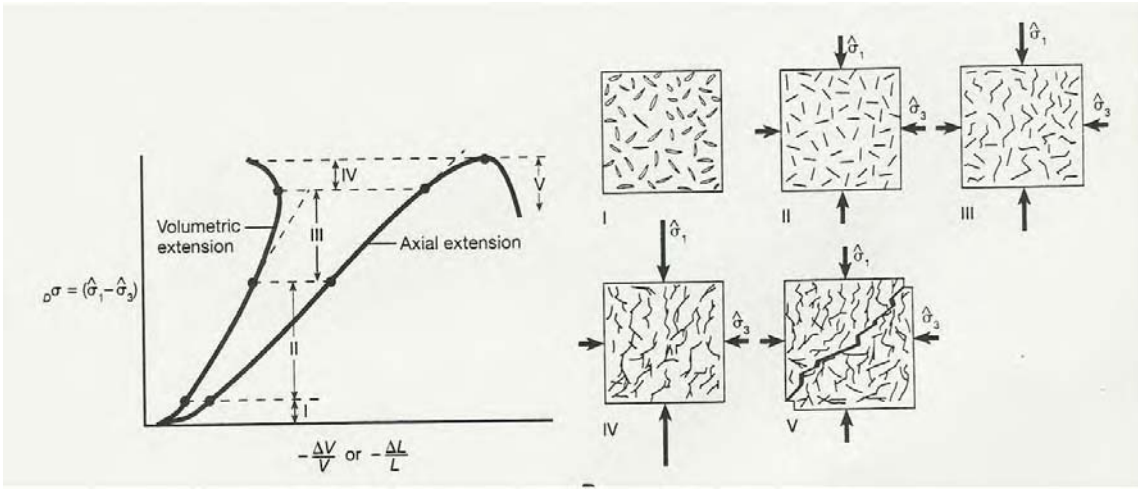

Fig. O-6 Schematic representation of the Griffith material model

Mathematical models for matrix permeability behavior under stress indicate a thin slit-like pore geometry (Ostensen 1983). If individual grains in the matrix are taken to represent the base material and the slit-like pore throats behave analogously to the Griffith micro-fractures, the model becomes a reasonable mechanical analog to a tight gas sandstone.

A backscatter SEM image of an Almond Formation (Amoco Production Co., Champlin 254B-2, T20N, R93W) natural fracture. The image (fig. O-7) shows the grain scale detail as the open extension fracture propagated through the rock. The bright white material is a barite fracture fill. Scattered throughout the section are other short segments of pressure solution surfaces or incipient fractures (pink arrows) that did not fail. The fracture skirts the grains along planes of weakness that are presumably the “slit-like” pore throats. Given the general pressure dependent behavior of the permeability as described by Ostensen, it can be argued that the slit-like pores are grain-bounding microfractures.

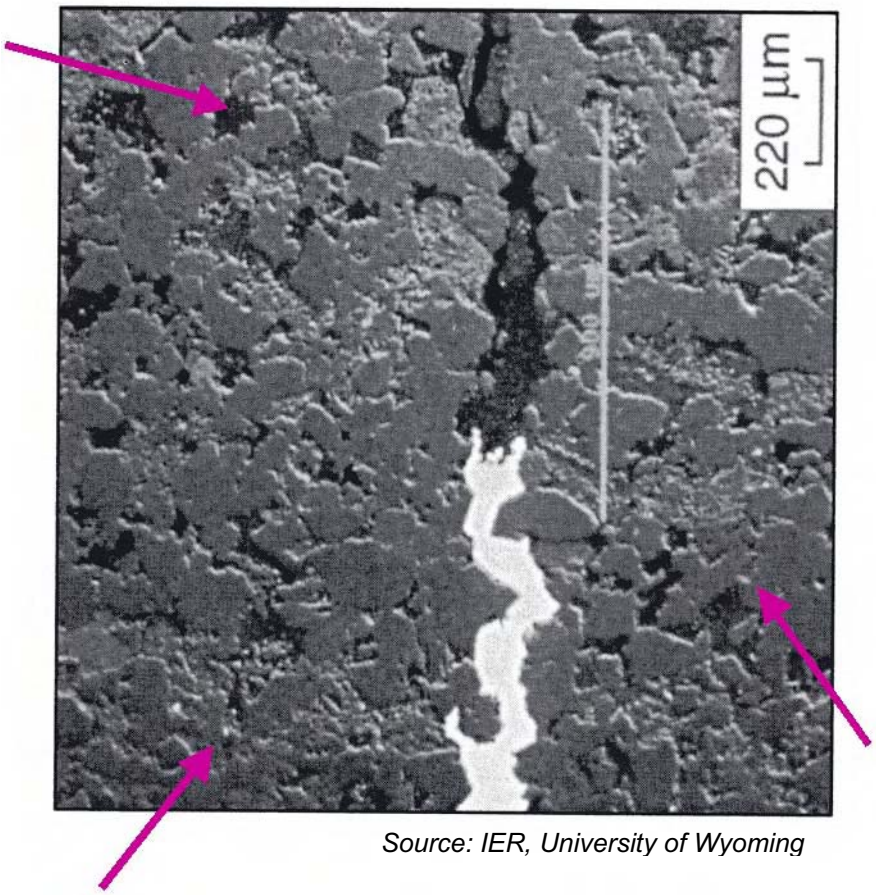

Source: IER, University of Wyoming

Backscatter scanning electronic microscope (SEM) image of an Almond natural fracture (Amoco Production Co., Champlin 254B-2, T20N, R93W). The fracture was originally oriented near vertical. (The horizontal textural change near the bottom is remnant bedding.) The fracture forms as a coalescence of smaller fractures and avoids the major grains for the most part. Other faint planar segments are visible across the image. The bright fracture fill is barite.

Fig. O-7. Almond unloading fracture

3. The Role of Temperature

Temperature cycles associated with burial and uplift of reservoir sediments are major factors responsible for stress generation and release.

Published data show that quartz, a major constituent of sandstone reservoirs, is one of the more thermally sensitive minerals commonly found in clastic rocks. Calcite and orthoclase feldspar are also significantly sensitive to thermal changes. These materials expand and contract with cycles of temperature change during burial and uplift generating large intra-basinal stresses. Unless the basin margins are allowed to expand and contract in concert, temperature-driven volume changes of these materials, within the basin fill, generate large isotropic stresses, apart from and in addition to any lithostatic or tectonic stresses.

Warpinski (1989) noted significant impact of thermally generated stresses and associated strain in his viscoelastic simulations. In his Piceance basin analysis, the strains generated by temperature effects were the same order of magnitude as tectonic strains. This is easier to visualize by first considering the volumetric impact of heating on a single spherical grain of quartz (fig. O-8).

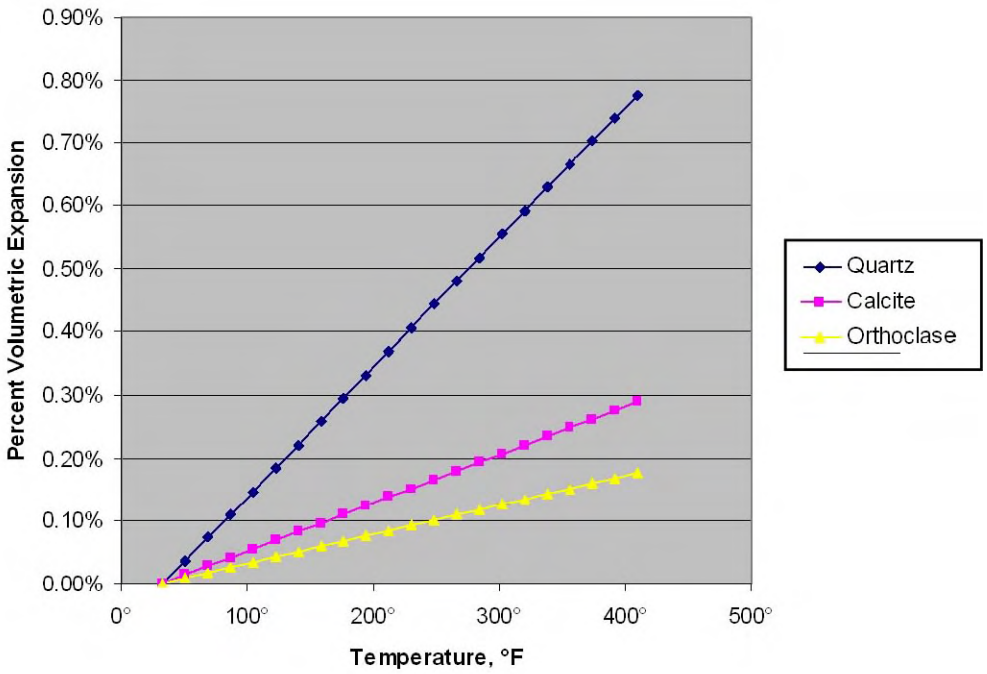

Thermo-elastic stress generated by grain expansion is a major (~40%) component of burial stress. Quartz is significantly more sensitive to temperature than other common constituents of the reservoirs.

Fig. O-8. Thermo-elastic expansion of a spherical quartz grain

The coefficient of thermal expansion (CTE, mm/m-°C) for quartz is well constrained because of its use in the semiconductor industry. It varies between optical axes with the a and b (equal) axes being approximately twice that of the c axis (~8 mm/m-°C). An initial hypothetical sphere of quartz becomes oblate, increasing its volume by nearly 0.8% when heated to 400 degrees Fahrenheit. Calcite, the next most thermally sensitive common reservoir component increases its volume only 0.3 % and orthoclase still less at 0.18 %.

These general relationships hold true when the minerals are included in composite systems (fig. O-9). Granite (with the most quartz as a constituent) has the highest coefficient of thermal expansion. The thermal behaviors of other types of igneous rocks also reflect their mineral compositions. On balance, the more quartz there is in a rock, the higher the coefficient of thermal expansion.

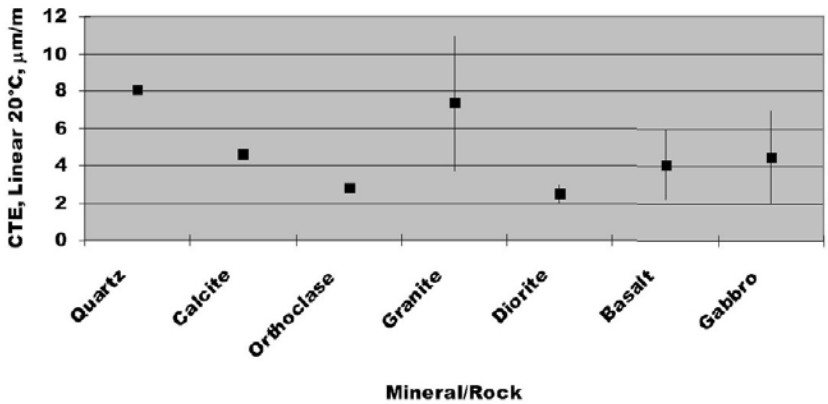

Fig. O-9. Coefficients of thermal expansion of common constituents

Fig. O-10 illustrates a mechanism proposed for microfracture generation by cooling of the matrix. Assuming roughly spherical (0.17 mm radius) quartz grains, packed tightly at 300 degrees Fahrenheit, the grains will shrink anisotropically along the crystallographic axes, proportionally, according to their respective coefficients of thermal expansion.

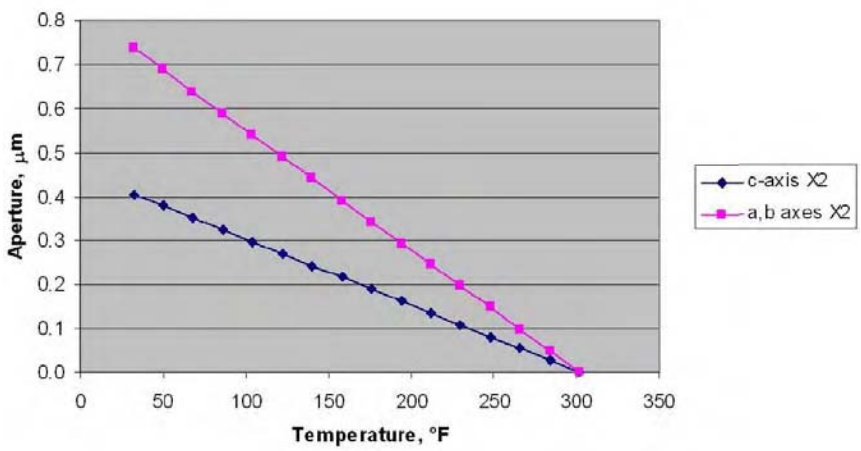

Maximum potential microfracture aperture generated between adjacent quartz grains cooled from 300 F° (.17 mm original radius)

Fig. O-10. Generation of grain bounding microfractures through cooling

If we assume the grains are stationary with respect to each other, a microfracture aperture will open to a width controlled by the relative relationships between the axes of the cooling grains. This is shown diagrammatically in fig. O-11. Ostensen (1983) used mathematical analysis of stress-dependent permeability behavior in tight-gas sand cores to postulate tabular pore geometries with comparable apertures.

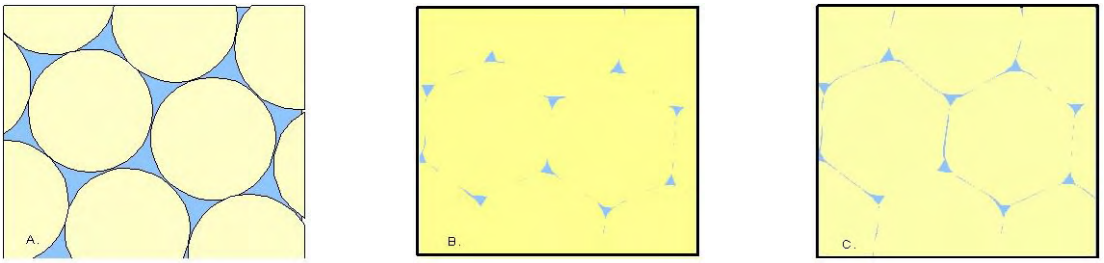

a. Schematically depicts an original closest packing arrangement of the sand grains.

b. Depicts the sand at its maximum burial when most of the original porosity has been destroyed, the grains are in pressure solution contact, and the remaining porosity is isolated.

c. Illustrates a 0.04% decrease in grain radius from cooling during the uplift process. This would be the equivalent of being uplifted from 15,000 to 10,000 feet subsurface. Sediment composed of pure 0.00017 radius quartz grains would generate grain-bounding cracks between 0.2 and 0.4 microns disseminated throughout its matrix.

Fig. O-11. Cycle of thermal expansion generates internal stresses

Thermal expansion of the constituent grains generates internal stresses that contribute to the process. These diagrams (fig. O-11) illustrate this cycle (exaggerated for visibility). The aperture range depends on orientation with respect to the crystallographic axes. These values for microcrack permeability in tight gas sandstones are comparable to those calculated by Ostensen (1983). In an ideal case, if sediment behavior were truly elastic and the grains not interpenetrating or cemented, the composite rock volume would simply shrink as its temperature fell. In actuality, once diagenesis occurred the grains were sutured by pressure solution, and cements. The shrinkage stresses the inter-grain boundaries, thus the weaker sutures will fail first.

A logical inference from matrix shrinkage and progressive development of microfractures during cooling is that matrix permeability will improve as the reservoir cools. If this process proceeds isotropically, there seems to be little reason to expect any permeability anisotropy to develop in the horizontal plane. However, this is not the case.

We recovered eleven cores from the Greater Green River basin (GGRB) that had undergone three-directional permeability measurement tests in the 1980's and 90's. Most cores showed significant permeability anisotropy (two-fold or greater). Notably, core from the Ericson formation exhibited the greatest permeability anisotropy (figs. O-12a and O-12b).

(a)

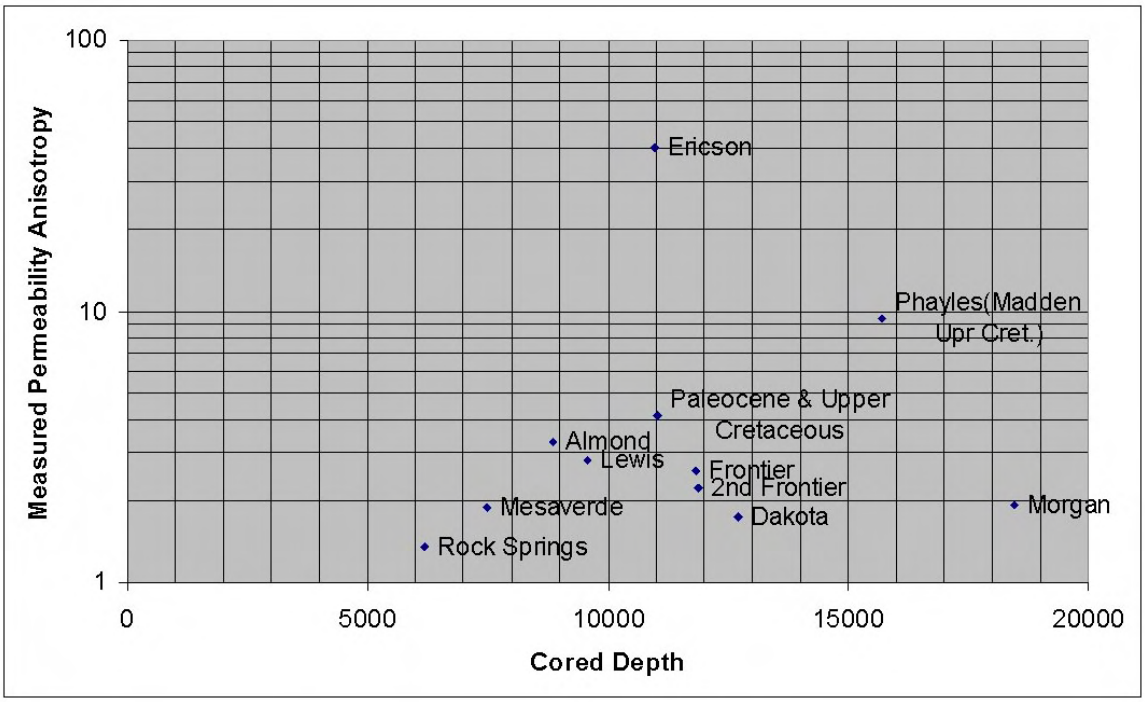

(b)

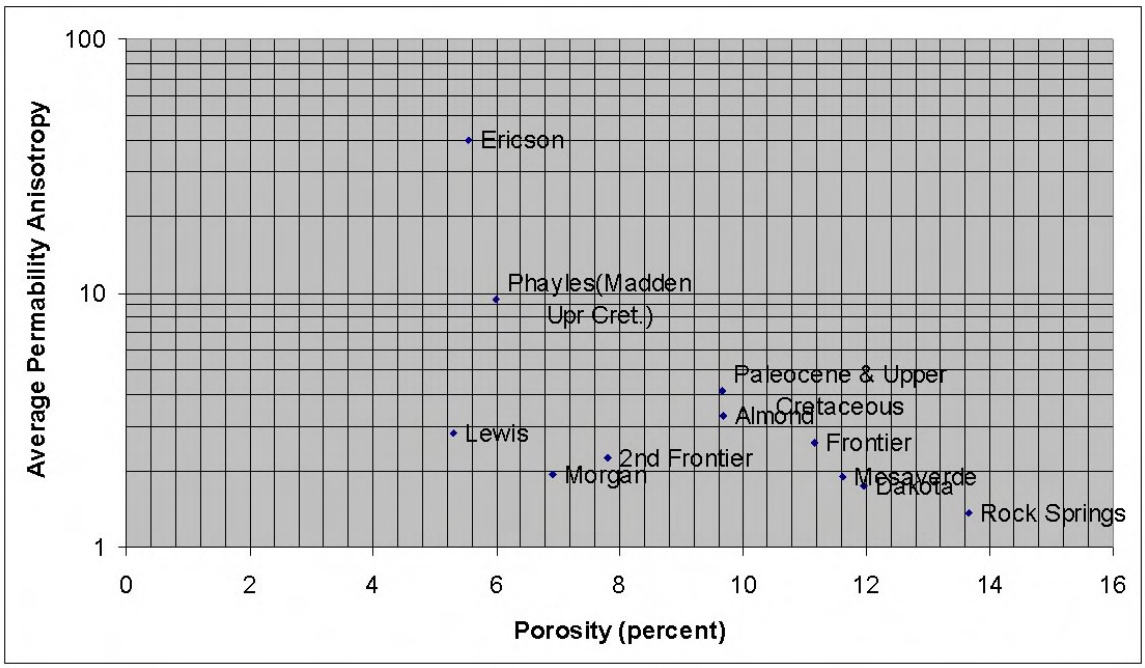

Historical whole core, two direction, porosity and permeability data collected during this project shows that the greatest permeability anisotropy is observed in the Ericson, a quartz-rich member of the Mesaverde group. The Ericson has less porosity than other units, even though the other cores were recovered from greater depth. To the extent it reflects true conditions in the subsurface, this data also suggests a significant amount of permeability anisotropy may be present at the grain scale in the subsurface.

Fig. O-12a & O-12b. Permeability impact of cooling & composition

Traditionally, such anisotropy was attributed to confining stress release associated with the coring process. Re-examination of this data, however, suggests mineral composition (thermoelastic contraction) may have a significant influence on the rock response. If the relative subsurface stress component associated with temperature predicted modeling is correct, then the composite coefficient of thermal expansion (determined by rock mineral composition) becomes a major permeability control.

4. Tectonic Influence

Regional tectonics plays a multi-faceted role in the development of tight gas reservoirs. In addition to profoundly affecting the basin development, subsidence, stratigraphy, and structure, it also can have a diagenetic impact on the sediments. Warpinski (1989) estimated the lateral strains in the multi-well experiment (MWX) area of the Piceance to be approximately the same magnitude as the thermoelastic fraction.

If burial stress crushes grains and promotes pressure solution, basin scale tectonic stresses probably will have a similar impact. Significant differential lateral stress will preferentially compress the sediments. This imparts a weak fabric of planar compressional strain features such as pressure solution boundaries and vertical stylolites. *Generally these planes will be oriented perpendicular to the principal horizontal stress and reach maximum development in areas of the greatest shortening strain.*

Laboratory experiments (1979 Lajtai and Allison) have shown that wet mortar—stressed, allowed to solidify, and released—will fracture perpendicular to the applied principal horizontal stress and even generate some load parallel fracture sets to accommodate the extension. Present day maximum principal horizontal stress is commonly oriented perpendicular to the inferred (from macro structural relationships) paleo principal horizontal stress.

Fig. O-13 diagrammatically illustrates a potential tectonic relaxation fabric with secondary porosity generation. Planar features with secondary porosity development, as illustrated by Webb, et al (2004), are relatively common in Rocky Mountain tight gas sands areas. Fluids under-saturated in calcite, moving through such a pore system, could very likely be responsible for leaching cements or unstable components.

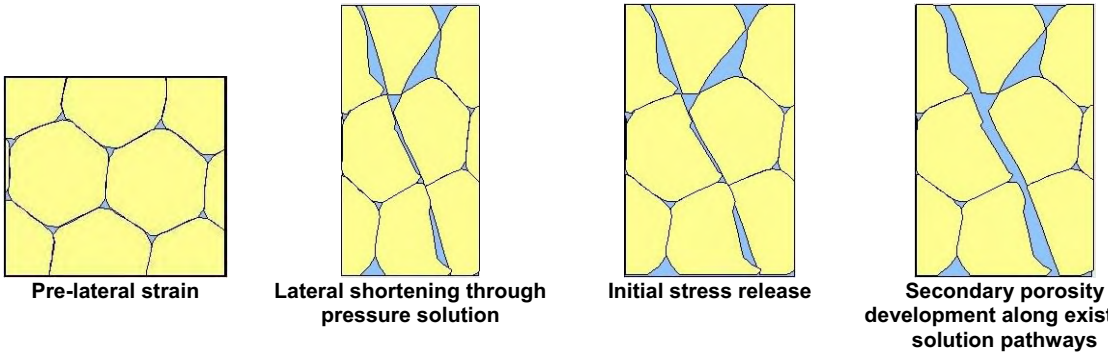

These diagrams schematically illustrate the potential for development of pressure solution surfaces along grain-to-grain contacts that may then relax and dilate after active compression and/or uplift. Circulation of undersaturated fluids along these pathways has great potential to foster development of secondary porosity on uplift.

Fig. O-13. Strain and pressure solution

5. Uplift Model Validation

ARI validated this uplift model for permeability development using two data sets acquired by independent groups, published fifteen years apart. Keighin, Law and Pollastro (1989) published the results of an extensive petrology and reservoir property study on the Almond formation of the GGRB. The study contained detailed petrography, core analysis, and vitrinite reflectance (Vr) results, from twenty-five Almond cores.

Roberts, Lean and Finn (2004) published a detailed assessment of oil and gas generation timing covering the USGS general southwestern Wyoming assessment area. These two data sets were interpreted and integrated to show uplift as a significant influence on permeability.

Keighin, Law and Pollastro (1989) collected petrographic, petrologic, core analysis, and maturity data on Almond cores from across southern Wyoming during resource assessment activities. They studied twenty-five cores, collecting analysis data (phi, k) for twenty-three cores (Table O-2).

Twenty-two cores contained usable, paired core analysis and maturity data values. Four of the twenty-two used had projected percent vitrinite reflectance in oil (Ro) values.% These findings underscore a recognizable but poorly understood relationship between core analysis properties and organic maturity as indicated by Vr.

Table O-2. Porosity, permeability, & Vr data from cores in Almond Fm, SW Wyoming

Well No.	Well Name	Location	Core Interval (ft)	Porosity (range & average %)	Permeability (range & average md)	Ro %	Norm_k	Proj Max Burial Depth	Amt of Uplift
1	Colo Interst Gas 2-8-14-92 Blue Gap 11	SW ¼ SW ¼ Sec 8 T. 14 N, R. 92 W	9,059 – 9,091	1.7 – 10.0 (5.0)	0.01– 5.9 (0.75)	0.80	0.15	11,598	2,523
2	Pan Am Barrel Springs 3	NE ¼ NE ¼ Sec 11 T 16 N, R 93 W	8,407 – 8,441	7.4 – 16.1 (12.0)	0.01– 0.30 (0.07)	0.70	0.0058	10.838	2,418
3	Amoco 1 Champlin 535 Amoco A	C SW ¼ Sec 17 T 16 N, R 97 W	13,645 – 13,674	2.4 – 11.5 (8.0)	0.02– 1.7 (0.34)	1.64	0.0425	14,951	1,301
4	Amoco Champlin 336 Amoco A-1	NEI ¼ SW ¼ Sec 21 T 17 N, R 94 W	10,626 – 10,649	2.6 – 12.0 (5.9)	0.01– 0.65 (0.08)	1.12 P	0.0135	13,405	2,770
5	Champlin Higgins 13A	NW ¼ NE ¼ Sec 7 T 17 N, R 98 W	6,992 – 7,013	8.2 – 17.1 (13.8)	0.02– 1.9 (0.48)	0.59	0.0347	9,873	2,873
6	Amoco 1 Champlin 440 Amoco A	NW ¼ NW ¼ Sec 11 T 17 N, R 98 W	8,590 – 8,638	1.5 – 6.2 (3.9)	<0.01– 4.9 (0.35)	0.84	0.8974	11,873	3,253
7	Amoco 1 Champlin 534	C SW ¼ Sec 31 T 18 N, R 96 W	10,969 – 10,990	3.9 – 11.0 (7.8)	0.02– 0.1 (0.07)	0.76	0.0089	11,307	327
8	Champlin Federal 44-4	SE ¼ SE ¼ Sec 4 T 18 N, R 98 W	6,841 – 6,897	2.3 – 19.2 (12.4)	0.03– 24.0 (2.40)	0.75	0.1935	11,232	4,372
9	Champlin UPRR 44-9-2	SE ¼ SE ¼ Sec 9 T 18 N, R 98 W	6,780 – 6,836	10.5 – 17.5 (14.6)	0.24– 6.06 (1.83)	0.71	0.1253	10,919	4,119
10	Texaco Table Rock 68	NE ¼ SW ¼ Sec 19 T 19 N, R 97 W	6,577 – 6,731	0.8 – 17.7 (8.1)	<0.01– 2.39 (0.33)	0.73	0.4074	11,078	4,438
11	Marathon 1-23 Tierney II	C SW ¼ Sec 23 T 19 N, R 94 W	N.A.	N.A.	N.A.	N.A.	N.A.	N.A.	N.A.
12	Forest 9-G-1	SW ¼ NE ¼ Sec 9 T 19 N, R 98 W	5,754 – 5,770	14.0 – 21.4 (17.7)	0.23– 41.0 (12.02)	0.62	0.6790	10,151	4,391
13	Forest 3-19-2 Arch	SW ¼ SW ¼ Sec 19 T 19 N, R 98 W	N.A	N.A.	N.A.	N.A.	N.A.	N.A.	N.A.
14	Forest 1-8 Arch 70	SE ¼ NE ¼ Sec 1 T 19 N, R 99 W	4,794 – 4,812	11.5 – 23.9 (19.8)	3.1– 102.0 (23.57)	0.68 P	1.1904	10,673	5,873
15	Forest 63-2-2 Arch	SE ¼ SE ¼ Sec 2 T 19 N, R 99 W	4,485 – 4,527	14.9 – 23.2 (19.5)	1.5– 88.0 (31.0)	0.67	1.5897	10,589	6.089
16	Forest 20-23-4 Arch	SW ¼ NE ¼ Sec 21 T 19 N, R 99 W	4,497 – 4,528	18.8 – 25.6 (22.1)	0.21– 135.0 (43.96)	0.57 P	1.9891	9,682	5,172
17	Amoco Champlin 441 Amoco A	C SE ¼ Sec 21 T 20 N, R 95 W	9,142 – 9,178	0.9 – 5.7 (3.5)	0.01– 0.09 (0.03)	0.80	0.0085	11,598	2,438
18	Forest Mustang 1-22-1	NE ¼ SE ¼ Sec 22 T 20 N, R 97 W	7,452 – 7,513	12.3 – 18.9 (16.1)	<0.01– 0.9 (0.4)	0.60	0.0248	9,967	2,477
19	Luff 1-23 Champlin-Playa	SE ¼ SE ¼ Sec 23 T 20 N, R 99 W	4,577 – 4,600	7.6 – 16.7 (13.0)	0.08– 13.0 (2.94)	0.60	0.2261	9,967	5,377
20	Luff 4-29 Champlin	NW ¼ SE ¼ Sec 29 T 20 N, R 99 W	3,474 – 3,481	14.7 – 19.6 (17.3)	0.43– 18.0 (7.9)	0.47 P	0.4566	8,648	5,170
21	Amoco Champlin 527 Amoco A-1	C SW ¼ Sec 19 T 21 N, R 95 W	8,971 – 9,061	2.3 – 15.2 (10.7)	0.01– 0.93 (0.20)	0.65	0.0186	10,417	1,402
22	Amoco 1 Champlin 446 Amoco A	NE ¼ SW ¼ Sec 15 T 22 N, R 90 W	14,256 – 14,271	1.0 – 8.1 (4.5)	0.01– 0.14 (0.07)	1.34	0.0155	14,219	-45
23	Amoco 438 Amoco A	C SE ¼ Sec 5 T 22 N, R 96 W	9,910 – 9,931	3.6 – 7.9 (5.1)	0.08– 0.22 (0.11)	0.82	0.0215	11,738	1,818
24	Mich-Wisc Red Dessert 1-33	NW ¼ SE ¼ Sec 33 T 24 N, R 94 W	12,515 – 12,586	3.4 – 9.1 (6.5)	<0.01 (<0.01)	1.64 P	N.A.	N.A.	N.A.
25	Energy Reserves 2-24 Nickey	NW ¼ SE ¼ Sec 24 T 24 N, R 96 W	11,884 – 11,916	1.8 – 7.6 (5.3)	<0.01– 1.8 (0.18)	1.60	0.0339	14,872	2,972

P = projected vitrinite reflectance
N.A. = Not available

Roberts, Lean and Finn (2004) interpreted the timing of petroleum generation in southwestern Wyoming as part of an overall petroleum system assessment. Burial histories and seven synthetic Vr curves were constructed and calibrated to recorded Vr values. A burial history curve defined the relationship between depth of burial (used to calculate temperature), time (related to stratigraphy), and Vr.

Vitrinite reflectance acted as a proxy for depth in areas where the relationship was calibrated. Because Vr continuously increased with maturity (depth), it reflected the maximum depth of burial. The Adobe Town (south central Washakie Basin) calibration was used as the standard Vr-depth relationship for purposes of our project.

We calculated a maximum depth of burial for each of the Keighin study Vr samples. This was done by digitizing the continuous (estimated) Vr curve published by Roberts, Lean and Finn (2004) to generate a fourth-degree polynomial fit. The resulting equation was used to calculate a maximum depth of burial for the core Vr values.

Fig. O-14 shows the original calculated Vr curve (Roberts, Lean and Finn 2004), the original calibration points (squares), and the calculated depths of burial for the Almond Vr samples (triangles). We adjusted the final maximum burial-depth value calculations by a linear shift of 3,200 feet to account for recent uplift and erosion in the Adobe Town area (Roberts, Lean and Finn 2004).

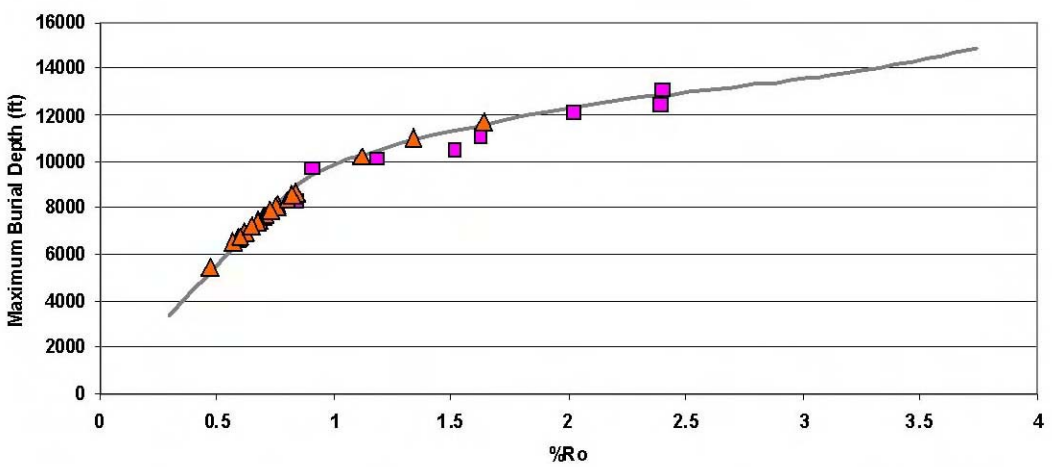

This graph illustrates the excellent fit between the

- Adobe Town easy %Ro model—*grey line*—(Roberts, et al)
- Original burial history calibration points—*squares*—(Roberts et al)
- Back projected maximum burial depths for the I petrographic/Vr data set—*triangles*—(Keighin, et al)

Fig. O-14. Vr (% Ro) maximum burial depth calibration

An estimated amount of uplift was calculated for each core location by subtracting the core depth from the estimated maximum burial depth. The Adobe Town area is very near the deepest portion of the present-day eastern GGRB. The resulting amounts of uplift were positive with only one exception, which calculated at fifty feet (for all practical purposes, 0). Thus, the different vintages of Vr data are comparable; the burial history calculations and synthetic Vr profiles are reasonable; and the overall scheme used here to estimate the amount of uplift is ascertained valid.

Permeability (k) was normalized to porosity (phi) in order to correlate the reported permeability values (of Keighin) between cores. We recorded the data as mean values of each attribute for each core. Mean permeability was divided by mean porosity to obtain a normalized permeability value for each core in terms of millidarcies (md) per porosity unit. Keighin noted increasing degrees of scatter in the cores of lower porosity. This is most likely due to the permeability anisotropy observed in whole core analyses (as previously discussed).

A cross-plot of estimated uplift versus normalized permeability is shown in fig. O-15. The x-axis is the estimated uplift in feet vs. the normalized k on the y-axis in millidarcies/porosity unit (md/pu). The data show a strong positive correlation between increasing uplift, as projected from Vr differences, and normalized permeability from the core studies.

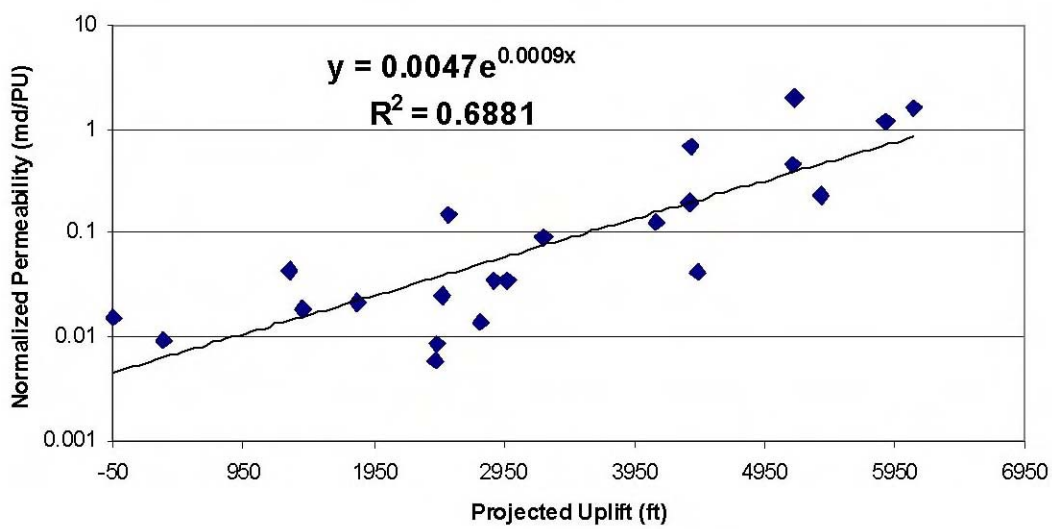

Fig. O-15. Projected uplift vs. normalized permeability

There is some scatter to the relationship but the variance remains similar in magnitude across the range of uplift values. This scatter is due in part to the permeability anisotropy observed in whole core analyses noted previously. It may also reflect differences in structural setting at the individual wellsites.

This analysis confirms a relationship between core analysis results and Vr first observed by Keighin, Law and Pollastro (1989). However, the relationship is indirect and thus is defined by both maximum depth of burial *and* amount of later uplift. Rocks buried at shallow depths retain more of their original textures and gain little permeability upon uplift.

Sediments within areas of above average confining stresses (depending on their mineralogy) will exhibit either above average matrix permeability or more extensive opening mode fracturing and perhaps both. The Griffith energy concept as applied by Engelder and Fisher (1996) predicts the outcome. The practical experiment with cement by Lajtai and Allison (1979) demonstrates it in the laboratory.

Thus, when a tectonic load is applied laterally the rocks should behave similarly as when they are buried and uplifted. This conclusion is supported by the concentration of opening mode fracturing in the paleo compressional areas observed at the RCP site during this project.

5. Prospect Generation

The general process of prospect generation via geomechanical modeling is illustrated in fig. O-16. Regional geology, core or borehole imagery studies and depth-converted fault planes derived from seismic are the major inputs of the modeling process. Once built and executed, the model outputs were matched to observed fracture types and their role in the reservoir to establish an interpretive framework.

Prospects are generated using the standard components of structure and stratigraphy together with the added permeability information derived from the geomechanical modeling. The prospect generation model is calibrated and controlled by matching the prospect generation model output with existing production (where available) in an iterative process.

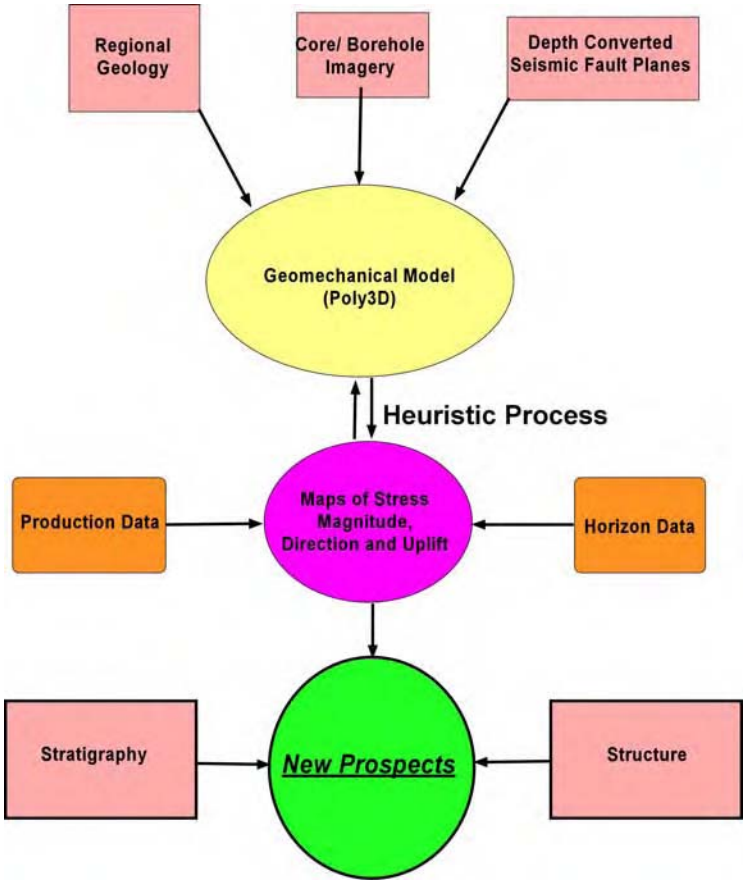

Fig. O-16. Prospect generation via geomechanical modeling

E. Resources

Work performed during this project conformed to generally accepted principles of petroleum geology and geochemistry. No laboratories were used as part of this study. All seismic data for the Anadarko project was purged from ARI facilities and the original media returned to Burlington Resources, in accordance with the project agreement. The majority of the project work was performed at ARI offices in Denver, CO.

The following specific trademarked commercial software packages were used during the interpretive or documentation phases of this project:

Ant Tracker algorithm of Schlumberger's Petrel™ workstation software.

ArcCatalog™, ArcMap™, ArcPublisher™, Spatial Analyst™ (ESRI, Inc)

Canvas 8™ and Canvas 9™ (ACD Systems, Inc)

Comet 3™ (Advanced Resources International, Inc.)

Microsoft Office Suite (Microsoft Corporation)

Petra, Petraseis™ (Geoplus Inc.)

Surfer 8™, Grapher 5™ (Golden Software, Inc.)

Veritas Inc. supplied time-depth relation for the RCP seismic

The following non-commercial research software programs were used:

NextGen™ (ARI, Inc)

Poly3D (A. L. Thomas, Stanford University 1993)

FracGen™ (discrete fracture network modeling, NETL)

RESULTS AND DISCUSSION

I. Study Area #1: Waltman/Cave Gulch

A. Overview

The WRB is one of the largest and least explored deep gas-prone basins in the Rocky Mountains. The United States Geological Survey (USGS) estimates the basin holds 995 trillion cubic feet (tcf) of gas in place in a series of Cretaceous-age, low permeability basin-centered formations. These formations are targeted by the DOE/NETL for technology-based development of new natural gas supplies.

The Frontier Formation (Fm), the target of this field demonstration of natural fracture exploration technology, is estimated to contain 150-tcf gas in place, with 111-tcf in deep, tight and over-pressured sands below 15,000 feet. Finding areas of natural fracture enhanced permeability in this deep, gas charged, basin-centered formation was considered the key technology for effective extraction of the gas in place.

B. Purpose

The primary purpose of the Waltman/Cave Gulch field project was to test and demonstrate the use of geomechanical technology (using boundary element modeling) to identify areas with intense clusters of natural fractures. The geomechanical model uses fault geometries derived from seismic to calculate the local stresses around these seismically mappable faults and from this the associated volumes of fractured sediments. Such fractured sediments are colloquially known as “sweet spots” in otherwise low permeability reservoir settings.

Developing improved technologies for predicting the location and extent of these “sweet spots” before drilling has long been one of the highest technology priorities of the industry and the DOE/NETL’s natural gas program for low permeability reservoirs.

C. Site Selection

The Waltman/Cave Gulch area (fig. I-1) was chosen as a demonstration site for the multi-site project for several important reasons:

1. The area is underlain by the deep Frontier Fm, a major natural gas resource target for industry and the DOE/NETL’s low-permeability R&D program.
2. The reservoir sands in this area are tight, requiring the presence of extensive natural fractures to support economic rates of gas flow.
3. Prior well drilling and 3D seismic had confirmed the presence of a significant fault system and natural fractures in the field area.

4. The gas play was being pursued by an operator looking to significantly improve the placement and performance of the new Frontier Fm exploration wells on the Bullfrog unit of the Waltman/Cave Gulch field.

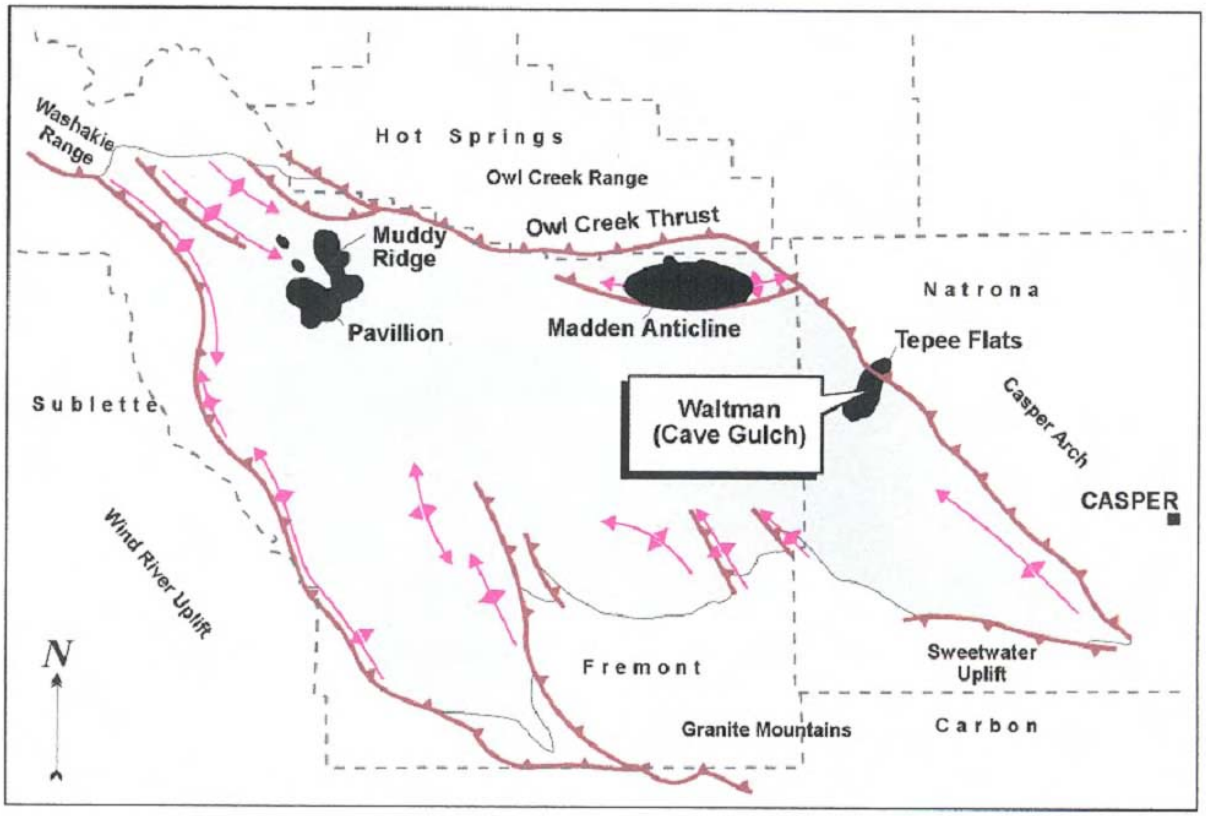

Fig. I-1. Barrett Resources test site – Wind River basin

Evidence of fractured reservoir behavior and interest in the demonstration and implementation of new exploration technology supported the applicability of the geomechanical approach to natural fracture prediction in the Waltman/Cave Gulch area.

The goal of this field-based research effort was to identify, using geomechanical technology, areas with fracture enhanced permeability in the Bullfrog Unit (Frontier Fm) of the Waltman/Cave Gulch field. It was assumed that technologies developed and applied at this site would be applicable to other areas in the WRB and with potential for other low-permeability natural gas basins in the Rocky Mountains.

In the eastern WRB, at the Bullfrog, Cave Gulch, and Teepee Flats units of the Waltman field, the Frontier Fm, is at 18,000 feet subsurface and highly overpressured. As such, it presents a challenging and costly target for well drilling, formation testing and reservoir characterization. Prospects require significant volumes of reserves per well to support commercial development.

A series of exploration wells were drilled into the Frontier Fm at Waltman field, in the early- and mid-1990s with the generally disappointing results:

- The initial exploration results were promising as three of the wells tested high gas rates and produced at 8 to 11-MMcfd; one well, the Federal #1-27 was dry.
- However, the gas production decline rates of the wells were steep, limiting ultimate gas recoveries. One of the wells (Bullfrog #2-7) watered out, limiting gas recovery to 2.8-bcf. The other two wells, Tepee Flats #16-1 and #18-1, have ultimate gas recoveries of 3.7-bcf and 6.4-bcf respectively.
- The wells in this deep tight formation were generally completed with small hydraulic fractures or without any stimulation, relying on the presence of natural fractures to provide enhanced permeability and connection with the reservoir.

The deep Frontier natural gas play remained dormant until 1997, when Barrett Resources drilled and completed the Cave Gulch #16 on the crest of the Cave Gulch anticline. The initial production from this well, at nearly 13-MMcfd, was encouraging and led to the drilling of a series of additional deep gas wells on the Cave Gulch and Bullfrog unit anticlines. However, some of the additional wells began producing high rates of water, contrary to normal expectations for a basin-centered formation, severely impacting gas flows and economics.

As discussed next, the difficulty in locating naturally fractured areas that did not also produce high volumes of water led to the suspension of this deep gas play. An improved understanding of the reservoir conditions and settings that would support economically productive wells in the deep Frontier was required for this gas play to be revitalized.

Discovery and Development History

The deep Frontier natural gas play in the Wind River basin was discovered and tested in 1981 by the Tepee Flats #16-1 well in S.16, 37N 86W. The well was drilled to 18,568 feet total depth (TD) and completed unstimulated in the First Frontier sand. The well tested at 11-MMcfd with a trace of water. Gas production peaked at 8.4 millions of cubic feet per day (MMcfd) with 22 (barrels of water per day (bwpd) at the end of 1981. The well has produced 3.7 billion cubic feet (bcf) of gas and 26 thousand barrels of water before being recompleted in the Muddy Fm in mid-1999.

Delineation Wells

Three subsequent wells were drilled and completed in 1982 and 1984 to further delineate this deep gas play, the Bullfrog #2-7, the Federal #1-27 and the Tepee Flats #18-1.

The Bullfrog #2-7 well was drilled to 20,830 feet (TD) in S.7, 36N 86W, tested the First through Fifth Frontier Fms and was completed unstimulated in the First Frontier. It had an IP of 6.5-MMcfd with 430-bwpd. Gas production peaked at 8.2-MMcfd in late 1984. The well recovered 2.8-bcf of gas and nearly 64 thousand barrels of water before being recompleted in the Fort Union Fm in 1993.

The Tepee Flats #18-1 well was drilled to 22,403 feet (TD) to test the Madison and Lakota in S.18, 37N 68W. The well was plugged back to the First Frontier Fm and perforated from 18,054 and 18,070 feet. The operator completed the well with a small water and sand frac. The well tested at 4.1 MMcfd and 25-bwpd in the First Frontier. Gas production peaked at 7.9 MMcfd in early 1992 (after a lengthy period of being shut-in). The well recovered 6.3-bcf of gas and 49,000 barrels of water before being shut-in in late 1999 and plugged and abandoned (P&A) in 2002.

The Federal #1-27 well was drilled to 21,382 feet (TD) in S.27, 37N 86W in 1982. It was completed unstimulated in the First and Third Frontier sands. The well flowed at 85-bwpd with a small gas flare in the Third Frontier, had no gas flow in the First Frontier and tested tight in the Fourth Frontier. The well was P&A'd..

Recent Wells

After more than a decade without further development, Barrett Resources drilled the Cave Gulch #16 in 1997 in an attempt to revitalize the dormant deep Frontier Fm gas play. The well was drilled to 19,106 feet in S.32, 37N 86W on the crest of the Cave Gulch anticline. The well was completed with a small frac (that screened out) in the First and Third Frontier sands. It tested at 10. 2-MMcfd and 334-bwpd in the Third Frontier.

Gas production peaked at 12.7-MMcfd in mid-1999 with 264-bwpd. The well has produced 4.6-bcf of gas and 101 thousand barrels of water through the end of 2002. The gas rate at year-end 2002 was about 190 MMcfd. (Additional detail on the Cave Gulch #16 well is provided in Appendix 1.5).

Next was the Deep Cave Gulch #3-29 well in S. 29, 37N, 86W. The well was drilled to 21,964 TD and produced 9.7-bcf from the Muddy and 0.2-bcf from the Lakota before being recompleted in the Frontier at the end of 2000. The Frontier horizon was completed with a 175,000 lb sand and 3,400 barrel "thermagel" frac at 18,095 to 18,102 feet. Two zones, the First Frontier at 17,894 to 17,940 feet and the Third Frontier at 18,018 to 18,148 feet were placed on production. Gas production peaked at 9.3-MMcfd with 72-bwpd in late 1991. Since early 2001, the well has produced 2.6-bcf of gas and 33 thousand barrels of water.

D. Regional Geologic and Tectonic Setting

The Waltman/Cave Gulch field demonstration site is located on the northeast flank of the WRB where the Waltman Arch is over-ridden to the southwest by the South Owl Creek thrust. The Bullfrog, Cave Gulch and Waltman units of the Waltman field were developed on a series of wrench and thrust related structures downthrown to the South Owl Creek fault. Accumulations in the area range in origin and trapping mechanism from shallow stratigraphic traps in the Fort Union Fm to deeper combination stratigraphic/structural plays in the Paleozoic through Cretaceous units (Madison, Tensleep, Morrison, Sundance, Lakota, Muddy, Frontier, Mesaverde, Meeteetse and Lance).

The area is one of the few, if not only, successful sub-thrust, overhang plays to have been discovered and developed in the Rockies in the last decade. The strategy for complex and costly deep gas play in fields is to drill wells with multiple objectives, capable of providing reserves of 10 to 20-bcf.

The focus of this project is the Frontier Fm in the Bullfrog/Cave Gulch Unit, one of the multiple, deep reservoir objectives. The area has been presented to the Wyoming Oil and Gas Conservation Commission (WOGCC) by the operators as a relatively simple conventional structure (fig. I-2).

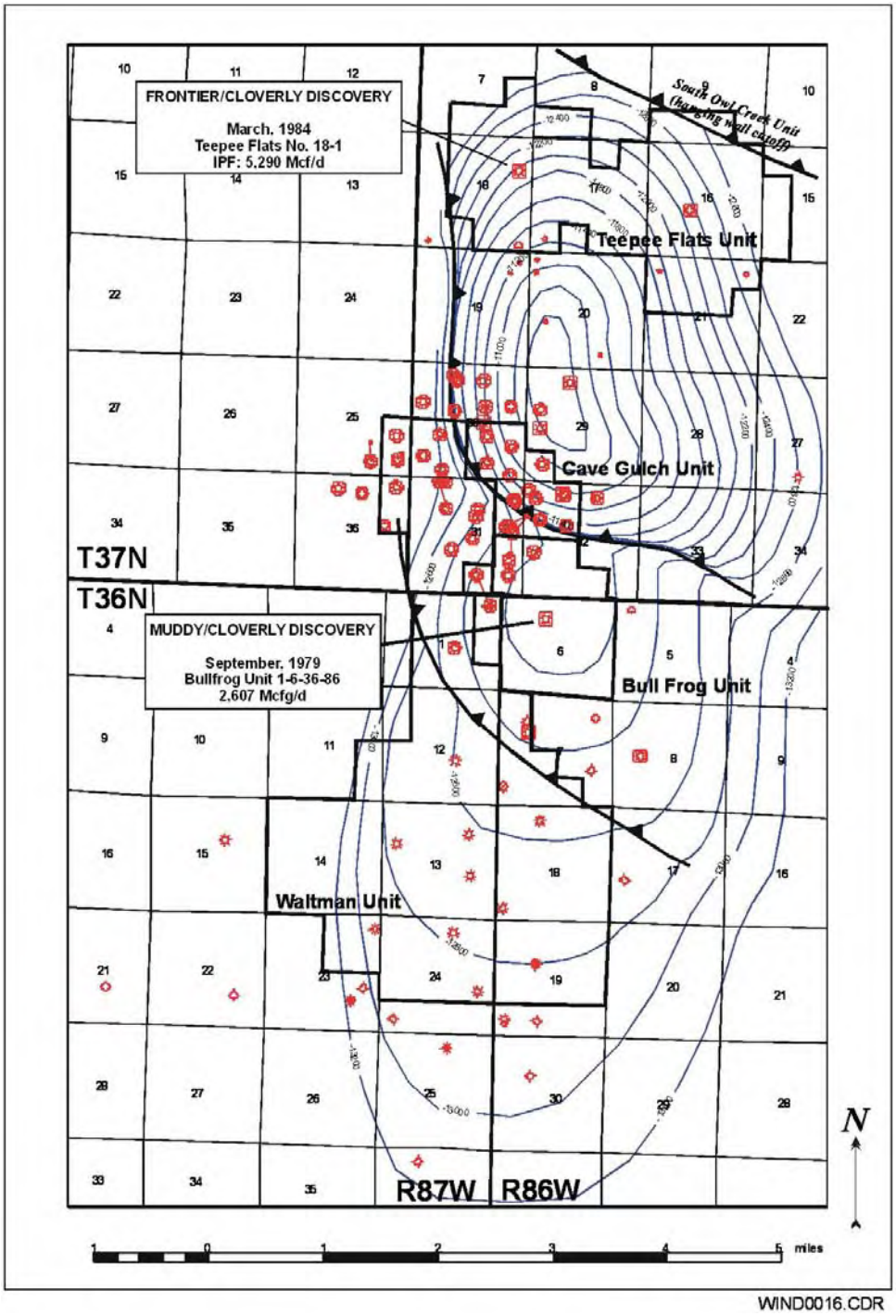

Fig. I-2. Structure Map, top of Frontier Fm, Wind River basin

Development of this large and potentially significant deep discovery is complicated by the unconventional behavior of its primary reservoir units. Barrett Resources reported in hearings before the WOGCC that, through August 1998, only two zones in two wells appear commercially viable.

Frontier Stratigraphy

The Frontier Fm in Wyoming is depicted on maps and cross sections as a widespread clastic depositional system of Upper Cretaceous age that overlies the Mowry shale and underlies the Carlisle shale (fig. I-3). The heart of the depo-system lies in west central Wyoming as judged from the sandstone isolith map. The limits of the system lie in southeastern Wyoming. There is a northwest-southeast elongation to the sandstone trends. This may reflect distributary systems controlled by an underlying structural grain.

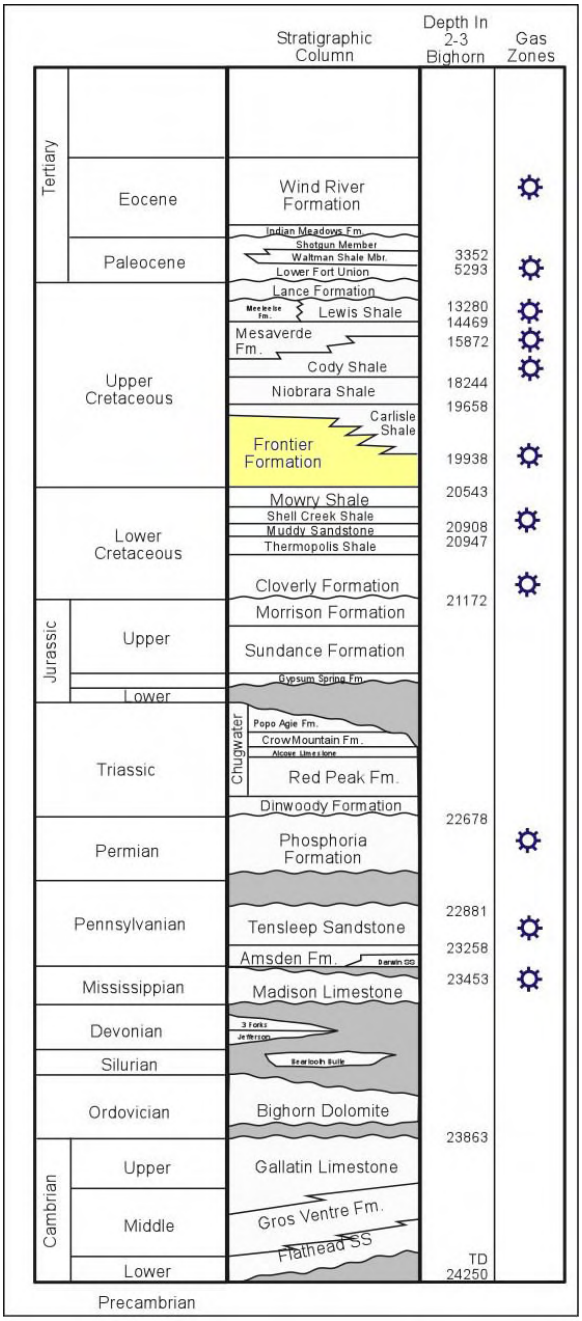

Fig. I-3. Generalized stratigraphic column, Rocky Mtn. area

Although the available isolith map (fig. I-4) represents composite sand content, there is a suggestion that stillstands during episodic regression and transgression were oriented in a northeast-southwest trend in southeast Wyoming and northwest-southeast in northeastern Wyoming. This may reflect an emerging structural grain. Overall, the formation appears more regressive at the base and retrograde near the top.

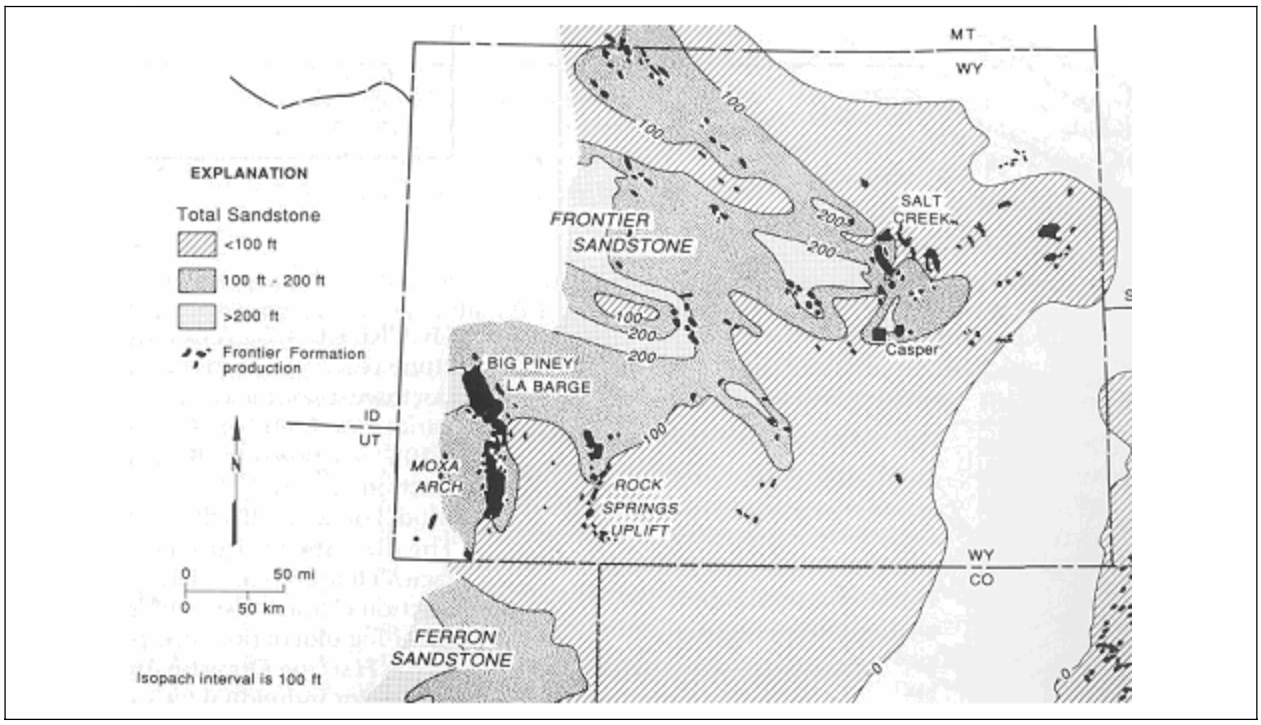

Eastern Wind River Basin Field Area, Cave Gulch Field. Adapted from Barlow and Haun file map, Atlas of Major Rocky Mountain Gas Reservoirs, NM Bureau of Mines, 1993

Fig. I-4. Isolith map of total Frontier Sandstone in central Rocky Mtn. area

The Frontier Fm is composed internally of several coarsening upward sequences of shale and sand. Marine influence is greatest near the bottom of each cycle and builds through delta front or shoreline sands. The marine sand cycles may be capped or removed by non-marine distributary channel facies.

Conventional nomenclature has the first sand in the Frontier as the top and the sands named in subsequent order of penetration, i.e., 1st Frontier, 2nd Frontier, 3rd Frontier etc. In very old scout tickets, one sometimes sees the individual sand within a given cycle named as benches thus the second sand in the 3rd Frontier becomes "2nd bench, 3rd Frontier" etc. Barrett Resources generally targets five Frontier sand cycles in the Cave Gulch area although there are more individual sands present (see stratigraphic cross-section). The marine sand facies in the Frontier appear bar-like in nature, are probably better quality reservoirs, and have continuity for a few miles based on field well control (see section on Structure). The continuity of the non-marine channels (bell shaped log signatures) is less predictable.

The Cave Gulch Deep area has several Frontier cycles present with about 150 net feet of sand. The major local sand accumulation probably lies to the east. Examination of log data presented to the WOGCC indicates the most robust Frontier sands are the first, third, fourth, and fifth. The third is the main pay in the CG#16 well as shown on the Frontier type log.

The base of each Frontier cycle in the CG#16 well is a "clean," low silt marine shale. Thus, the stratigraphic cycle juxtaposes the most ductile shale against the most brittle sand. The sand shale ratio in this unit is also near ideal for theoretical sealing of faults and reservoir compartmentalization. No small faults are indicated on any of the available maps yet they are potentially present.

Sufficient Frontier sand is available in the Cave Gulch area to support numerous prospects. The stratigraphic setting is sufficiently stable that a step-out of a few miles should still have Frontier sand present in at least some of the benches. Porosity and permeability, as discussed later, are the key risk factors.

Structural Setting

The WRB is a rhombic-shaped, physiographic basin located in central Wyoming. The Tertiary Wind River Fm is at the surface for most of the geomorphic basin area. The western margin of the basin is formed by the eastern limit of the Wind River Mountains. The southern margin of the basin is defined by the outcrop of several northwest trending (imbricate) reverse faults whose hanging walls form a series of plunging noses.

The northeast and northern boundary of the basin is formed by the South Owl Creek thrust and the Owl Creek thrust with the east-west trending Madden Anticline as the dominant feature on the north side. McKutcheon (2001) cites studies detailing the sinistral oblique strike-slip nature of the Owl Creek thrust. The eastern limit of the basin is the Casper Arch. The basin is asymmetric to the north and east where the greatest thickness of sedimentary section (25,000'+) is preserved, immediately downthrown to the major basin bounding thrusts.

The Waltman Arch (Barrett, informal name) is a cross-basin structure traceable to a surface outcrop in T33N, R88W. The structure to which Barrett relates the Waltman Arch contains a reverse fault (Roux 2002) that likely juxtaposes Archean against Cody. Such a motion would suggest several thousand feet of lateral shortening which would require a similar amount of shear displacement.

The fault's position on the north flank of the thrust suggests the shear should be dextral in nature. Mapping upthrown to the Owl Creek is complicated by the fact that the Cody is the dominant formation at surface. The fault timing is inferred as first the Waltman thrust, then the Owl Creek/Casper thrust. The Bullfrog-Cave Gulch structure is a hanging wall ramp/shear with respect to the Waltman thrust/shear trend and a footwall imbricate zone to the Owl Creek/Casper thrust.

If substantiated by exploration work, the cross-basin shears analogous to the Waltman feature will provide the means to generate deep basin structures to the north and west of the study area. This could provide a natural fracture and enhanced permeability generation mechanism to facilitate the extraction of the gas resources in this deep portion of the basin.

Reservoir Properties

In the deep portion of the Wind River basin, the Frontier is a 600 to 1,050 foot thick sequence of interbedded shale, siltstone and sandstone overlying the rich source rocks in the Mowry shale. The formation is gas bearing and highly overpressured (pressure gradient of .70 to .77-pounds per square inch (psi) in all deep wells drilled to date, suggesting that a widespread basin-center gas accumulation may exist in this area. The Frontier contains from 4 to 6 stacked sandstone intervals having an aggregate thickness of 100 to 300 feet, (fig. I-5.) In the deep portion of the basin, the sandstones generally have less than 8% porosity and have extremely low permeability.

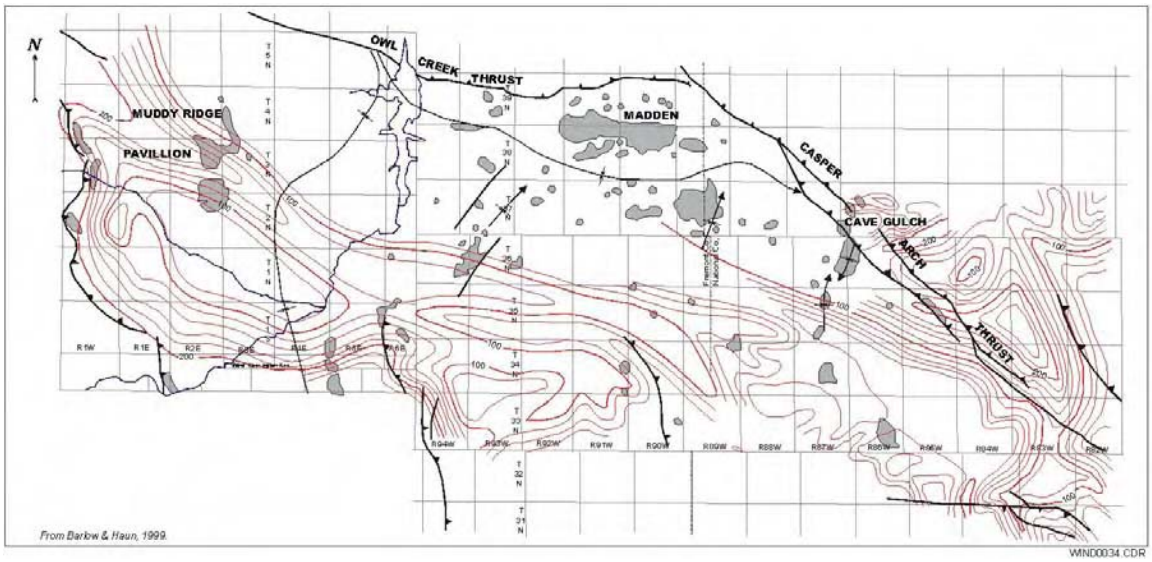

Fig. I-5. Gross Sandstone Isopach, Frontier Fm, Wind River basin

At Waltman/Cave Gulch, the productive Frontier sandstones are continuous across the accumulation, can be as much as 125 feet thick, have 8% porosity, and have extremely low matrix permeability. The existence of good quality reservoirs in deep basin settings have been explained by diagenetic processes favoring reservoir preservation and/or enhancements The Muddy sandstone discovery at Waltman/Cave Gulch demonstrates the potential for high quality production from the deep basin setting (Tables I-1 and I-2).

Table. I-1 Reservoir characteristics—Waltman/Cave Gulch field

Parameters	
Depositional Environment	Fluvial
Reservoir Continuity	Continuous
Reservoir Thickness (feet)	125
Aggregate Reservoir (feet)	125
Porosity (%)	5-10, 8 Avg
Porosity Type	Matrix/Local Frac
Importance of Natural Fractures	F>>M
Permeability (md)	<.001
Depth (feet)	16700-19500
Drainage Area (acres)	Unknown

Table I-2. Production characteristics—Waltman/Cave Gulch field

Parameters	
Hydrocarbon Column (feet)	1500
Avg Initial Reservoir Pressure (psi)	13,482-14,802
Avg Pressure Gradient (psi/ft)	.73-.77
Avg. Reservoir Temperature (oF)	284
Drive Mechanism	Depletion
Gas Characteristics (BTU)	1021
CO2+N2	1.45% CO2
GOR	High
Gravity (API)	0.581

E. Site Characterization

Reservoir Overview

We modified the Bullfrog site plan to be a back-cast (post-appraise) demonstration to accommodate the operator's rapid pace of activities. The site was characterized, data collected and interpreted for prospect generation, and two newly drilled wells were back-cast from the prospect maps. In addition, we made recommendations for future activities to the operator. The operator was discouraged by the high risk of excessive water production from the deep Frontier and did not immediately pursue our location recommendations.

The Bullfrog site is located in Townships 36N 86W and 36N 87W in the southeastern part of the WRB along the Waltman Arch and immediately south of the Waltman/Cave Gulch field (fig. I-6). The primary reservoir objective of the project is the Frontier Fm, which lies between 17,000 and 18,000 feet subsurface.

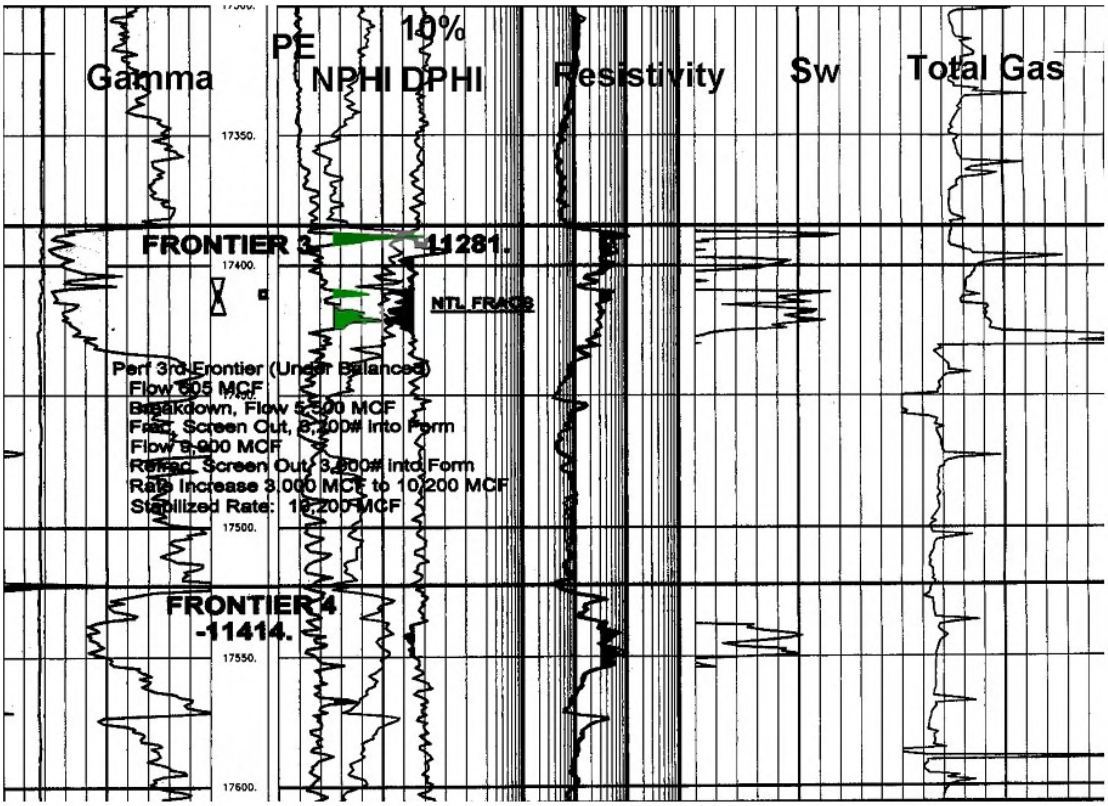

Portion of electric log showing Frontier Fm. pay zone in the Cave Gulch #16. High values of Photoelectric effect (green, above), frac screen-outs, and anomalously high productivity are believed to reflect the influence of fractures in the Frontier reservoirs of Cave Gulch.

Fig. I-6. Frontier Fm pay zone in the Cave Gulch #16

The Frontier Fm at the Waltman/Cave Gulch site is a naturally fractured tight gas reservoir. Matrix permeability reported from core is <0.001-md (WOGCC proceedings). The Frontier Fm exhibits multiple "unconventional production characteristics" including multiple reservoir compartments, sporadic occurrence of thief and kick zones, and a poor completion success record (F. Barrett 1999) and WOGCC documents.

Indirect evidence such as photoelectric effect (PE) curve deflections, hydraulic fracture screenouts and anomalous productivity are common. FMI logs also indicate numerous natural fractures in the section. The operator believes natural fractures in the reservoir are essential to establish economic production.

Data Collection

Initial data collection for the Bullfrog field site included assembly of data presented during public hearings before the WOGCC and meetings and telephone conversations with Barrett Resources personnel, as well as a review of the reservoir data assembled for the Deep Wind River basin gas study, prepared by ARI for the Gas Research Institute (GRI).

Barrett Resources, Inc., the operator, contributed approximately twenty-six square miles of licensed, depth converted Frontier Fm seismic. Barrett Resources personnel interpreted the horizon (fig. I-4). Barrett also provided a series of wireline logs from prior wells drilled in the area. The wellbore FMI was delivered on CD-ROM in Proprietary Schlumberger Format (PDS) files.

ARI and Barrett Resources geophysical staff jointly completed a detailed fault interpretation in Barrett's offices in Denver. Access to the seismic data was provided by Barrett Resources with ARI acting as consultant to Barrett Resources during this interpretation.

The fractured nature of the reservoir was confirmed early in the project via core and electric logging (see fig. I-7 and Appendix A) setting the stage for core and stress interpretations to support the geomechanical model building process.

Disarticulated, bed bound natural fracture from Frontier Fm at 17,818 md in Barrett, Bullfrog #5-12. The fracture is lined with euhedral carbonate crystals 2-3mm in size. Note non-planar geometry of the fracture face.

Fig. I-7. Fractured Frontier Fm. Barrett Bullfrog #5-12

Petrophysics

The Frontier Fm is known regionally as a lithic-rich unit that seldom exhibits good reservoir qualities and almost never yields easy petrophysical characterization. The Frontier Fm at Cave Gulch is no exception and, in fact, may be even more difficult to characterize. Petrographic analysis of rotary sidewall cores indicates the marine sand units are clayey, very fine-grained sublitharenites with 10 to 20% feldspar and 6 to 10% clay. Indicated log porosity is in the 6% to 8% range. The permeability was measured at 0.002 md. (WOGCC proceedings).

The reservoir quality of these sediments is so poor that engineers have difficulty rationalizing sufficient permeability and storage to justify a production well. (WOGCC proceedings). One of the best arguments for natural fracturing in this area is that the sediments cannot produce at the observed rates from demonstrated matrix properties alone. (The Bullfrog core (discussed later) appeared tight and similar in nature to the sidewall cores taken in Well #16, however the Bullfrog core did have some larger grain sizes present.)

The poor reservoir quality of these sediments can be explained by their lithic components and their post-depositional structural history. The Cave Gulch area is located immediately downthrown to the Owl Creek/Casper Arch and was probably in the deepest portion of the basin prior to uplift. No specific amount of uplift can be determined without more data but there is likely from 5,000 to 10,000' of uplift associated first with the Waltman Arch and the Owl Creek thrust. The high pressures suggest a relatively static and confined system (little fluid throughput) that might also explain the lack of secondary porosity development.

Natural Fractures

Prior to examining the core from the Bullfrog #5-12 well, there was considerable indirect evidence supporting an interpretation of the Frontier at Waltman/Cave Gulch as a fractured reservoir. Teufel (1991), Laubach and Lorenz (1992), and others have characterized the Frontier Fm. as a fractured reservoir from regional work in the GGRB. The DOE/UPRC/ARI work at Rock Island demonstrates the Frontier as a fractured reservoir.

In addition, work by Laubach and Lorenz (1992), and Billingsley and Evans (1995) demonstrates the presence of open fractures at depth in the Frontier at the Frewen unit in the eastern Green River basin. Outcrop studies of fractured Frontier pavements (Poison Spider field, Wind River basin, scanned images) have been performed on exposures from the upthrown block. Production modeling of deep Frontier wells in the WRB has been used to demonstrate evidence of fractures in the reservoir.

The Bullfrog #5-12 well core provided direct evidence for natural fractures. The fracture observed in the well core itself was part of a larger swarm of natural fractures. Crude reconstruction of the projected in situ aperture suggested 3/16-5/16" aperture width. Permeability of such a feature would be extreme and storage at that depth and pressure is potentially significant.

The extent of the fracture and whether it is connected with others of similar nature is the major question. Good data was reported from the Bullfrog FMI, which may provide additional direct fracture information. The remainder of the evidence from the field derives from production anomalies, shows, lost circulation and PE logs.

Fracture Porosity

The sampled rocks have low matrix porosity and permeability, from both core and log data, yet the production rates definitely imply considerably high gas storage and early time gas flow. The large aperture fracture from the Bullfrog 5-12 core could hold significant gas at these pressures. Given the structural position and history of Cave Gulch, at least in part, the producing reservoir is composed of sheared zones wherein porosity has been generated in brittle rocks because of deformation. When the zones are not very thick and are oriented according to the stress and strain history of the structure, they are difficult to identify using tools and techniques designed for conventional reservoirs.

These zones will appear as semi-random thief/kick zones that would potentially absorb mud, give a PE signature on logs and not be obvious on other tools. (Although continuous sampling FMI should see these fractures.) Such a reservoir would be nearly impossible to properly characterize using conventional petroleum engineering tools.

On the basis of the available data, which is still limited, the deep Frontier reservoir in the Waltman/Cave Gulch area is a complex amalgamation of poor matrix porosity, regional fractures, fault related fractures and tectonic porosity generated as the brittle reservoir rocks deformed during the formation of the structure. Intra-structure seals may be present because of the sedimentary stacking pattern. The interbedded nature of the sands and shales of the Frontier Fm, with the introduction of even small scale faulting, would develop into a very complex reservoir system. A mix of small and large scale faulting adds to the complexity of the reservoir geology.

While the Waltman/Cave Gulch area has been characterized as a “field,” it lacks the geologic homogeneity necessary to be engineered or exploited as a single hydrocarbon accumulation. Barrett’s arguments during the WOGCC hearings regarding the high degree of heterogeneity seem well founded.

Bullfrog 5-12 Core Interpretation

See Appendix A.

Bullfrog 5-12 Log Analysis

Dipmeter Interpretation

A six arm Dipmeter/caliper was run 9,500' to 16,340' measured depth (MD) in the well. We examined the log for indications of borehole ovality. No digital data was available for this examination. We observed several intervals of slight to moderate ovality in the wellbore. Fig. I-8 is an example.

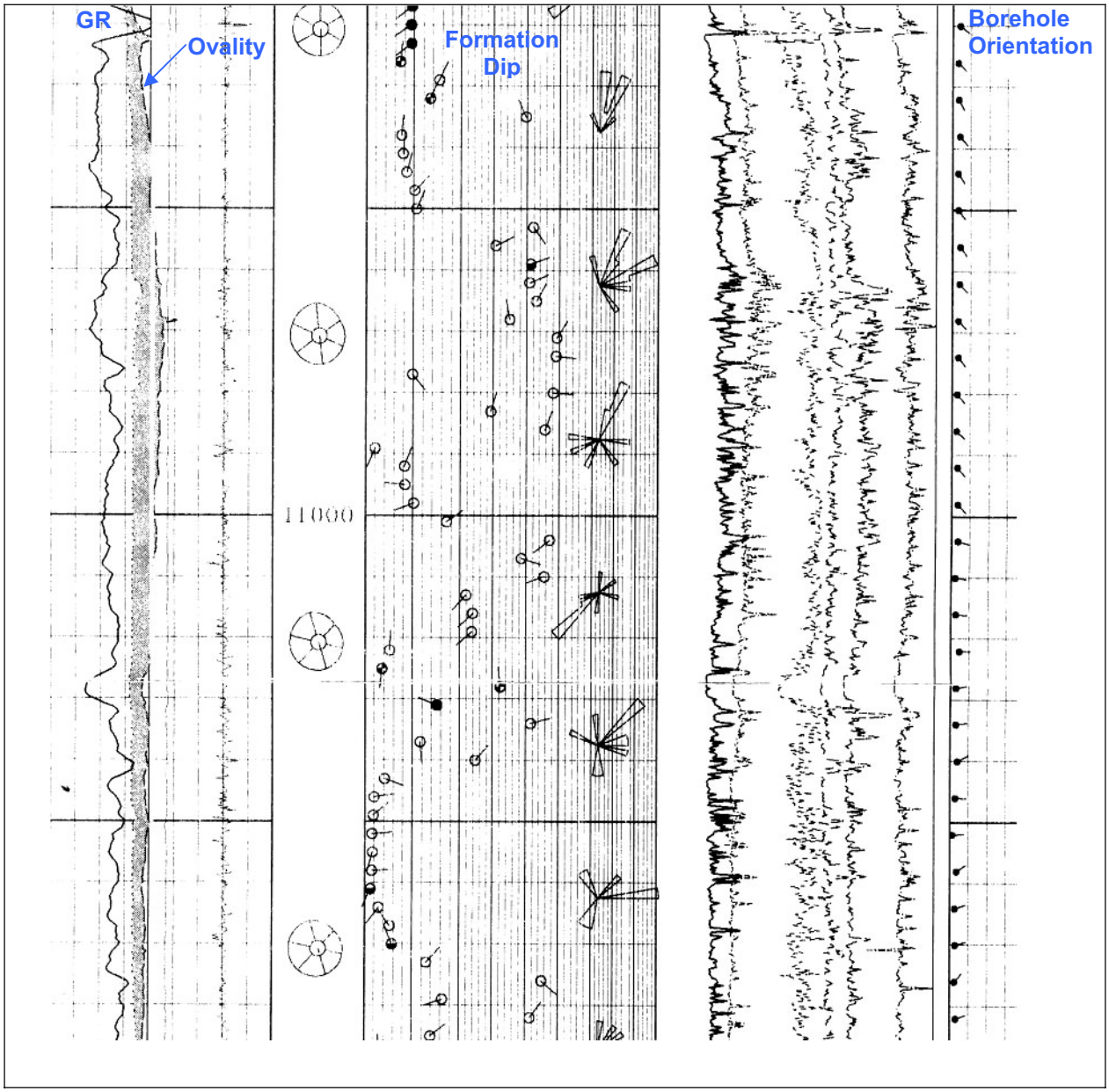

Fig. I-8. Bullfrog 5-12 dipmeter segment

The shaded area in the left track indicates the presence of ovality. One division in the track represents 0.1" difference between the maximum and minimum caliper readings. Longer intervals of consistent readings are viewed as more reliable than short intervals with changeable values. The small wellbore symbols in the depth track display the computed geometry of the wellbore in cross-section. The dip tadpoles in the right track indicate the section is nearly flat lying. This interval demonstrates a slight ovality towards the NNW. Others are similarly weakly developed and generally indicate ovality between NNW and NNE. Overall, the wellbore displays a weak, qualitative NNW to NS ovality over several intervals in the shallow section. Ovality decreases towards the base of the logged interval.

These observations indicate the area around the wellbore is weakly stressed (present day) with the principal horizontal stress in an E to ENE direction in the shallower portions of the logged section. The decline in ovality qualitatively observed with depth is inferred to reflect relatively less present day differential horizontal stresses at depth.

FMI Interpretation

A Schlumberger FMI log was collected in two runs by displacing the oil based mud with a water-based pill for logging operations. The log was interpreted in Schlumberger's Denver Computing Center. Schlumberger's interpretation of fractures and other wellbore features has been largely accepted for this evaluation. No fracture apertures were calculated because of the highly resistive mud system. The log and compiled fracture statistics were reviewed in hardcopy and raster formats.

Borehole ovality was also very weakly developed at depth on the FMI. Few intervals exhibited ovality at all. The few that did show some ovality seemed to agree with the information derived from the dipmeter. A poorly documented rose diagram purporting to be derived from "drilling induced" fractures was presented but no indication was present on the log to demonstrate the phenomenon so identified by the interpreter.

In (fig. I-9) the overwhelming E-ENE trend of the observed fractures in the wellbore is demonstrated. Other directions are represented sparsely. The predominant type of conductive fracture observed was characterized as bed-bound with significant numbers partially healed. The azimuth rose diagram demonstrates a strong ENE trend. Significant scatter is observed in the dip rate as displayed on the Wulff stereo net.

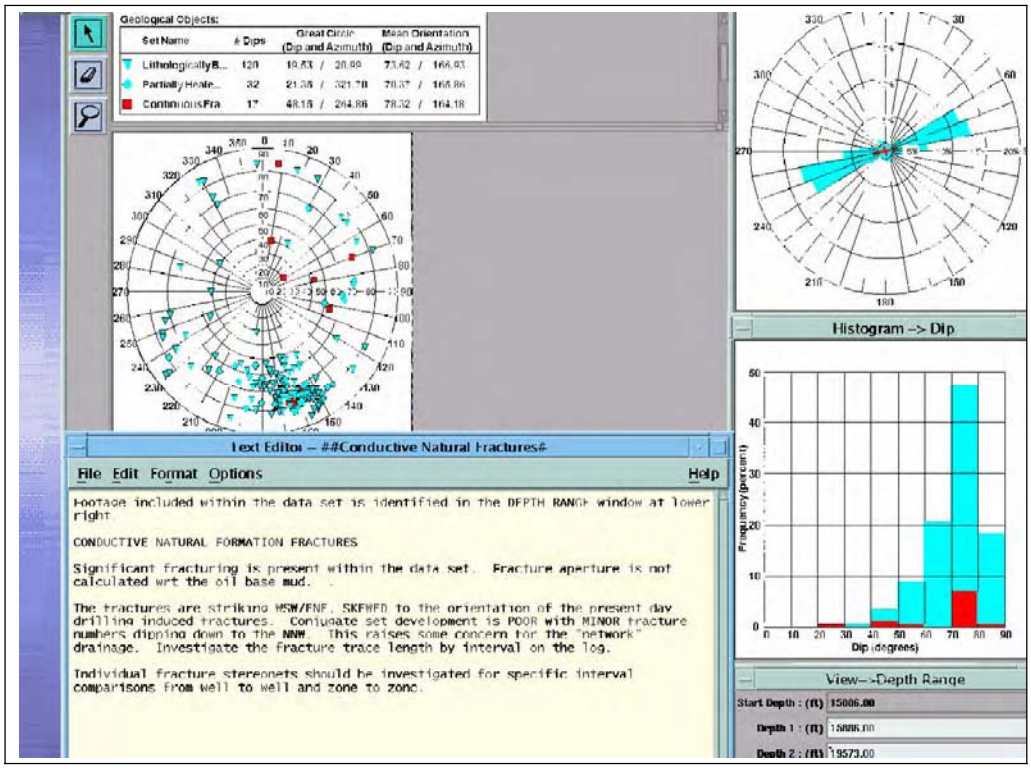

Fig. I-9. Bullfrog 5-12 FMI summary

Typical regional opening fractures are near vertical in attitude whereas this population appears to have a pronounced consistency to its strike azimuth but considerable variability to dip. Bedding presently is near flat so rotation of the fractures from near vertical because of folding seems unlikely. A more likely origin for the orientation would seem to be variability in origin within an episodic, evolving stress field, which is supported by the number of major faults involved in the structural development of this area. Regardless, the general fracture population as observed on the FMI is consistent in strike and diverse in dip.

Observations

Our examination of the dipmeter and FMI logs lead to these observations:

1. The poorly developed borehole ovality (borehole breakout) suggests the area around this wellbore is under the influence of minor NE-E differential horizontal stress at this time. Any previous stress appears to have been absorbed and accommodated as strain in the form of fractures, faults and folds;
2. The general direction of the maximum horizontal paleostress represented in the observed fractures is inferred to be ENE to E in origin;
3. There are no well developed conjugate pairs of shears indicative of failure in the Coulomb envelope present within the sampled dataset; and
4. Consistent strike azimuth and diverse dips within the population suggests multiple but as yet, poorly understood, origins for the fractures.

Fig. I-10 shows the general area and setting of the geomechanical modeling in cross-section view. The prospective area is a deep imbricate thrust complex with the modeled faults labeled on the cross-section. Two main thrust faults (RLB_1, RLB_X) and three back-thrusts (BT_1, 2, and 3) were modeled for three model combinations. The original proposal called for one geomechanical model run. However, a single run was inadequate to characterize the setting and eventually three models were built and evaluated.

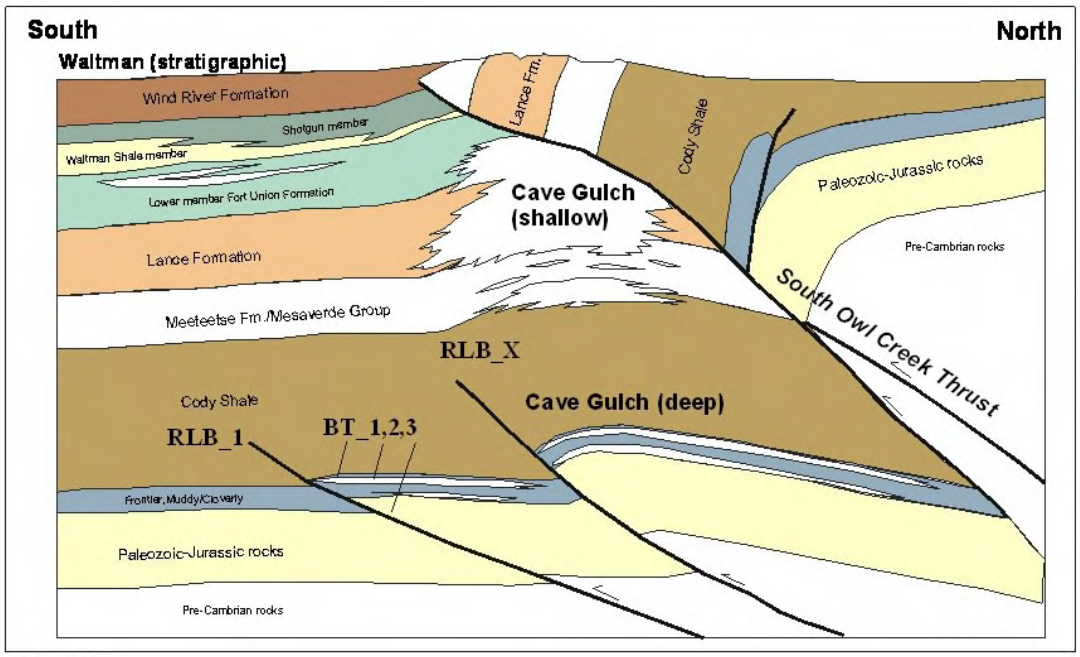

Modeled faults are indicated by labels.

JAF01931.CDR

Fig. I-10. N-S Diagrammatic cross-section of the Bullfrog/Waltman area

Our geomechanical models are based on a detailed interpretation of the fault planes and their geometry. Special attention was paid to fine scale interpretation and line-tying, especially around the edges of the faults where the discontinuity will be the most severe. Small inconsistencies in the interpretation will generate large stress anomalies.

With Poly3D modeling faults cannot be allowed to intersect or the model will fail in execution. Fig. I-11 is a perspective view of the RLB_1 system and its three genetically related back thrusts.

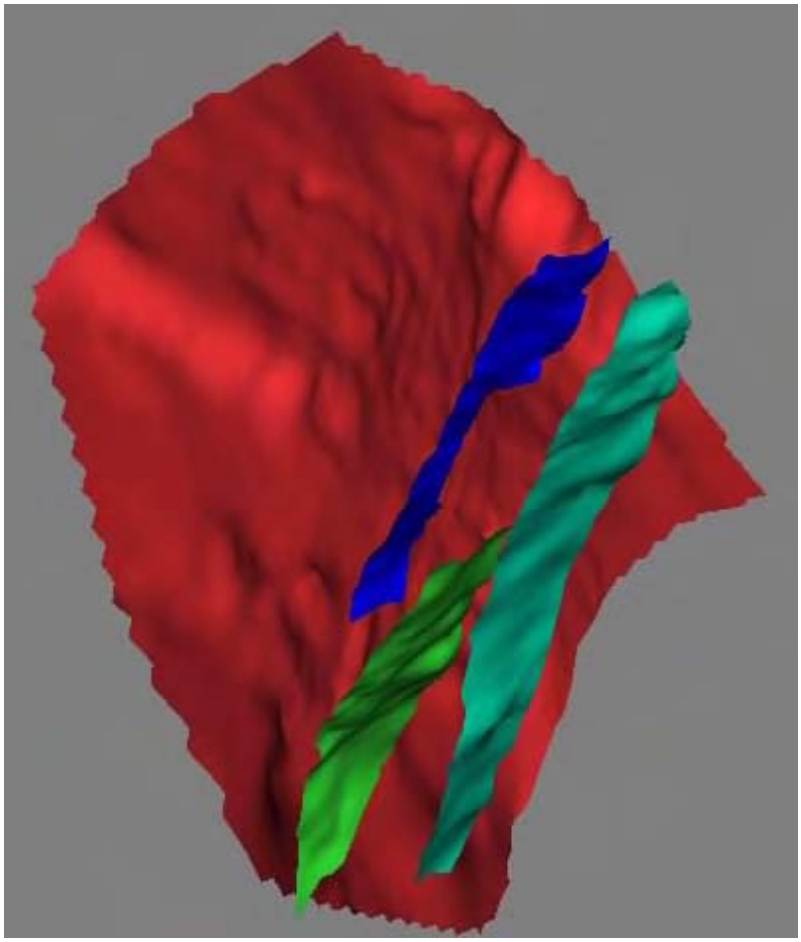

This perspective figure illustrates the ramps and back-thrust geometry relationship of the four modeled faults. The basal thrust, RLB_1 is in red and the associated back thrusts are in blue, green and aqua. The illustration was generated using experimental software from the Rock Fracture Project at Stanford.

Fig. I-11. Perspective view of the Bullfrog fault system

The back thrusts are significant faults in their own right (1000'+ of displacement) and actually form the Bullfrog prospect (fig. I-12). The undulations apparent in the shaded relief display are judged to be real, forming above the lateral ramps developing along the fault trend as individual sub-seismic imbricate thrust faults coalesce into a single seismically resolvable fault plane.

Fig. I-13 is a generalized structure contour map on the Frontier horizon. The culmination drilled by the Bullfrog 5-12 lies on the upthrown side of the most downdip (with respect to Rlb_1) back-thrust.

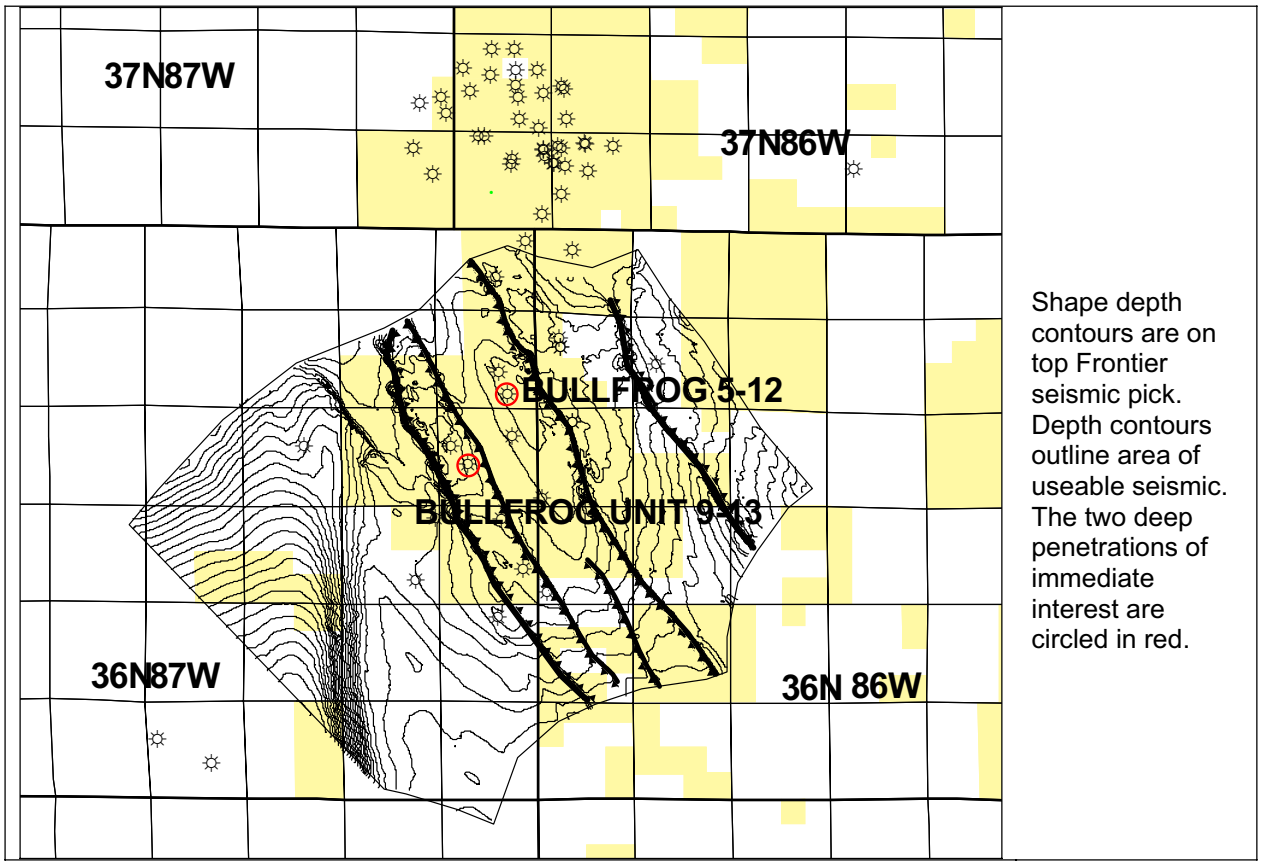

Fig. I-12. Basemap of the Bullfrog/Cave Gulch project area

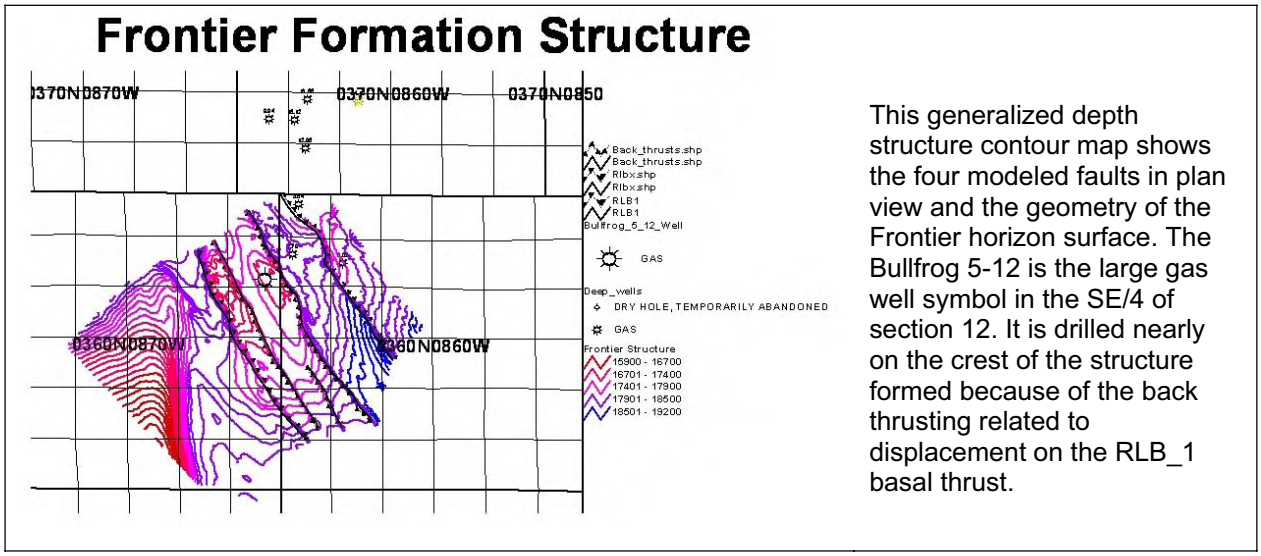

Fig. I-13. Generalized structure contour map on the Frontier Fm horizon

Geomechanical modeling (to project fault related stresses in the subsurface) offers a number of choices and assumptions, guided by the quality of the input data available. In the Bullfrog field demonstration site the fault geometries, and stress directions are reasonably well constrained compared to the reservoir rock properties, the actual displacement amounts, directions and their distribution along the fault surface. Given these conditions, we chose to run the models in stress mode by applying a unit stress (1 stress unit, from N70E) at the boundary and making the fault surface frictionless. All outputs are in stress units, and displacements in feet, relative to the discontinuity (fault).

This type of model will generate a map of relative stress (within the model) but no absolute values for comparison to outside controls. Any attempt to calculate true stress would require considerable correction, often involving more assumptions. For the Bullfrog field demonstration, we decided to use relative stress within the model rather than introduce additional uncertainties into the process.

Implementation of a new technology to map non-visible attributes required a set of controls to ensure consistency and reliability of the results. In the geomechanical model, quality control is provided by mapping calculated fault displacements, which are compared to the generated structures (with the real mapped structures). For fault generated structures, the contours of displacement should agree in shape with the observed structure contours (derived from seismic).

A sample of such a map is presented in fig. I-14. This map was generated from the RLB_1 thrust model without the backthrusts. Boundary conditions were set at 1 stress unit, N70E azimuth. The reds are positive (up) relative motion, blues are negative; all are relative to the fault plane itself.

Validity of the boundary condition assumptions was achieved by superimposing the structure contours and fault traces on the grid of displacements, then visually comparing the fit. In this case, the red colors generally parallel the trend of the underlying ramp and lie within the band of mapped backthrusting. The backthrusts are thus interpreted to be genetically related to the uplift associated with the ramp, and the parallelism of the trends supports the N70E azimuth of stress as reasonable.

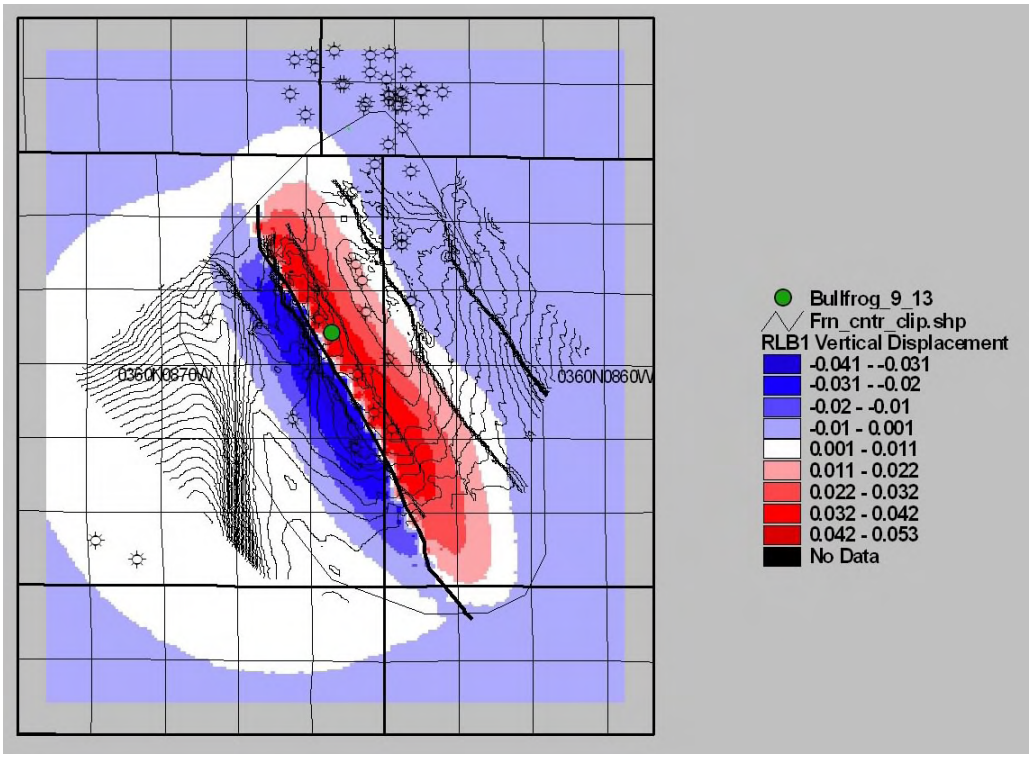

The colors in this figure are gridded model output values representing the calculated uplift associated with fault displacement on the main basal thrust, RLB_1. The limits of the grid are the limits of the model. The superimposed contours represent the limits of true data within the model. Values along the edges of the model outside the structure contours are projected values of unknown reliability. The area of maximum uplift (red) is parallel to the back thrust trend indicating the back thrusts are forming to accommodate the uplift along the ramp.

Fig. I-14. Generalized Frontier structure map and simulated displacement

F. Prospect Generation

The Bullfrog structure provides an excellent trap for the Frontier sands and forms an upthrown closure against the Carlisle-Niobrara shale sequence. The Bullfrog structure is located approximately 2.5 miles down plunge on the Waltman Arch and fault separated from the Cave Gulch culmination. Barrett has mapped approximately 1200’ of displacement across the key reverse fault This displacement should be sufficient to juxtapose the entire Frontier objective section against the 2000’ Carlisle-Niobrara shale interval.

As discussed previously and shown from the Bullfrog core, reservoir sands, although of marginal quality, exist in the Frontier in this area. The major risks with this prospect will be encountering sufficient permeability in the form of matrix or fracture permeability and assuring that the sands are fully gas charged. A successful well in this structure must encounter a sufficiently connected fracture system to effectively drain a large area of marginal quality reservoir or a sufficient volume of tectonically generated porosity to supplement the low porosity Frontier sands. For this, the prospective areas on the Bullfrog structure will need to have undergone significant shear and extensional deformation during formation of the trap.

G. Well Drilling and Testing

During the project but before results were available, Barrett drilled two deep tests, the Bullfrog #5-12 and the Bullfrog #9-13. Core and borehole imagery were collected in the Bullfrog #5-12 well. This information was used in the construction of the boundary element model. In this case, project activities focused on establishing an effective interpretive flow, building the models and post appraising the second well.

Results

The interpretation of core, borehole imagery and production data indicates the large shear fracture cored in the Frontier represents the bulk of the production permeability. The cored fracture had failed through a rotational shear but showed no slickensides suggestive of actual lateral displacement. Two possibilities exist for conditions to give rise to such a fracture.

- Near the extreme tip of a fault after failure has occurred but before displacement.
- Shear failure as a volume of moving rock passes through a hinge area of a fold, as at the base of a thrust ramp in the transition from flat to ramp in a thrust system.

Both conditions exist at the Bullfrog 5-12 drill sit; therefore there is no single answer. Fig. I-15 is a detailed map of Poly3D model results for the Bullfrog #5-12 and #9-13 well areas. Both wells are located in an area with average Coulomb stress on the crest of the structure. Low Coulomb stress values would suggest a lack of pervasive shear failure. Neither well has exhibited, through production, indications of communication with a large well connected fracture system. Although both wells have produced significant amounts of water, the bulk permeabilities are relatively low. This is interpreted to reflect consistency with the modeling, which generally reflects low amounts of fault-related shear stress in the crest of the structure.

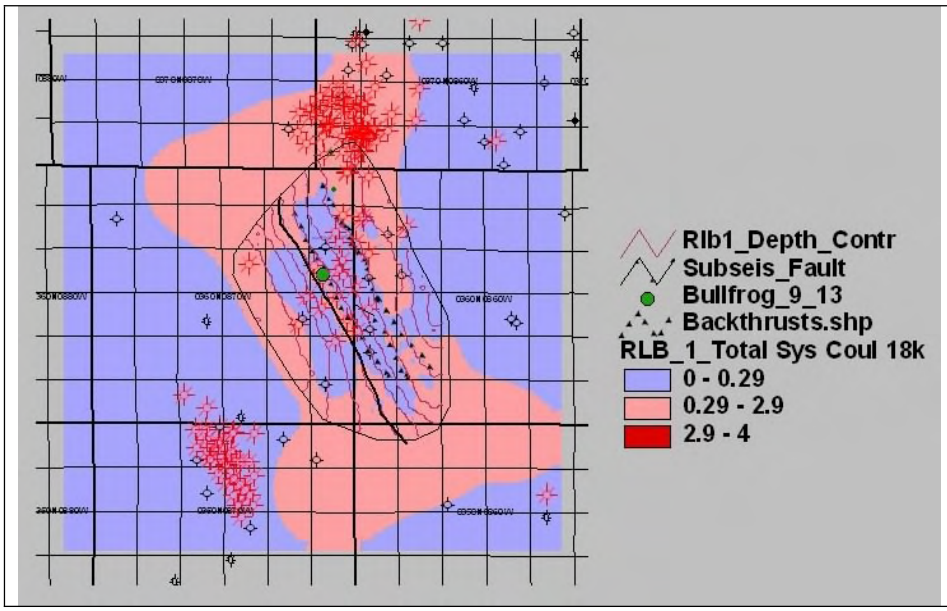

This map shows the distribution of Coulomb stress resulting from the entire RLB_1 system (including the back thrusts) along a flat plane at 18,000' subsurface. Background (average) Coulomb stress for the model was 0.29 stress units. Prospective areas will be defined relative to the model background Coulomb stress.

Fig. I-15. Distribution of Coulomb stress

In retrospect, we noticed that the Frontier structure contours had small apparent offsets that could reflect the presence of small subseismic faults. The undulations on the fault trace *might* reflect motion transfer zones occurring along a very complex fault system. If so, the small scale faults would be dying out towards the wells. Such faulting is theoretically necessary but not fully substantiated by the data available.

Subsequent Actions

In 2001 we recommended three potential offset locations to the operator (shown in fig. I-16). Two potential locations were in areas of above average shear stress along probable motion transfer zones related to the faulting. The third potential location lies midway along a small, subseismic fault, away from the main back thrust and down flank but in an analog setting to the crestal Bullfrog #5-12 well.

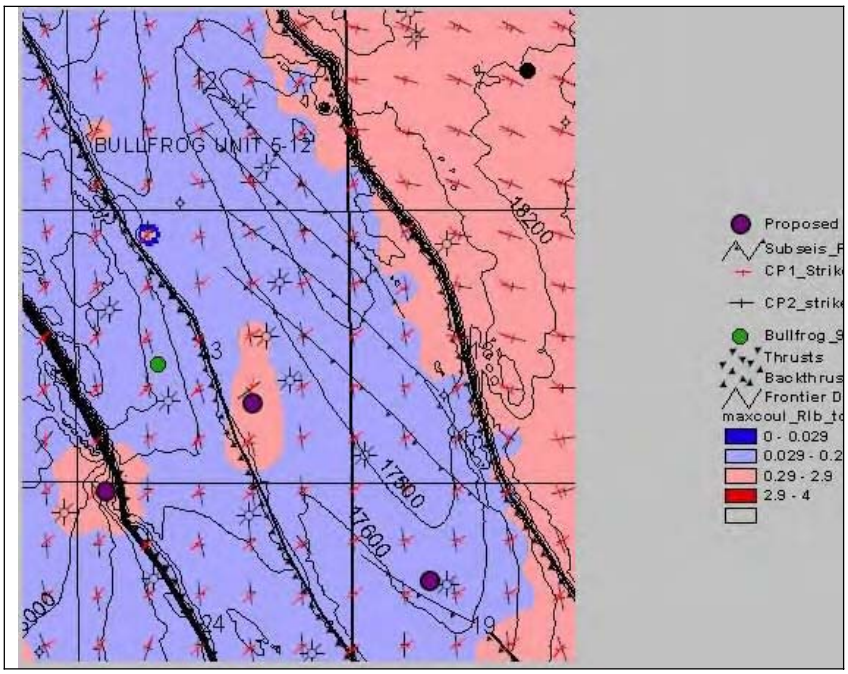

This illustration is the final prospecting map for the Bullfrog field demonstration site. The three purple circles are locations recommended for enhanced fracture permeability based on the core, FMI, seismic and geomechanical integration. Red tones are areas calculated to be areas of increased shear stress. The smaller, regularly spaced symbols are the intersections of the calculated shear failure planes with the modeled datum and as such, will reflect the trends of projected shear fractures.

Fig. I-16. Final prospecting map for the Bullfrog field demonstration site

The operator has not drilled the recommended locations as of 2005. This decision was based not on the projection of improved permeability from the project work, which was accepted; but rather on the increased risk of producible water, as encountered in the Cave Gulch #6-29 well discussed previously. The presence of producible water in the two exploratory wells in this perceived deep basin centered setting has had a negative effect on the operator's willingness to further pursue the deep Frontier Fm gas resources.

Impact Assessment

The Bullfrog field demonstration/back-cast yielded the following results when post-appraised with the geomechanical modeling approach:

1. Both wells drilled by the operator during the course of the modeling were drilled in compressive and slightly sheared locations that yielded mediocre results for the depth and cost involved.
2. The geomechanical modeling approach was able to appropriately back-cast the well results by integrating the information derived from core, FMI and seismic into an integrated stress model for the area.
3. The use of a relative measure of stress for mapping results is insufficient and needs improvement
4. The Bullfrog retains a slight ENE stress anisotropy originally generated during the structural development.
5. Further exploitation of the field demonstration area was halted after encountering significant water production in other exploration wells in the Waltman/Cave Gulch area.

Geomechanical models of the structure indicated the locations were in areas of high differential stresses related to displacement along the local reverse faults. The wells encountered NNW trending shear fractures as would have been expected. Extensional fracturing related to the faulting appeared to be minor as would have been expected by the compressional nature of the locations

Both wells found gas (Bullfrog 5-12 produced 2 BCF, Bullfrog 9-13 hi initial water) but produced unacceptably large amounts of associated water. The large aperture, open shear fracture encountered in the Bullfrog 5-12 is inferred to have allowed water movement, potentially across bed boundaries.

It is likely similar fractures exist across the crest of the structure. This style of fracturing may have allowed significant fractionization of gas and water in the structure. The location of the Bullfrog 9-13 very near the crest of the structure suggests any gas saturated intervals may be higher in the section, perhaps within the overlying Cody Shale.

The results of the Bullfrog geomechanical simulations were reviewed with Drs. Pollard and Aydin of Stanford University who gave several valuable suggestions and insights. They improved our understanding of the interpretational aspects by explaining several poorly understood artifacts of the modeling process. This in turn, improved our process for sizing models appropriately within seismic volumes to avoid misleading results.

From this field test we identified the need for several procedural changes and modifications to our approach. There was a clear need for improved visualization and interpretation tools, both for model construction and output presentation. These needs were incorporated into the NextGen package, then under development. In order to more effectively present simulation results, an attempt was made to establish realistic failure criteria using commonly understood units of rock mechanics

It was clear from the initial geomechanical experience at Bullfrog that there was a significant gap between the ability to theoretically simulate conditions favorable for natural fracturing and it's effective practical application under oilfield conditions

II. Study Area #2: Anadarko

A. Overview

The Anadarko basin was estimated to contain over 16 TCF of gas resources (mean) in the USGS 1995 assessment. An uncertain, but perceived significant, amount of these resources are contained in deep reservoirs or reservoirs whose behavior is believed to be influenced by natural fractures. Improvements natural fracture exploration methods will increase recoveries from these more difficult reservoirs.

Geomechanical techniques were employed to predict natural fracture related permeability in Paleozoic reservoirs along the Wichita Front area of the Anadarko basin. Core, electrical logging and production data were evaluated to demonstrate the role of natural fractures in production. Seismic data were used to map structure and fault systems at the reservoir levels. Poly3D models were built to simulate the structural development of the area. A discrete natural fracture network simulation was performed (incorporating 3D seismic and Poly3D simulation results) to develop a map of natural fracture permeability distribution. Prospects were generated using a combined stratigraphy and natural fracture permeability approach.

Twelve prospects estimated to contain approximately 60 BCFG, recoverable, were identified in the project area. Land issues precluded the drilling of the exact locations recommended. The operator has since drilled four wells in the project area. Three of the wells are judged to have fit the maps built during the project. One well was drilled to the objective interval, later completed in a shallower unit and is believed unsuccessful (at the objective horizon). Specific information about drilling and production results have been held confidential by the operator.

B. Purpose

A key goal of the Multisite project was to build credibility by demonstrating the geomechanical technology in a resource rich area outside the Rocky Mountain area in order to establish its applicability across multiple geologic terrains. A successful Anadarko basin field demonstration in conjunction with a technologically savvy operator would fulfill that goal. The project targets *immaturely developed Pennsylvanian-age tight gas formations* in the deep Anadarko Basin, holding 16+ tcf of technically recoverable resources. Effective development of these (and deeper) formations will be *essential for reversing declining natural gas production* in the Mid-Continent.

C. Site Selection

The required ingredients for a successful exploration field demonstration were considered to be a willing, technologically savvy operator, 3D seismic data, a naturally fractured reservoir and available exploration acreage. The Wichita Front where Burlington Resources, Inc. possessed a large 3D seismic data set and considerable undrilled acreage, was considered to meet all required criteria.

A favorable business environment was a fifth, unanticipated, component. Personnel shifts, corporate strategic shifts, and the fiercely competitive nature of the Oklahoma oil and gas business climate all combined to make the actual execution of the field demonstration a difficult challenge. Oil and gas operating rules in Oklahoma promote extreme secrecy not only to protect advantage but to protect acreage interest as well.

As a result, the detailed results of the Anadarko field test will remain confidential until March 31, 2007. Exact locations and certain diagrams, which might convey information counter to the best business interests of the operator, will not be released at this time. The intent here is to convey the essence of the demonstration and the result without compromising the operator's interest position.

The general area of the field demonstration was located in the Elk City area, Custer County Oklahoma. The initial study area incorporated approximately 35 townships and 250 square miles of 3D seismic (fig. II-1). The field demonstration involved exploration for a deeper objective that was common in the area.

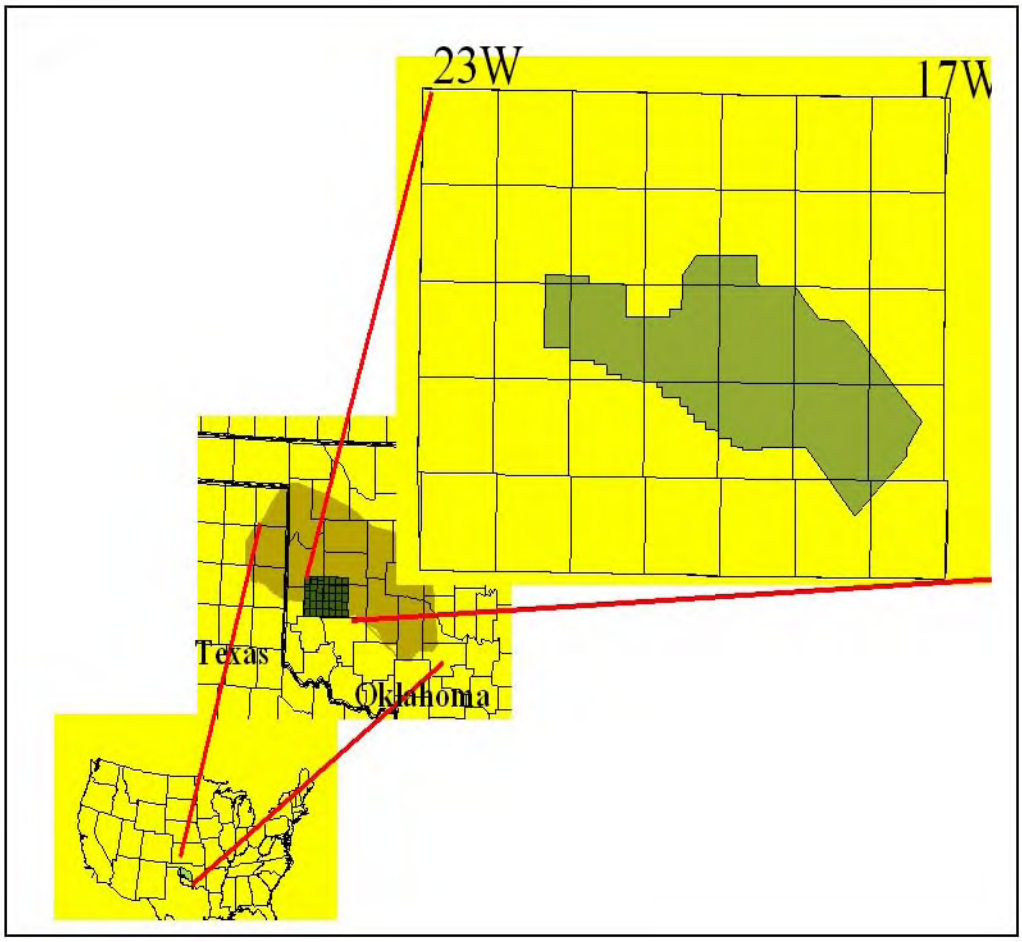

Fig. II-1. Anadarko basin field demonstration project area

D. Regional Geologic and Tectonic Setting

The Anadarko basin is an elongate, asymmetrical, northwest-striking foreland depression of late Paleozoic age, extending across 35,000 square miles of western Oklahoma, southwestern Kansas, and the northern Texas Panhandle (fig. II-2). The basin is structurally bounded to the east by the Nemaha Ridge, to the south by the Wichita and Amarillo Mountains, and to the west and north by shallow paleoshelf areas.

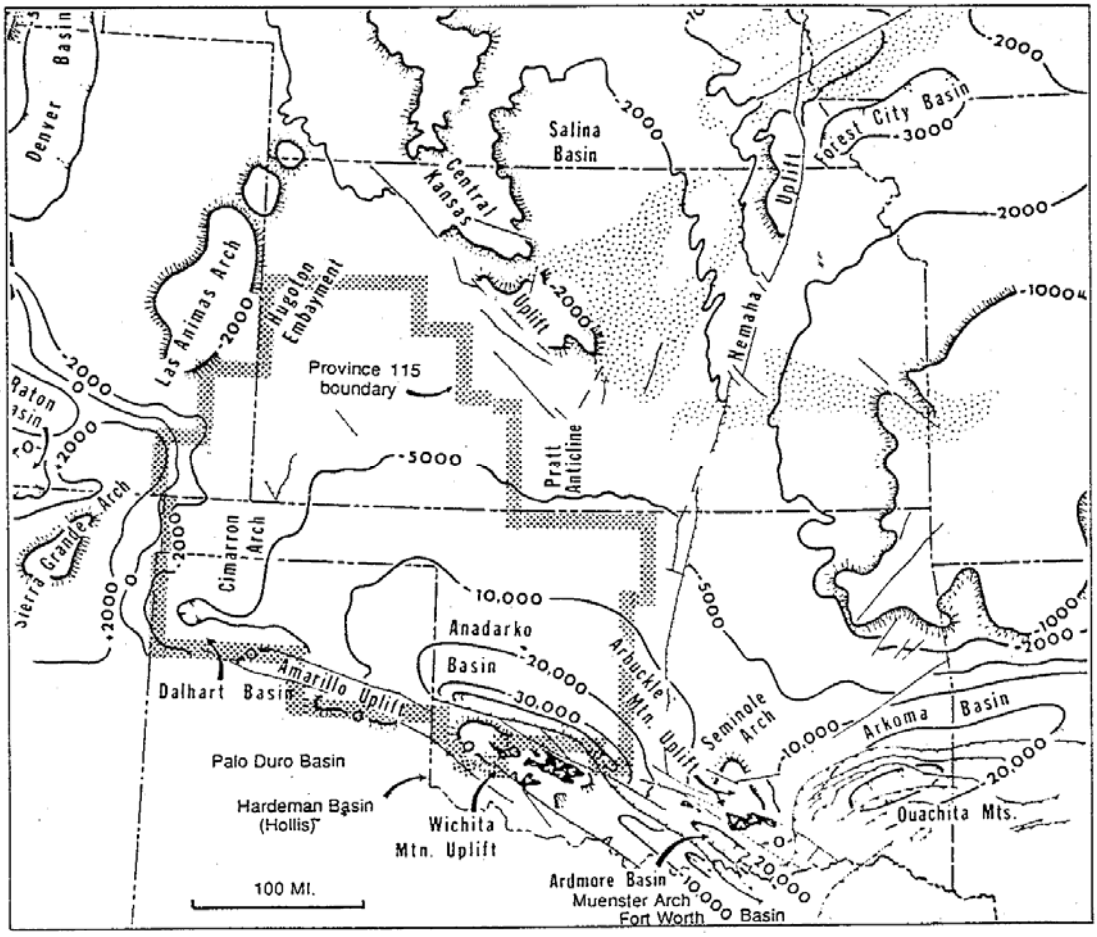

(Ball, Henry and Frezon 1991)

Fig. II-2. Basement structure, Anadarko basin & adjacent basins & uplifts

The "Deep Anadarko" basin, overlying the main structural axis of basin subsidence, covers an area of 11,800 square miles in Texas and Oklahoma. Arbitrarily defined by a depth-to-basement of 15,000 feet, the deep basin incorporates 22,000 cubic miles of sedimentary rock (fig. II-3).

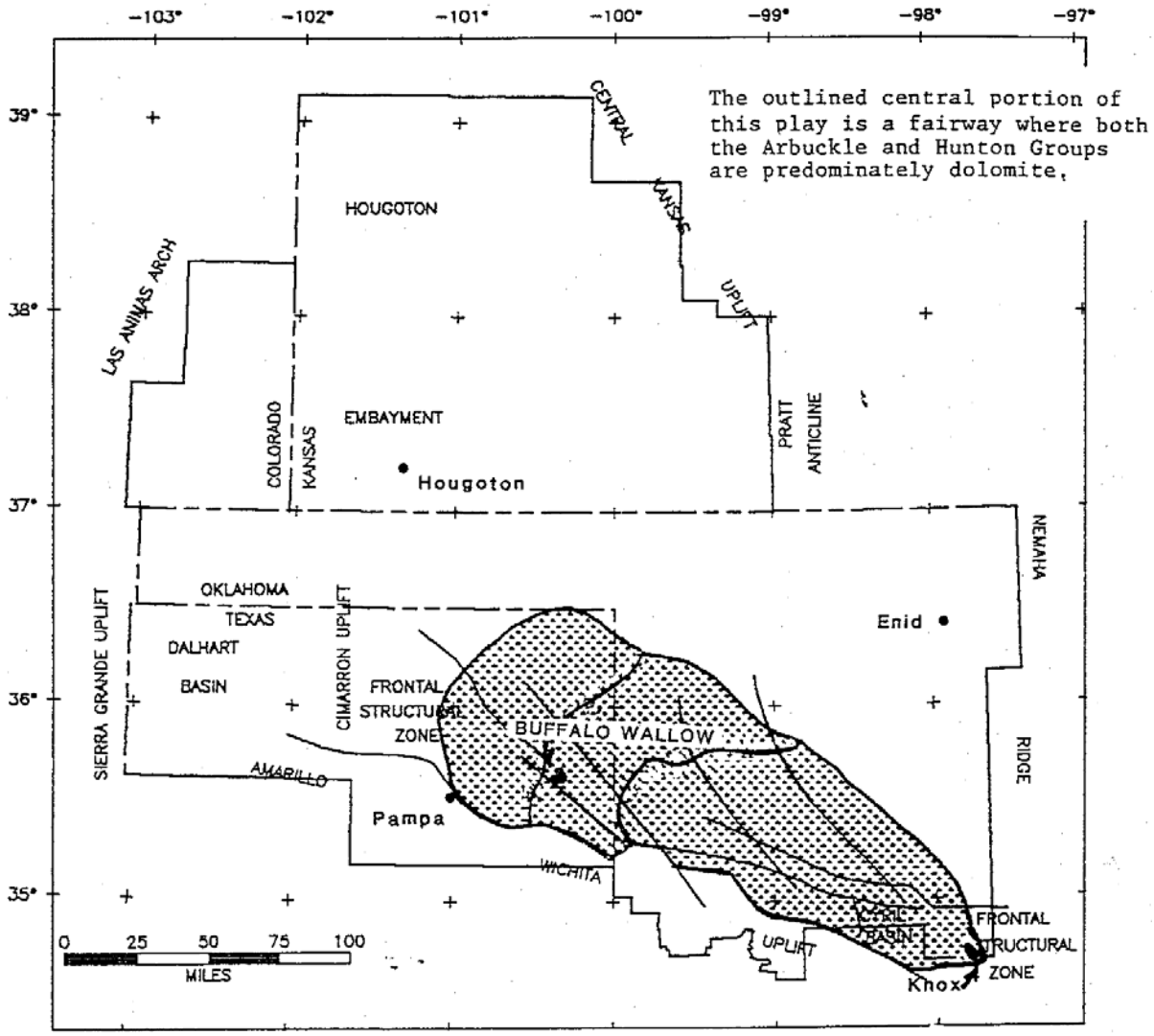

(Ball, Henry and Frezon 199l)

Fig. II-3. Deep Anadarko basin (stipple): basement depth > 15,000'

This structurally complex region is characterized by high-angle reverse faults, and normal and recumbent folds, overlain by relatively undeformed Permian strata (fig. II-4).

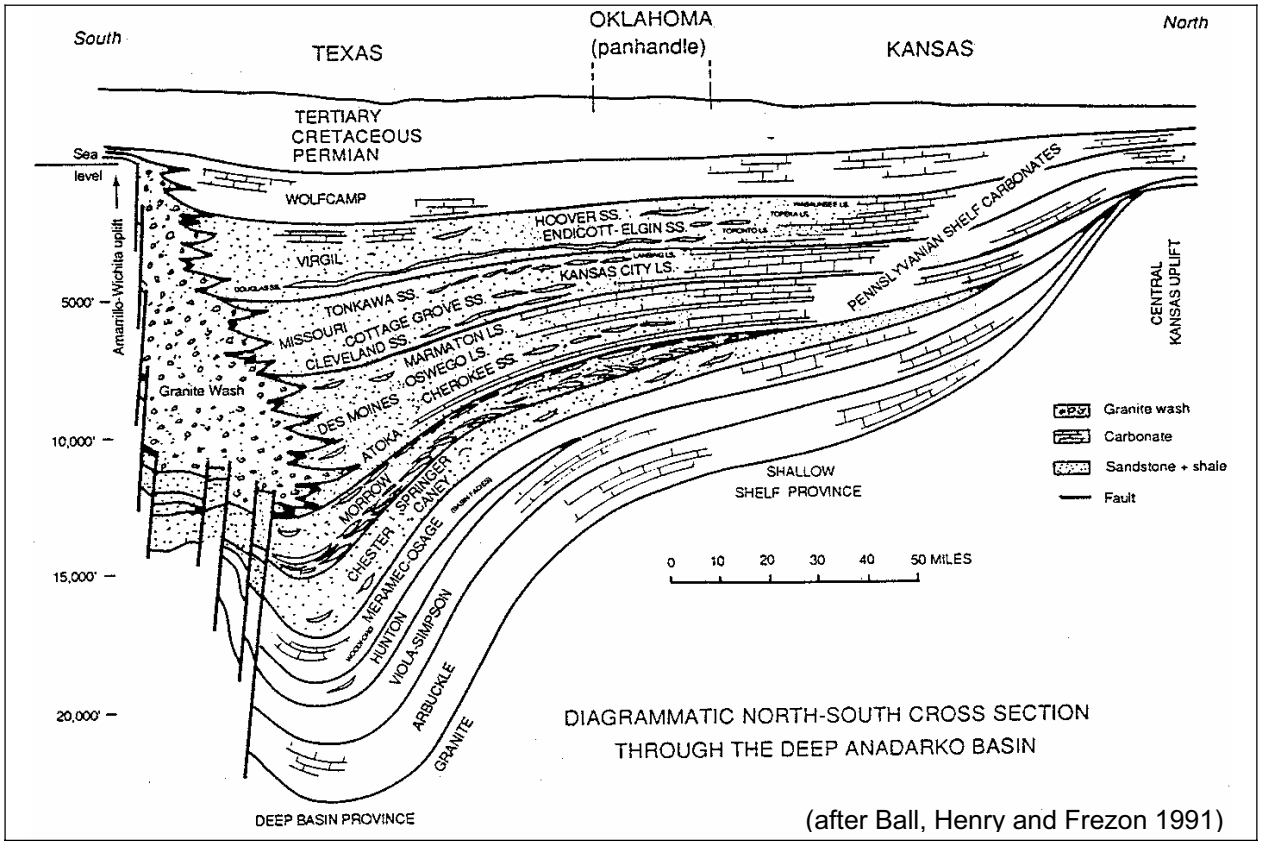

Fig. II-4. South (left) to north (right) cross-section of Deep Anadarko

Pennsylvanian and Permian rocks are primarily clastic in the deep basin, with hydrocarbon reservoirs mostly occupying stratigraphic traps. Cambrian through Mississippian strata are dominantly carbonate, with most known hydrocarbon reservoirs formed by structural traps related to Pennsylvanian faulting. Unconformities and facies changes make stratigraphic traps likely, especially in carbonate rocks of the Silurian – Devonian Hunton group.

The Anadarko basin is parallel to, and partially overlies, a late Proterozoic structural depression that may be part of a major northwest-trending transcontinental shear zone. Multiple lines of evidence show that fault activity along this deep-seated zone of "crustal weakness" has been chronic and persistent, with major episodes of deformation in the Anadarko region culminating during the early Cambrian and Pennsylvanian periods. Minor reactivation and reversal of fault offsets has occurred sporadically, as recently as Holocene time.

Wichita Fault System

The Wichita uplift is bounded by an extensive, northwest-trending system of anastomosing and overlapping faults (fig. II-5). The Meers fault zone is the most significant of these having some surface exposure. The Slick Hills are underlain by Cambrian to Ordovician carbonate rocks (mostly Arbuckle group) exposed in the overlap zone between the Meers fault to the south and east, and the Mountain View fault to the north and west (fig. II-5) (Donovan 1995).

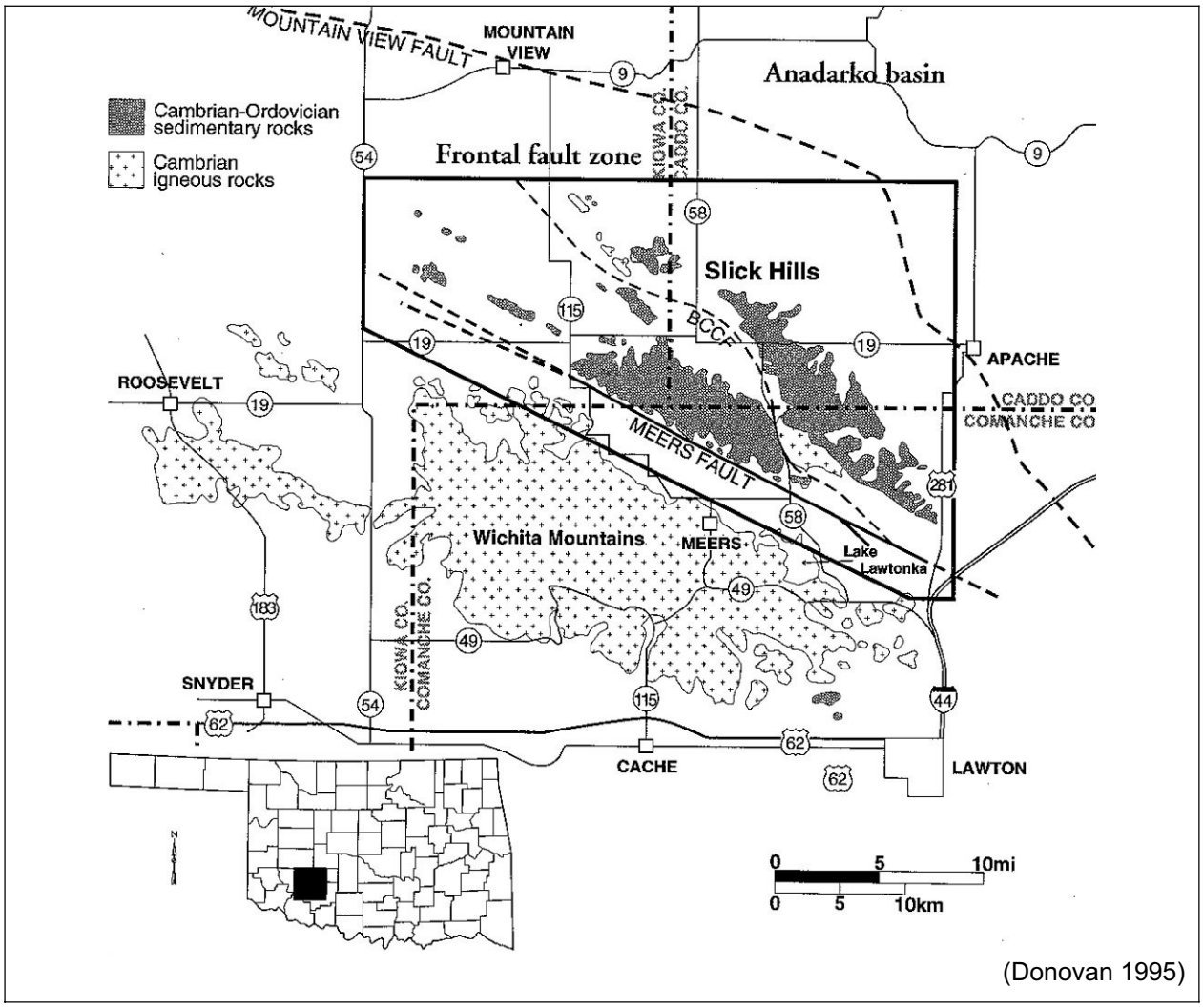

Fig. II-5. Frontal faults of the Wichita uplift, Slick Hills region

Magnetic lineations suggest that the Meers initiated during the early Cambrian as an extensional fault within the late Proterozoic trough. In the Arbuckle uplift to the southeast, the Washita Valley fault represents the northern margin of the aulacogen, juxtaposing Cambrian-age Colbert Rhyolite (Carlton equivalent) against Precambrian granite (Donovan 1995).

Transpressional, left-slip reactivation of the Meers, Mountain View, and other frontal faults during the Pennsylvanian created a series of shallow subsurface fault blocks stepping down from the uplift to the deep basin (fig. II-12), achieving a cumulative structural relief of more than 45,000 feet (Donovan 1995). About 6,500 feet of vertical offset occurred across the Meers fault; COCORP deep-reflection seismic traverses indicate that the Meers fault dips steeply $>70^{o}$ to the southwest, while the Mountain View displays moderate southwest dip at 30°-40° (Jones-Cecil, Donovan and Bradley 1995).

Most individual faults of the Wichita front, including the Mountain View, are buried under upper Pennsylvanian and Permian strata. The Post Oak Conglomerate suggests Permian reversal (up to the north) along part of the Meers fault (Jones-Cecil, Donovan and Bradley 1995). Minor, down-to-the-south offset along the Meers fault has occurred through Holocene time, accompanied by sinistral movement consistent with significant ENE-directed present-day compression (Hentz 1994) that created a prominent, 26-kilometer-long straight fault scarp about 1,050 years ago (Jones-Cecil, Donovan and Bradley 1995).

Miscellaneous Structures

Within the deep basin area is an en-echelon series of northwest-trending anticlines named (from east to west) Fort Cobb, Cordell, Sayre and Mobeetie. These folds suggest transpressional deformation along the Wichita fault system during Pennsylvanian time.

A prominent, NNE-trending isogravity high spans the Anadarko deep, oriented subparallel to and about 90 kilometers west of the Nemaha uplift. This (like most other anomalies in the isostatic gravity data) is assumed to reflect a change in basement lithology (Robbins and Keller 1992).

Hydrocarbon Production

This summary is based on the paper by Ball, Henry and Frezon (1991). Oil was first produced in the Anadarko basin in 1901 from Permian redbeds. The single most important accumulation is the giant Panhandle – Hugoton field in the shallow northwest corner in the basin, extending from the Texas Panhandle into southwestern Kansas. The trapping mechanism is the result of updip pinchout of carbonate rocks and granite wash on the Amarillo uplift, sealed by salt and anhydrite of the Permian Sumner group.

Eighteen additional giant fields (>100M boe) have been discovered. Three have EUR exceeding 100M barrels of oil equivalent (boe). These include the Sooner Trend on the northeastern shelf margin, producing from fractured Mississippian limestones; Cement field in

the southeastern basin, producing from Missourian-age quartz sandstone reservoirs; and the Postle field in the Oklahoma Panhandle, producing from Morrowan-age quartz sandstone.

There are ten gas fields with EUR exceeding 1-tcf. The Mocane – Laverne field of the Oklahoma Panhandle has an EUR of 5-tcf in Pennsylvanian quartz sandstone and Chesterian limestones. The Watonga – Chickasha trend, stretching north-northwest across nearly 90 miles in the southeastern Anadarko basin, contains an estimated 4-tcf in Morrow- and Springer-age quartz sandstones.

Nearly 700 fields have EUR > 1M boe; 107 are oil fields, 194 are gas, and 392 are classified as "neither" (gas + oil > 1M boe).

E. Site Characterization

Fractures and Stress

Several fracture studies have been conducted in the Anadarko region. Brevetti (1985) investigated subsurface fractures in Mississippian strata, and in the Devonian – Silurian Hunton Limestone, between depths of 9,000 to 9,330 feet in Kingfisher County, Oklahoma. The distribution was bimodal and orthogonal, with the dominant set trending north and the secondary set trending east. In Cambrian to Ordovician strata of the Slick Hills area, adjacent to the Meers fault, Wilhelm and Morgan (1987) found two populations of surface lineaments trending N30^{o} – 60 ^{o}W and N40^{o} – 50 ^{o}E, and explained these as northwest-trending left-lateral and reverse faults and northeast-trending right-lateral faults.

Donovan (1995) noted numerous tectonic stylolites and tensional fractures exposed in folds and near faults in the Slick Hills. Most of the fractures are calcite-filled. Some appear to be locally related to the folding, and may predate the formation of stylolites; most formed after the stylolites, but before the basal Permian unconformity. In the field and, a pervasive regional fracture pattern is observed that trends N40^{o} – 50°E (Donovan 1995), partially confirming the results of Wilhelm and Morgan's (1987) Landsat image analysis and implying a maximum horizontal stress orientation of N56^{o}E when these features were formed (fig. II-6).

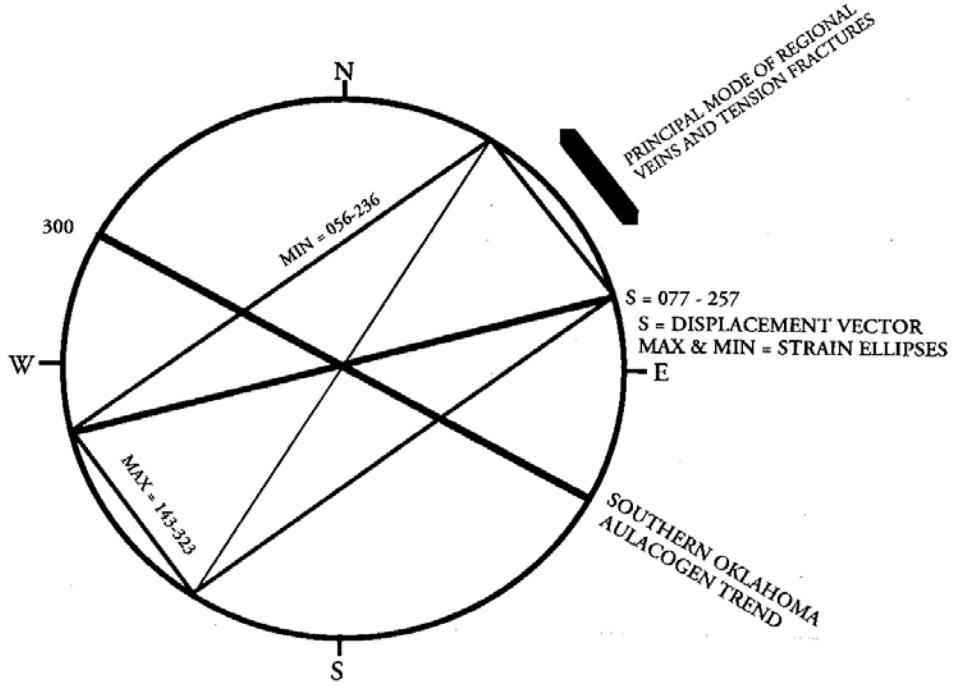

(1995 Donovan)

Fig. II-6. Fracture trends and strain orientations in the Slick Hills area

In the Marietta basin, on the south side of the Arbuckle uplift (fig. II-16), 84 natural fractures were identified intersecting six wells; these fractures had a mean orientation of N42^{o}E. However, 35 fracture-related wellbore enlargements observed in closely adjacent wells followed a N65^{o}E trend. This 27° offset may indicate the difference between paleostress orientation (natural fractures) and the present-day stress direction (wellbore enlargements).

In the Texas Panhandle to the west, vertical natural fractures are oriented N50^{o} – 60 ^{o}W at the Maxus Glasgow #2 well, and the present-day maximum horizontal stress orientation is inferred to be N75^{o} – 85°W (Hentz 1994).

Present-day stress orientations were based on wellbore enlargements measured in sixteen wells in the eastern Anadarko basin of Oklahoma (fig. II-7) (Dart 1990), at depths ranging between 2,450 and 13,200 feet.

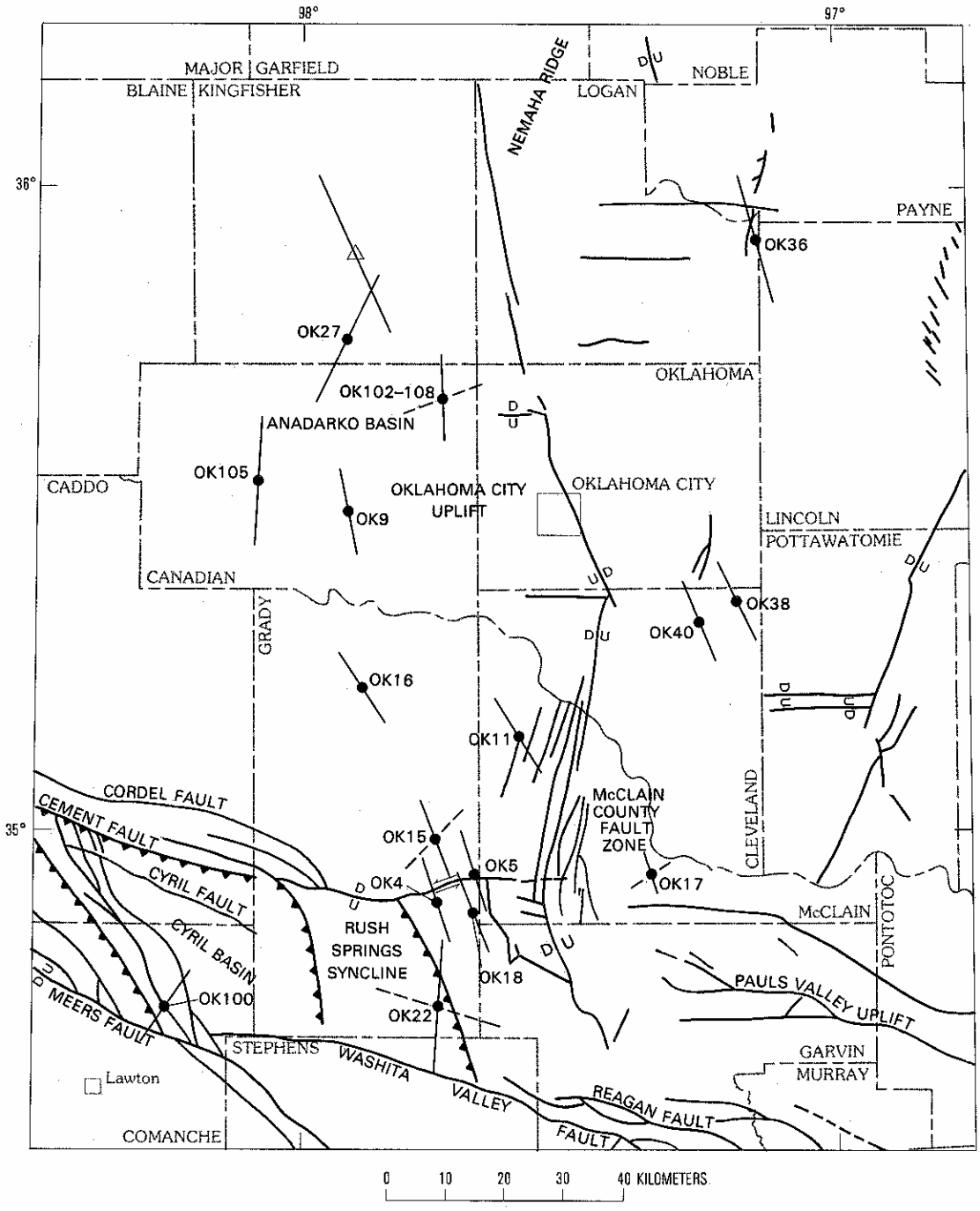

(Dart 1990)

Fig. II-7. Wellbore enlargements in eastern Anadarko basin

Dart assigned wellbore enlargements to one of two categories:

1. *Fracture enlargements* attributed to spalling from hydraulically-induced fractures, or natural fractures assumed to be oriented parallel to the present-day maximum horizontal stress orientation; or
2. *Wellbore breakouts* attributed to shear failure of the wellbore in a direction perpendicular to the present-day maximum horizontal stress orientation (fig. II-8).

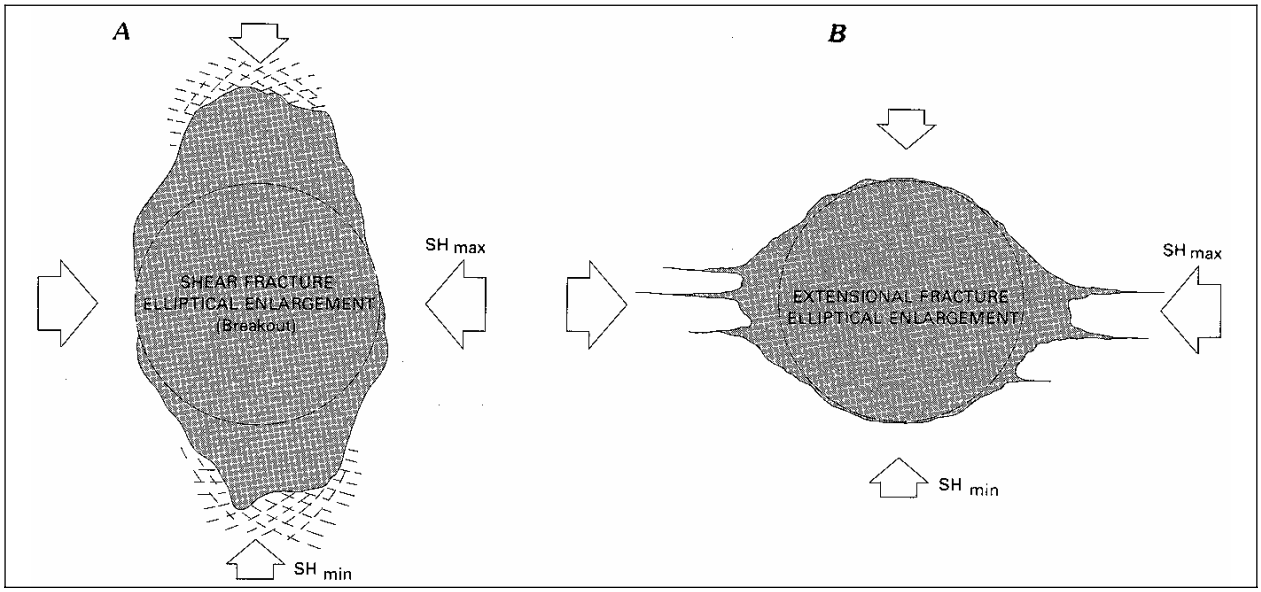

Wellbore breakout (A) vs. fracture enlargement (B) (Dart 1990)

Fig. II-8. Schematic illustration of wellbore breakout vs. fracture enlargement

Fracture enlargements in the eastern Anadarko wells were relatively infrequent. Most were considered true breakouts due to spalling, implying that natural fracturing may be rare. A marked decrease in borehole breakouts between about 6,000 feet and 9,000 feet suggests either increased tensile strength or decreased ratio of maximum vs. minimum horizontal stress over this interval.

The breakout orientations were remarkably consistent, yielding a present-day maximum horizontal stress orientation of N78^{o}E. The few fracture enlargements indicate an orientation of N51^{o}E. Hydraulic fracture data from a single well in Kingfisher County suggest an intermediate N65^{o}E direction.

Breakouts also investigated by Dart (1990) in adjacent regions (fig. II-9) exhibit bimodal distributions, but indicate present-day maximum horizontal stress orientation of N41^{o}E in the Marietta basin to the south, and N49^{o}E in the Bravo Dome area to the west. Dart (1990) attributes this azimuthal shift to a regional transition in stress regimes, from a normal-fault-dominated regime in the Texas Panhandle to strike-slip and reverse-slip dominated regimes in Oklahoma.

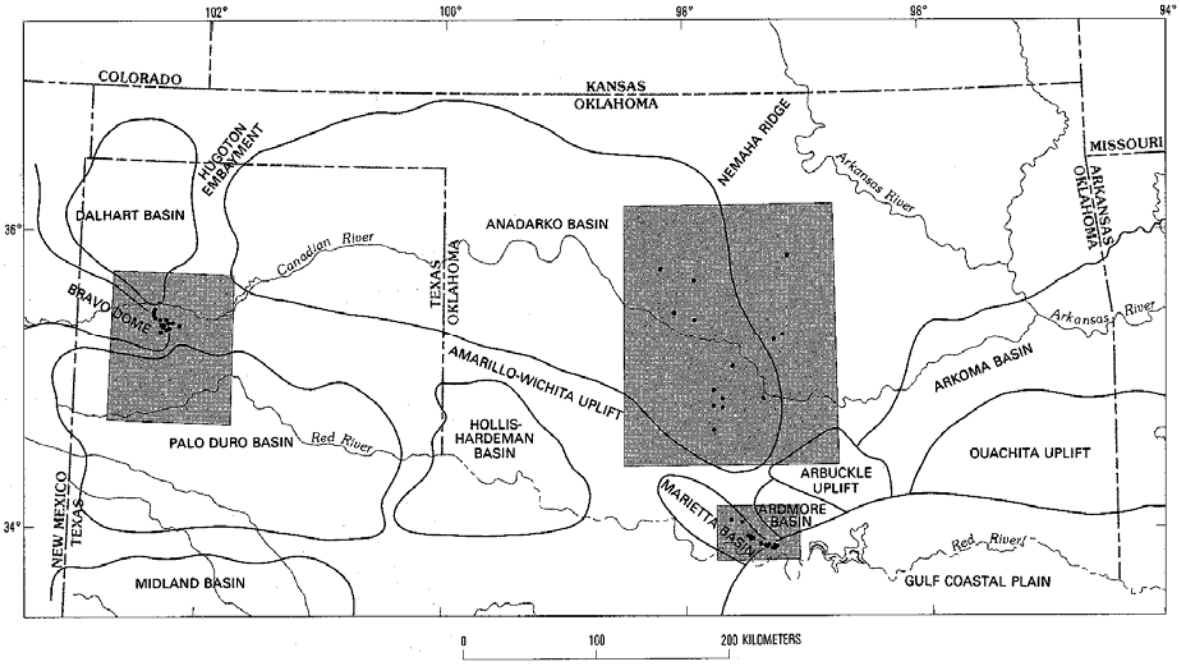

Detail from eastern Anadarko.

Fig. II-9. Locations of borehole breakout studies conducted by Dart (1990)

Core and logs from eight wells across the study area were examined for evidence of natural fractures, their orientation and impact on hydrocarbon productivity. The results are listed in Table II-1. While several contained some evidence of fracturing, the majority were filled with calcite cement and appeared ineffective from a permeability standpoint. In one case, fig. II-10, the fracture had not only been cemented it had been folded around adjacent clasts post cementation. Only one well, the Marie Walters 1-14, contained sufficient high quality data to build a compelling case for a naturally fractured reservoir interpretation.

Table II-1 is a summary of the core and image log observations for the Anadarko. See Appendix A for detailed core descriptions.

Table II-1. Core and Image Log Observation Summary

Well Name/ Location	Operator	Data	Formation	Data Interval	Interpretation
1. Walter Steffes 1-5 S. 5, 9N 19W	Kaiser-Francis	Core *(3/89)*	Atoka B	13,625'-13,662' 13,692'-13,727'	Major set of fractures, calcite filled
2. Simmons 2-31 S. 31, 12N 22W	Apache	Core *(6/88)*	U. Morrow (Puryear)	17,488'-17,548	Minor natural fractures
3. Marie Walters 1-14 S. 14, 10N 21W	Kaiser-Francis	FMS *(8/89)*	Atoka D	12,200'-13,918'	Major open natural fractures present
4. Flying J 3-11 S. 11, 9N Y	Burlington	EHI *(9/95)*	Cherokee/ Redfork	12,400'-13,651'	Minor Natural Fractures
5. Sunny Joe 2-35 S. 35, 10N 20W	Burlington	FMI *(4/99)*	Granite Wash/Atoka Morrow	12,550'-13,500' FMI 14,200'-15,024' FMS	Atoka: Healed natural fractures, wellbore breakout, EW trend Morrow: Poor Data
6. Cletus Pete 1-31 S. 31, 10N 20W	Burlington	EHI *(11/95-8/96)*	Cherokee/ Granite Wash	10,636'-10,969' 10,870'-11,851' 12,450'-13862'	Indication of limited natural fractures
7. Goodwin 1-11 S. 11, 11N 23W	Burlington	EHI *(9/81-10/95)*	Cherokee/ Granite Wash	12,316'-14,470'	Minor open natural fractures
8. Paul King 1-17 S. 7, 10N 21W	Trigg Drilling	Core	Morrow	15,863'-15,888	Minor open natural fractures

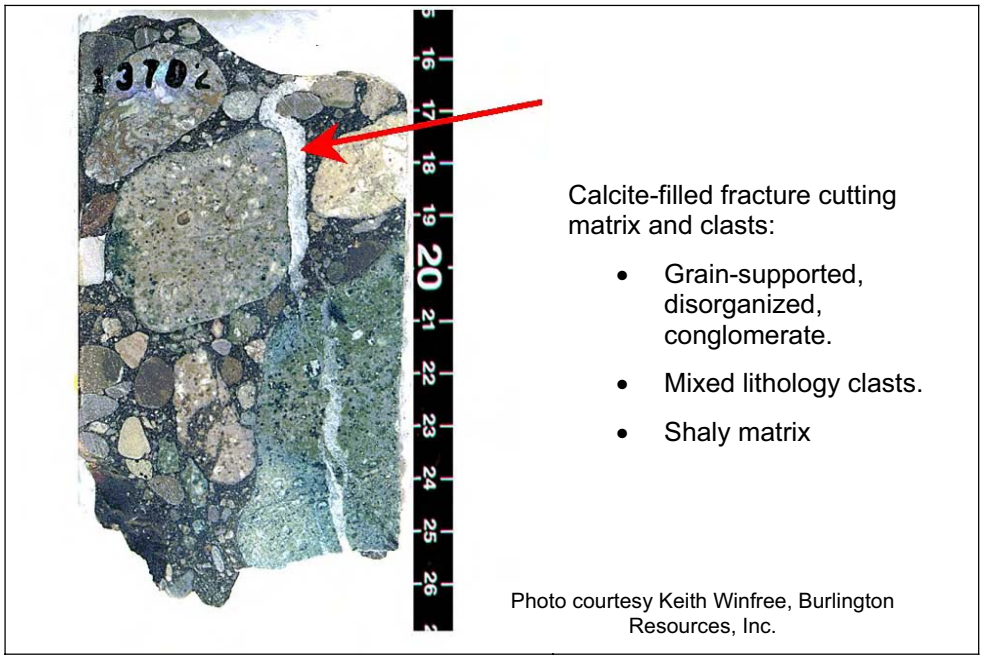

Fig. II-10. Atoka natural fractures

Key Well

The Marie Walters 1-14 (see location map, fig. II-11), drilled in section 14, TXN, RYW, is the key reservoir characterization well for the Elk City field demonstration. This well best illustrates the drilling, logging and production behavior characteristic of a naturally fractured reservoir. Other wells in the area exhibit anomalous production behavior or other characteristics but the *Marie Walters 1-14 was the only well encountered where quality reservoir characterization data was available*.

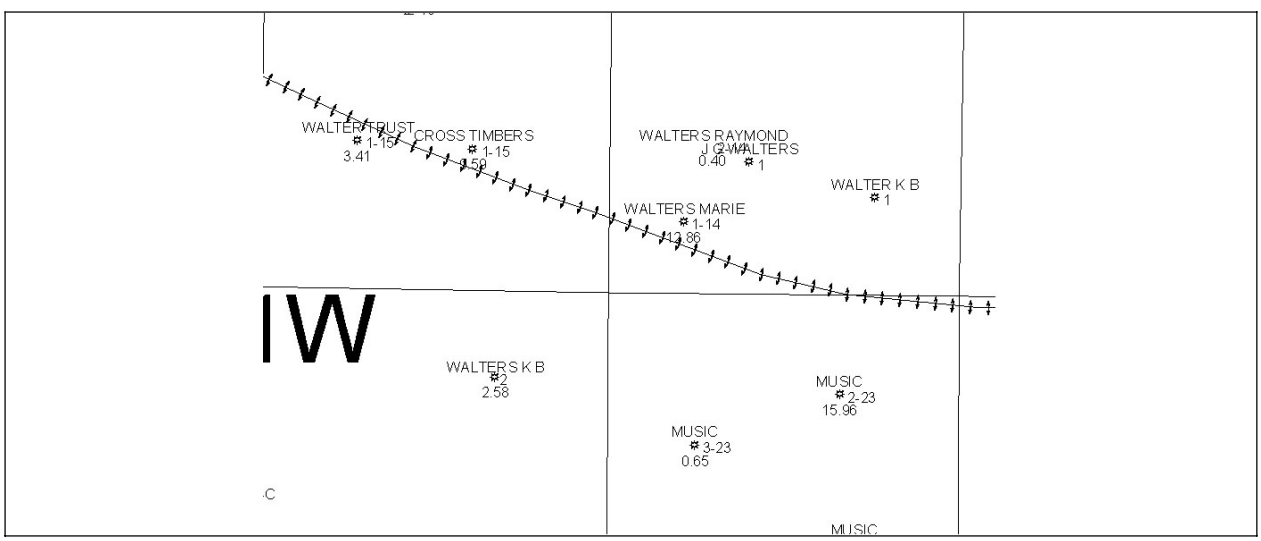

Fig. II-11. Marie Walters 1-14 location

The arbitrary seismic line in fig. II-12 shows the general shape of the Elk City structure. The Marie Walters 1-14 was drilled near the crest of the broad anticline. The broad anticlinal structure is nearly four miles wide but it has a sharp crest with relatively steep dips off to the flanks.

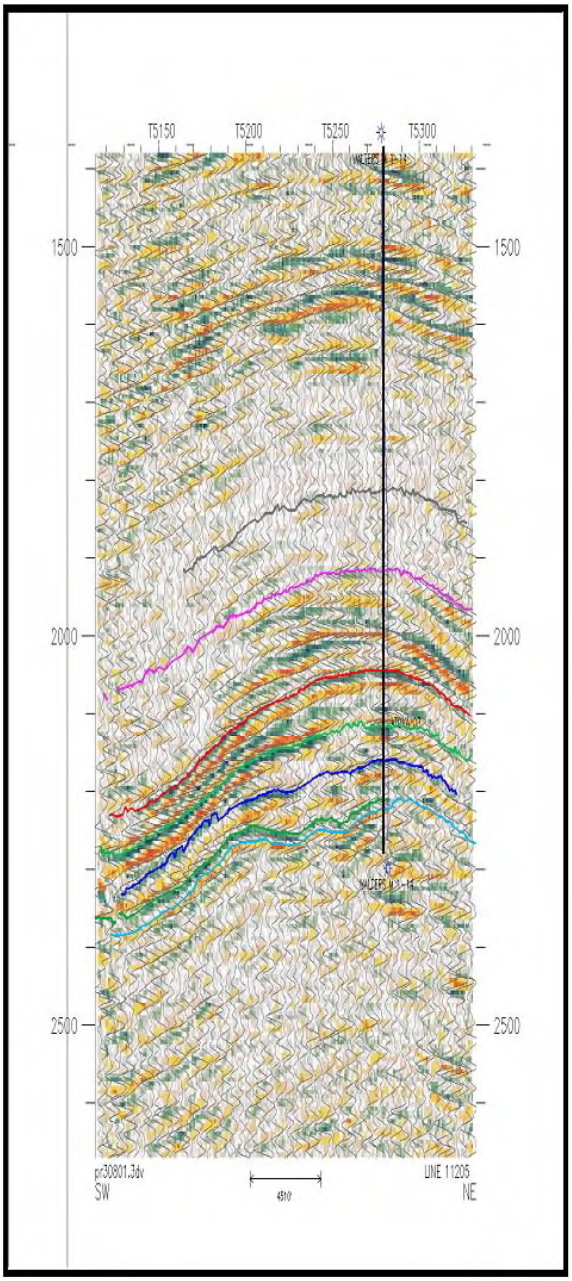

Arbitrary seismic line across the Elk City structure near the Marie Walters 1-14. Note the poorly imaged complexity below the pink horizon. Length of the seismic line is approximately 6 miles.

Fig. II-12. Marie Walters seismic transect

Drilling mud logs for the Marie Walters record a modest drill break and a 350 bbl mud loss when drilling an interval at 13,204' MD (Atoka). The formation micro-scanner (FMS) log run later indicates a single large aperture natural fracture extending over approximately 6 feet of the well bore (fig. II-13). The initial, untreated natural flow rate is reported to be 4.25 MMcfd. After a hydraulic fracture treatment using 142 kgal fluid, 12.5 klbs of 100 mesh sand and 150klbs 20/40 sand the well reportedly flowed 27 MMcfd calculated absolute open flow (CAOF).

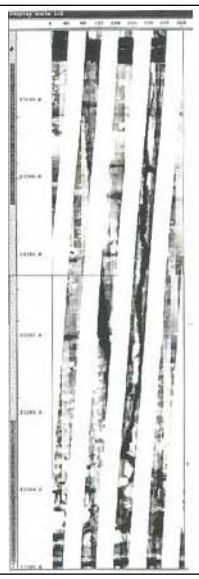

ESE Trending 6' shear fracture. 13,199'- 13,205' MD. 350 Bbl lost circulation zone. 2000 unit gas show. Tested natural 4.25 MMcfd

Fig. II-13. Marie Walters 1-14 FMS

The well produced consistently for ten years following its completion, yielding a cumulative 11.7 bcf and 193,000 barrels of oil (BO) respectively. EUR estimates by decline curve, pressure/cumulative gas, and PTA all yield values in the range of 13-17 bcf (G. Koperna, pers comm., 2000). PTA of the pressure drawdown over time further indicated long term bi-linear flow (1/4 slope on a log-log plot)-consistent with a fractured reservoir interpretation (fig. II-14).

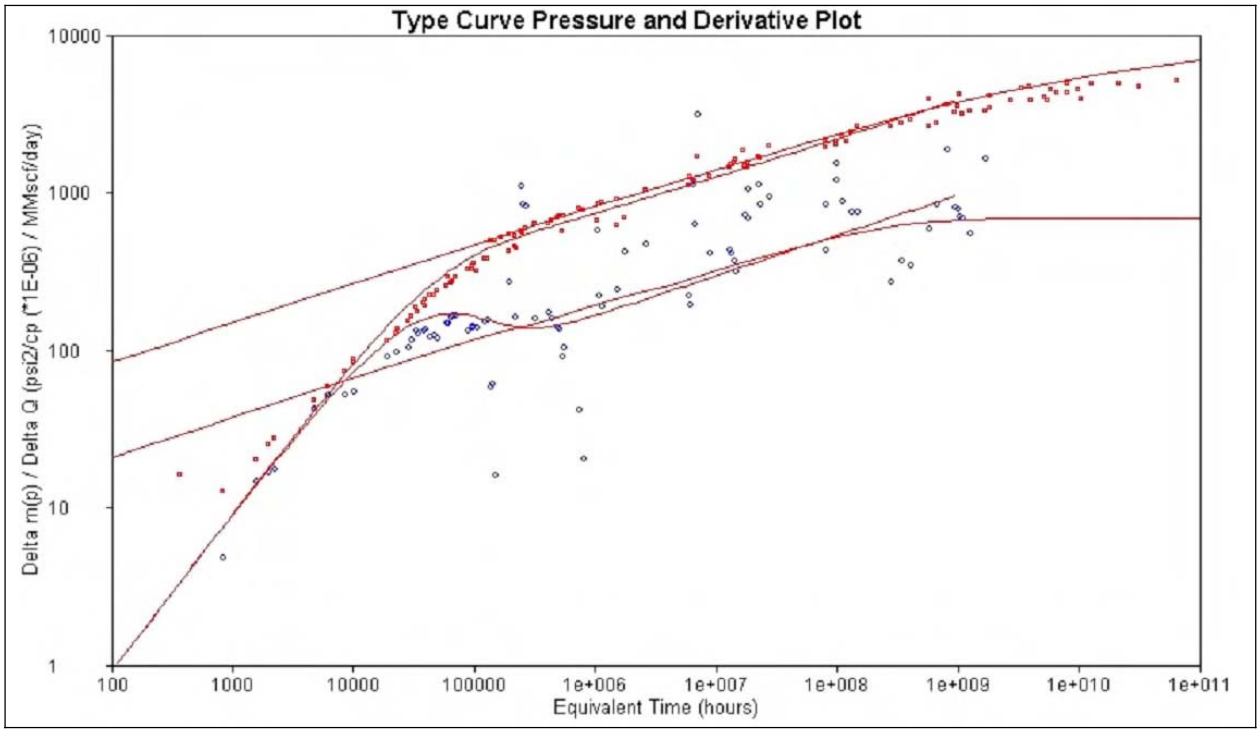

Ten years of production rates and reported pressures were used to construct a type curve pressure and derivative plot. Type curve analysis demonstrates long-term bi-linear flow behavior, equivalent to a finite conductivity hydraulic fracture model, i.e., log-log plot of data follows 1/4 slope (G. Koperna, 2000, pers comm).

Fig. II-14.Marie Walters 1-14 type curve pressure and derivative

Petrophysical evaluations of logs in the area must be specifically tailored for individual pay zones and are valid only over small areas. The upper Paleozoic reservoirs in the area are composed of immature sands and polymictic layers of conglomerate (fig. II-15). Conglomeratic clast compositions vary radically between carbonate, metamorphic and igneous as the adjacent Wichita Uplift was denuded.

Reservoir petrophysical properties, particularly grain density, must be calibrated locally to establish pay criteria. No local core data was supplied for calibration, which rendered accurate petrophysical interpretation nearly impossible.

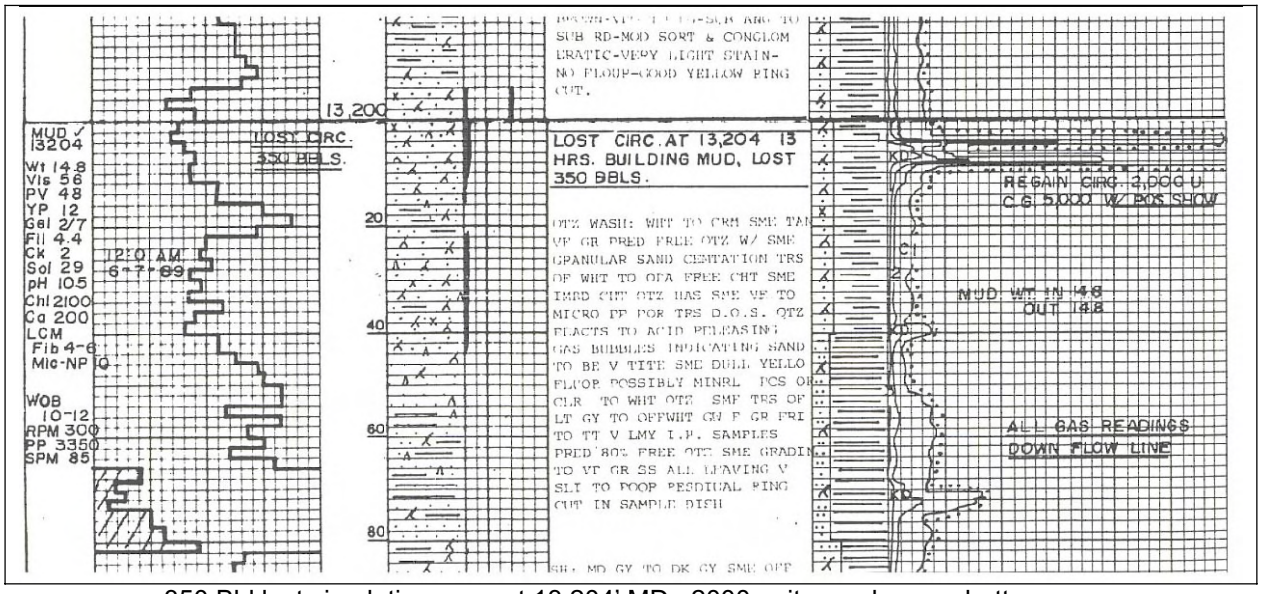

350 Bbl lost circulation zone at 13,204' MD. 2000 unit gas show on bottoms up

Fig. II-15. Marie Walters' mudlog

Summary

Characteristics of nearby productive analogs were used to frame the play concept for the exploration demonstration. The field demonstration targeted an irregularly distributed polymictic Paleozoic reservoir interval where natural fractures, particularly those involving a shear sense of movement, had enhanced the in situ permeability of the reservoir. The only known fracture definitively associated with production showed an east-southeast trend. The aggregate information regarding present day principal horizontal stress for the areas indicates a northeast to east direction.

Fracture Summary

- Image log in Marie Walters indicates large shear fractures play major role in production.
- Core study indicates Type 1 fractures tend to be cemented and likely tight.
- Reservoir modeled as dominated by shear fractures related to faulting.

F. Prospect Generation

The Elk City Field is located on a deep anticlinal structure downthrown and basinward of the main Wichita Uplift Frontal zone (fig. II-16). The target reservoir is an unnamed geopressured interval within the Pennsylvanian-Permian unroofing sequence derived from the uplift.

Prospect generation for the Elk City field demonstration incorporated the following steps:

1. Seismic interpretation
2. Boundary Element Modeling
3. Discrete Fracture network simulation
4. Integration with the reservoir distribution projection (operator supplied, confidential)
5. Calibration to production
6. Delineation of prospects

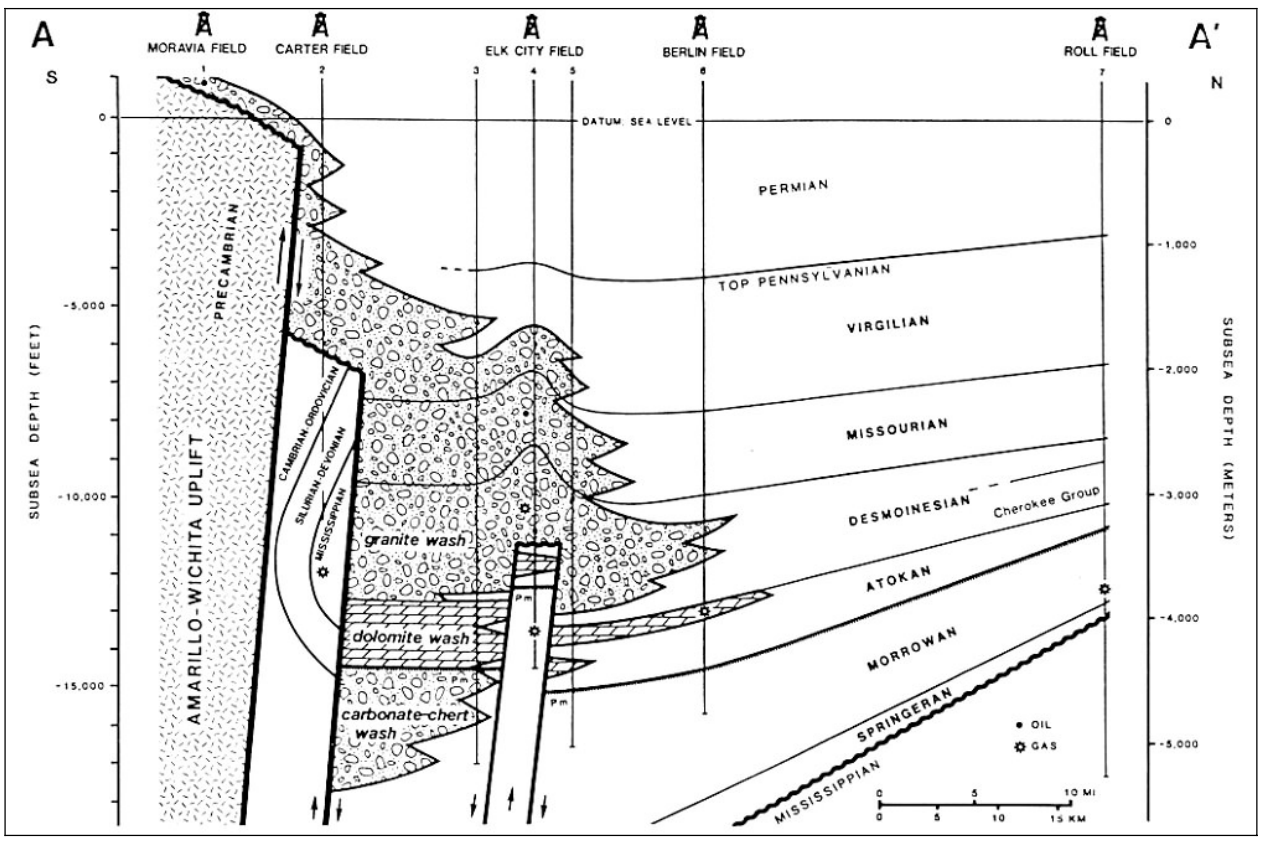

Typical presentation of Wichita Front structure: large vertical exaggeration (in this case, 12:1) results in apparent near-vertical fault geometry.

Fig. II-16. Anadarko-Pennsylvanian structure with exaggeration

Seismic Interpretation

The 3D seismic volume was interpreted to identify and depth convert the major faulting in the area of interest. Fig. II-17 is a time slice near the reservoir interval that shows the complexity of the faulting in the core of the structure where the objective was believed present.

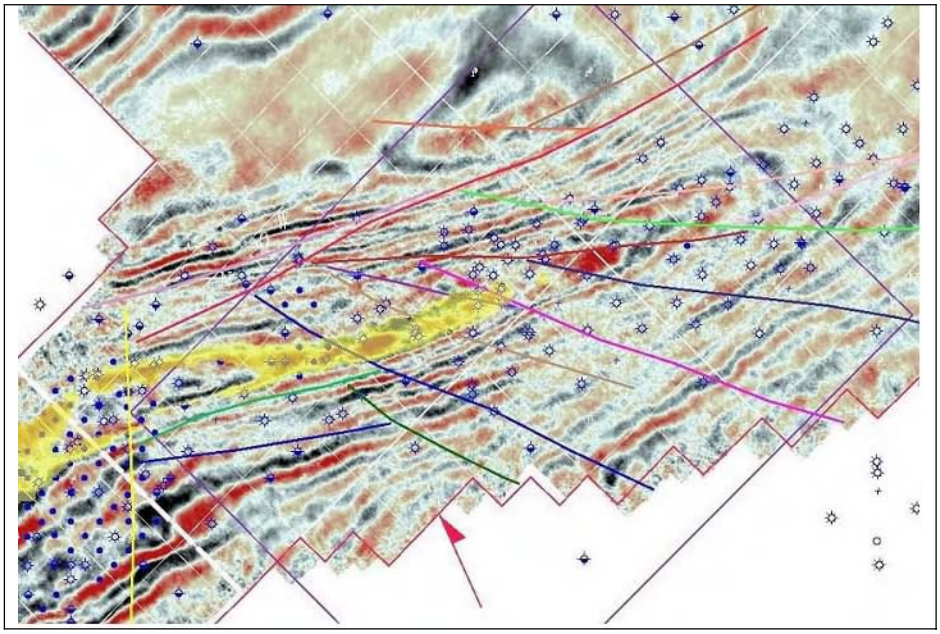

Fig. II-17. Faulting timeslice

Fig. II-18 is an arbitrary NE-SW section through the general area. The faults are interpreted to intersect and sometimes are themselves displaced across other faults. The overall style of deformation appears almost viscous in nature as might be characteristic of a syntectonic transpressional setting.

The faults were mapped in time and converted to depth for Poly3D modeling. The faulting in the seismic volume under consideration was more complex than could be reliably interpreted or simulated. The faults were screened to identify only the largest most significant features considered of prime importance to the development of the structure.

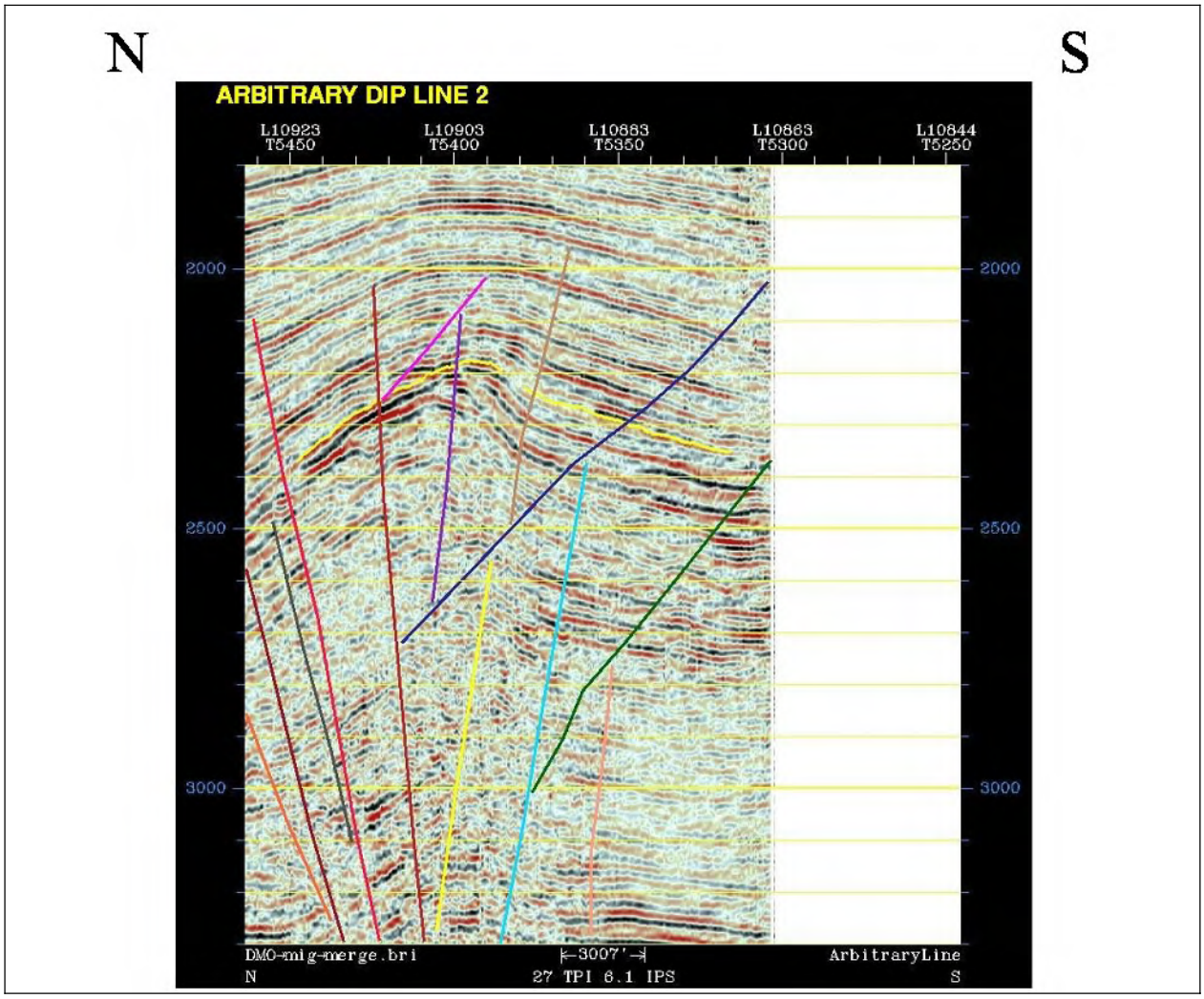

Fig. II-18. Vertical section

The faults generally strike northwest-southeast but dips range from southwest to northeast and were typically very steep. Fig. II-18 shows several faults and their complex structural style. In this view the fault surfaces have been gridded and meshed for input to the Poly3D simulation. The relative direction of fault plane dip is shown by the color of the mesh, red is high, blue is low.

Fault strike within the structure is generally around a NW-SE azimuth. The dip on the faults is steep and varies somewhat with the position relative to the anticlinal axis. Faults to the SW of the axis tend to dip steeply to the NE and vice versa for faults to the NE of the axis. Some faults appear to be antithetic in nature. Total shortening across the structure was not calculated but exceeds 30% by visual estimate.

Several faults were interpreted to cut the objective horizon. Fig. II-19 illustrates the relationship of the objective horizon (colored contours) and the faults (meshed edges). Minor offsets in the structure contours reflect the presence of uninterpreted and subseismic scale faulting.

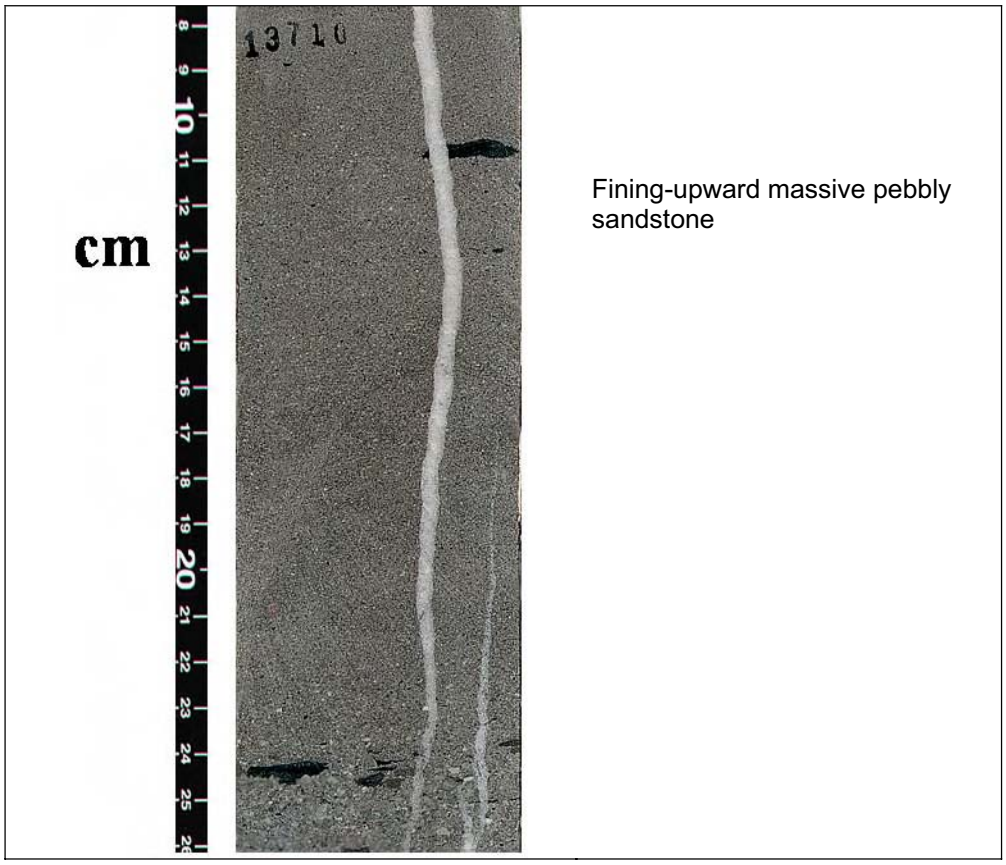

Fig. II-19. Atoka Steffes reservoir large calcite-filled fractures

Multiple strike and dip directions of faulting will probably generate several directions of fracturing which accounts for bi-linearity and lack of classical fractured reservoir production behavior.

Boundary Element Modeling

The core of the Elk City anticline is a challenging structure to model mathematically. The faults have complicated, anastomosing geometries that reflect a complex development history. No single event or feature could be isolated as controlling the structural development of the reservoir. The Elk City area differs from the Bullfrog area in this regard. Where the Bullfrog structure had a relatively simple kinetic style with identifiable elements, the Elk City structural elements show complex, almost ductile, kinetic relationships.

No realistic failure criteria were available for the reservoir and the large amount of shortening indicated system strain well beyond a simple elastic scenario. North 140 degrees east was used as the azimuth of principal horizontal stress. This agrees with calcite shortening directions presented by Harrison (1999, DOE).

Calcite twinning and differential stress values for areas in the Appalachians were outlined in van der Pluijm et al (1997). They report inferred differential stresses near the center of the Appalachian orogenic belt to be on the order of 100 megapasals (MPa). A remote stress of 100 thousands of pounds per square inch (kpsi) at an azimuth of N140E was used as the boundary condition for the simulation. This value may be high but the inelastic nature of the deformation (as evidenced by calcite twinning and convoluted structural style) preclude a meaningful brittle failure analysis and it simplifies the mathematics.

The seismic fault interpretation was generalized for modeling purposes. The interpenetrating faults in the core of the structure were first edited and then simplified in order to build an executable Poly3D model. Fig. II-20 illustrates an intermediate step in the iterative process.

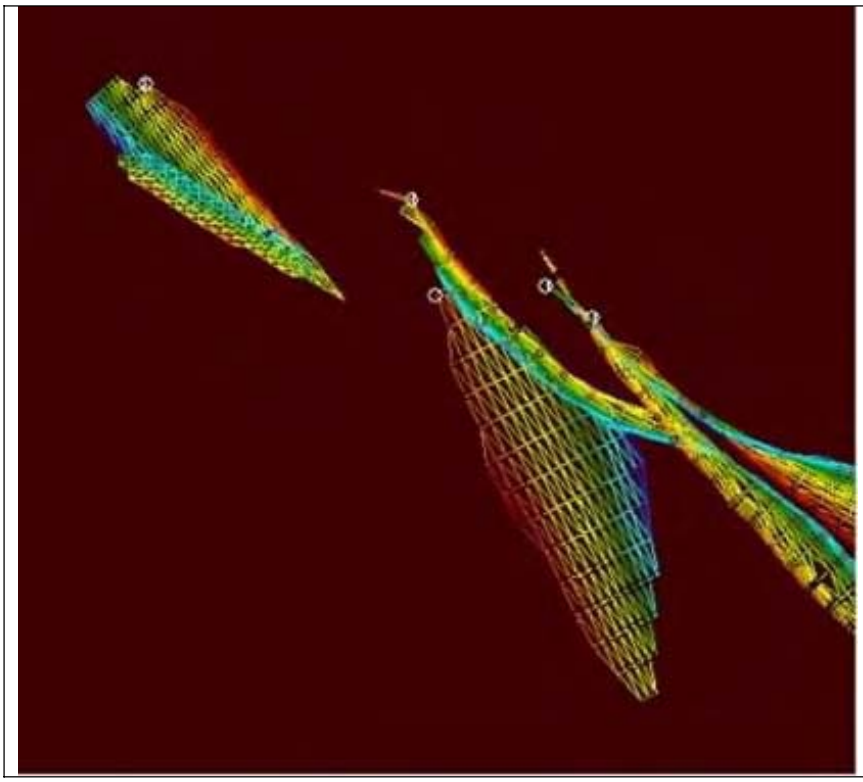

A screen capture from the model construction process showing some of the final fault surfaces gridded and meshed for the simulation. This model failed but this screen capture shows the complex fault pattern near the right side that delivers the best fit to the structure and productivity in the Steffes area. The faults in the upper left are in the area of the Marie Waters and must interpenetrate which caused this early model to crash.

Fig. II-20. Anastomosing, interpenetrating faults within the structural core of the anticline.

Fig. II-21 illustrates the relationship between the simulated fault planes and the reservoir horizon. Several small culminations occur along the anticlinal axis of the long narrow structure. The local culminations are the result of vertical displacements along the anastomosing reverse faults within the structural core.

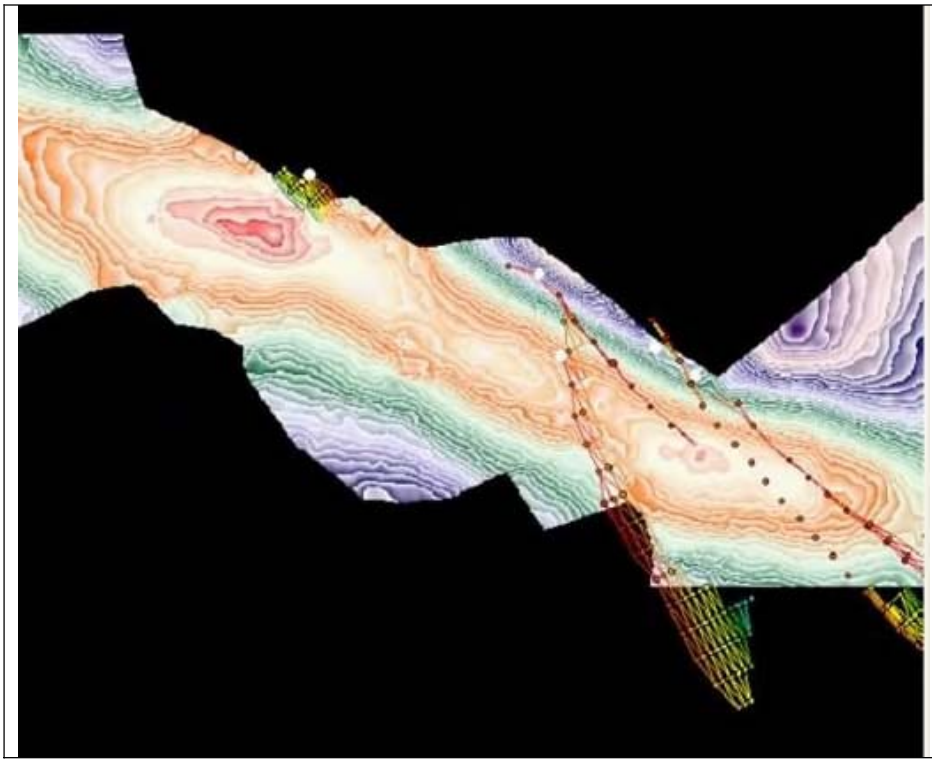

The faults with the reservoir depth map showing the relationship between the reverse faults and the local structural culminations. Red and Orange tones on the depth structure map are local highs.

Fig. II-21. Reservoir horizon and faults in depth.

Fit to present day structure was used as the major criteria by which to judge the simulation quality. Interference between the faults in the model was a major consideration during the simulation phase. The most likely explanation for this problem was that subsequent deformation had distorted the original brittle fault geometries. Fig. II-22 shows the vertical displacement calculated in the final simulation. The combination of fault geometry and stress orientation has resulted in the growth of a local structure on the hanging wall of a fault that agrees reasonably well with present day structure.

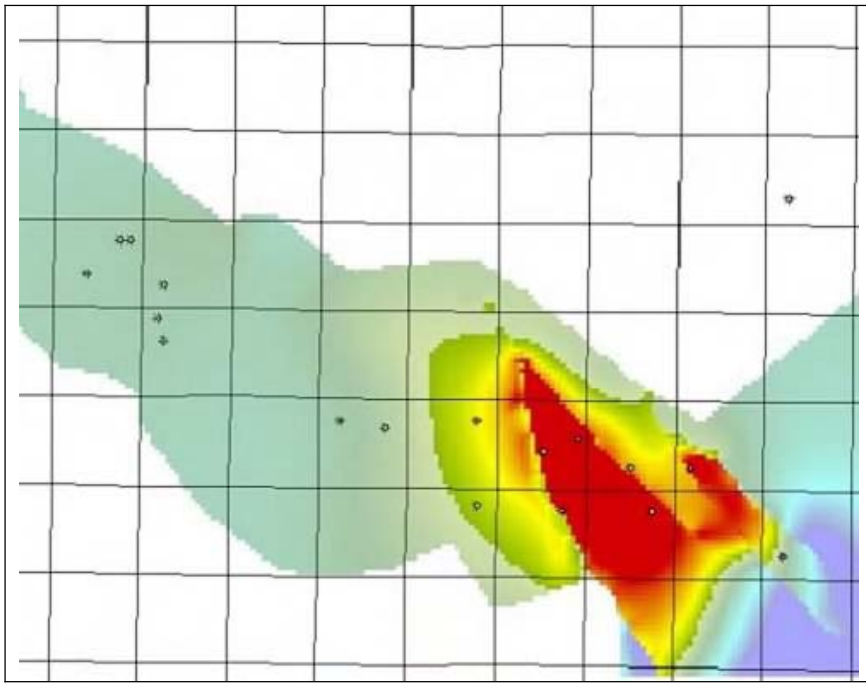

Vertical displacement was used to judge the quality of the model. If the positive (red) areas lie under the antiforms, then the model is a reasonable (but probably not unique) solution.

Fig. II-22. Simulated Vertical displacement of an area of the Elk City structure.

The Poly3D simulations indicate the crestal area of the structure has been subjected to considerable shear stress related to the propagation of the internal faults and growth of the Elk City structure (figs. II-23 and II-24). The simulation generates relatively large shear stresses (both Coulomb and Maximum, reds) along and between the faults along the axis of the anticline This was consistent with the nature of the Marie Walters FMS log and the lack of significant open undeformed extensional joints observed in the cores.

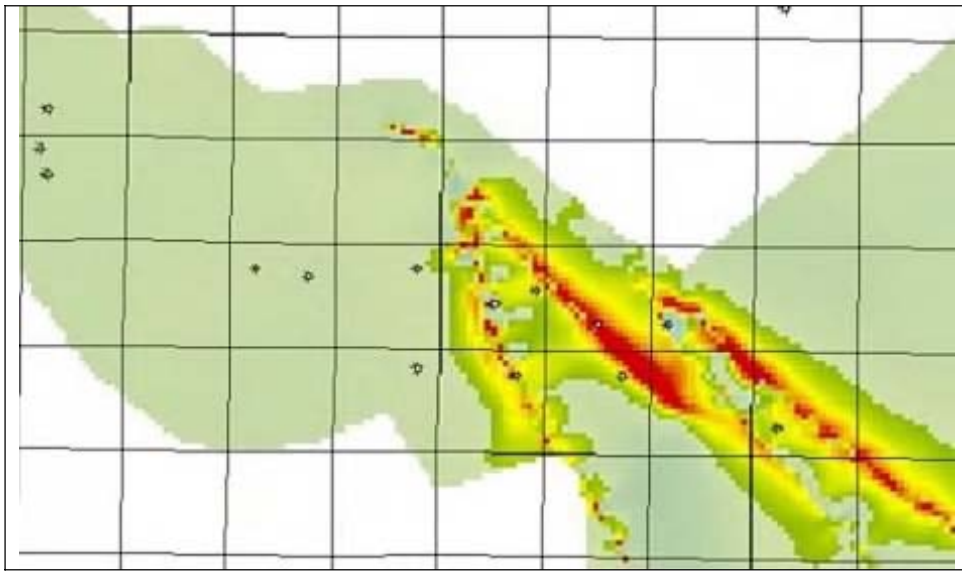

Note narrow bands of higher (red) Coulomb shear stress along and between faults.

Fig. II-23. Coulomb stress

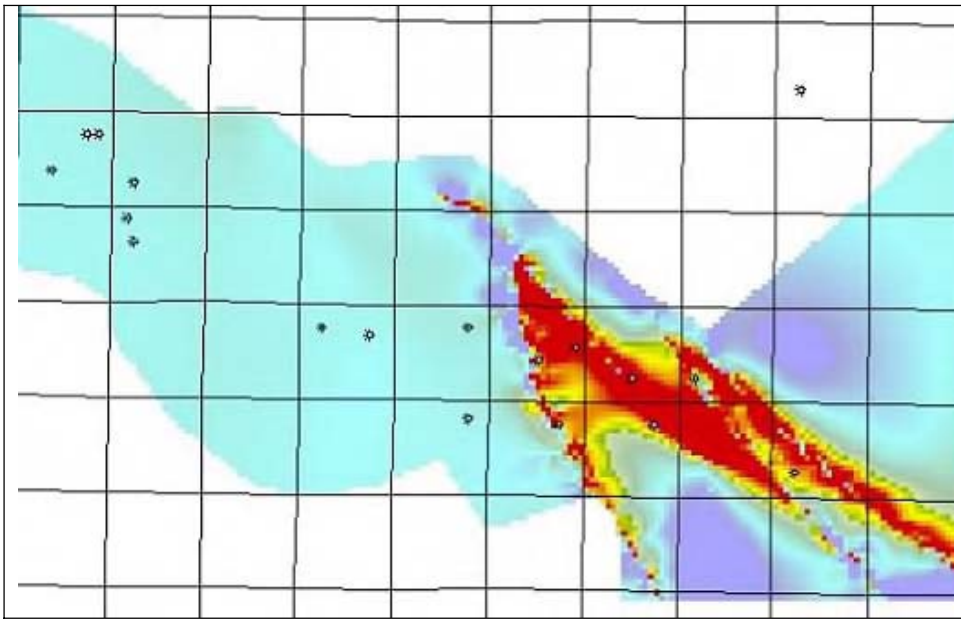

The red areas on this map indicate the areas of higher simple maximum shear stress generated along the faults and the crest of the anticline where the faults interfere.

Fig. II-24. Max shear

The simulation results, FMS log and core descriptions, taken in conjunction with the calcite twinning results from Versical reported by Harrison (1999) portray the structural setting of the Elk City structure as intensely compressional with significant inelastic deformation. Further pursuit of elastic mechanical simulation methods to predict the distribution of effective natural fractures in this setting was not justified.

FracGen Modeling

The complex nature of the faulting and inelastic shortening involved in the growth of the structure preclude effective use of elastic BEM techniques. Instead, FracGen, a DOE discrete fracture network software package, was used to predict a permeability grid across the project area. FracGen generates a statistically valid geographic distribution of natural fractures based on a set of hierarchical, descriptive input parameters.

The geographic distribution and characteristics of the resulting fracture network is controlled using attributes derived from seismic, well data or other interpretations. The hierarchical nature of the fracture network generation process allows for the incorporation of dependencies, if needed. FracGen itself was executed stochastically and the results summed across the project area.

The Marie Walters study well indicated the productive natural fractures in that well were shear fractures propped by asperities. Such fractures are related to the small scale faulting observed across the structure on the 3D seismic. In the absence of additional data, the FracGen input file was created using fracture population statistics from a Laramide transpressional structure (based on a more robust data set).

The orientations and locations of the faults are determined from a seismic time slice near the reservoir depth and the patterns of stress accumulation calculated by the structural simulation. The orientations of the subordinate fractures along the faults are adjusted to fit the Marie Walters FMS data (which indicated a general east southeast azimuth). Fig. II-25 is a screen shot captured during the construction of the FracGen model.

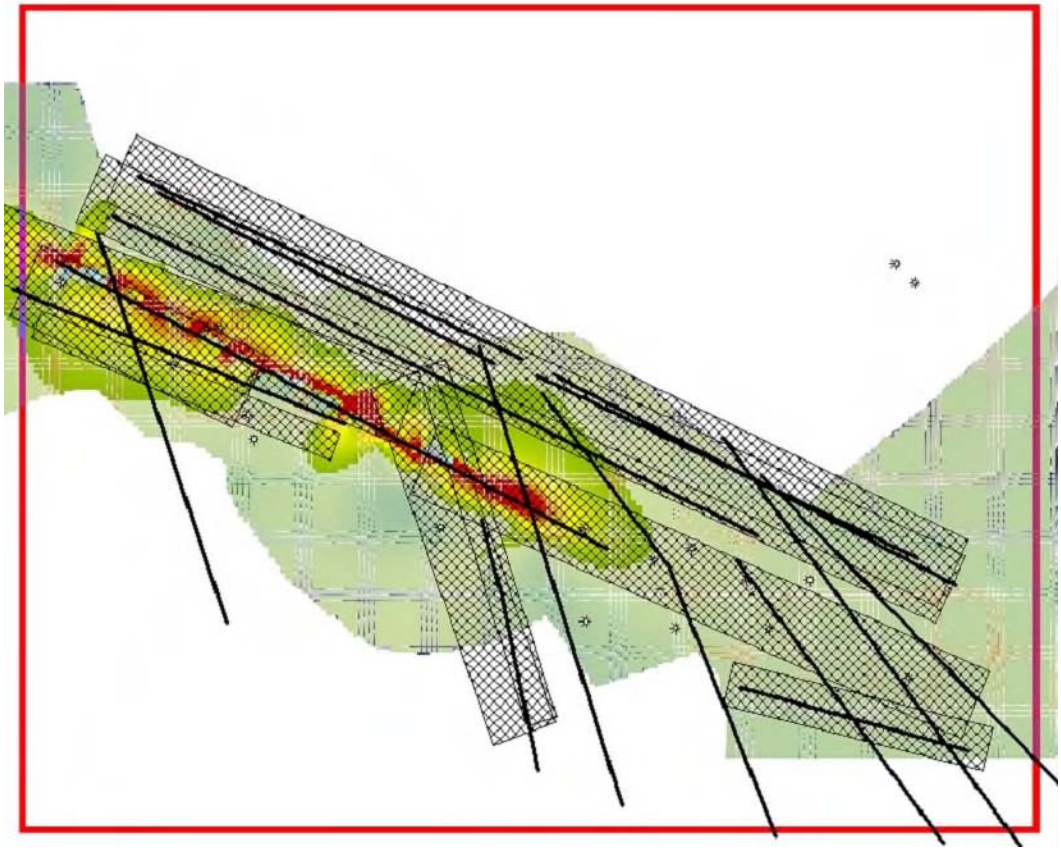

This is a panel from the Discrete Natural Fracture model. The black lines and hachured boxes are the loci for the generation of the stochastic fracture model. Each set has it's own character, aperture etc., described as statistics.

Fig. II-25. FracGen model-Coulomb stress example.

The FracGen model itself is stochastic in nature and the model was executed 100 times with the results stored in a database for later aggregation. End point locations and aperture are captured for each fracture of each run. Fig. II-26 is a screen shot of one realization.

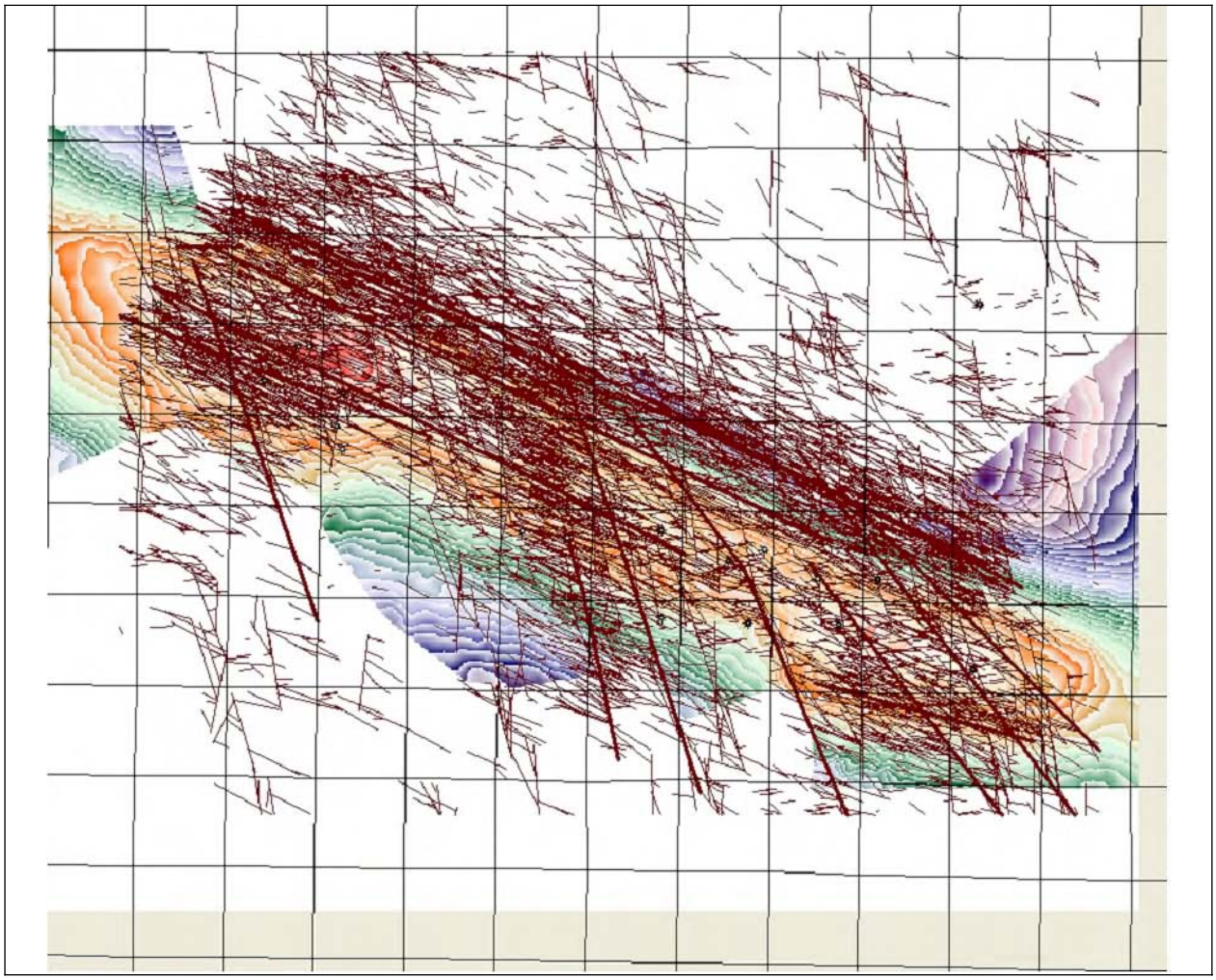

One realization of the final FracGen model superimposed on depth structure. Each fracture's aperture, length, etc., are summed in a grid and stored in a database for use in the perm transform. A significant degree of randomness was used to compensate for sub-seismic scale faulting.

Fig. II-26. FracGen model realization

A map of relative permeability (fig. II-27) related to the fracture system was prepared from the FracGen output. Cumulative aperture of all "fractures" present within individual grid cells was calculated using a cubic power function (permeability proportional to cumulative aperture cubed). No true permeability values derived from well control were available to establish a more exact calibration. All fractures (regardless of orientation) were assumed to be open and effective which was believed reasonable if they were all fault related shear fractures.

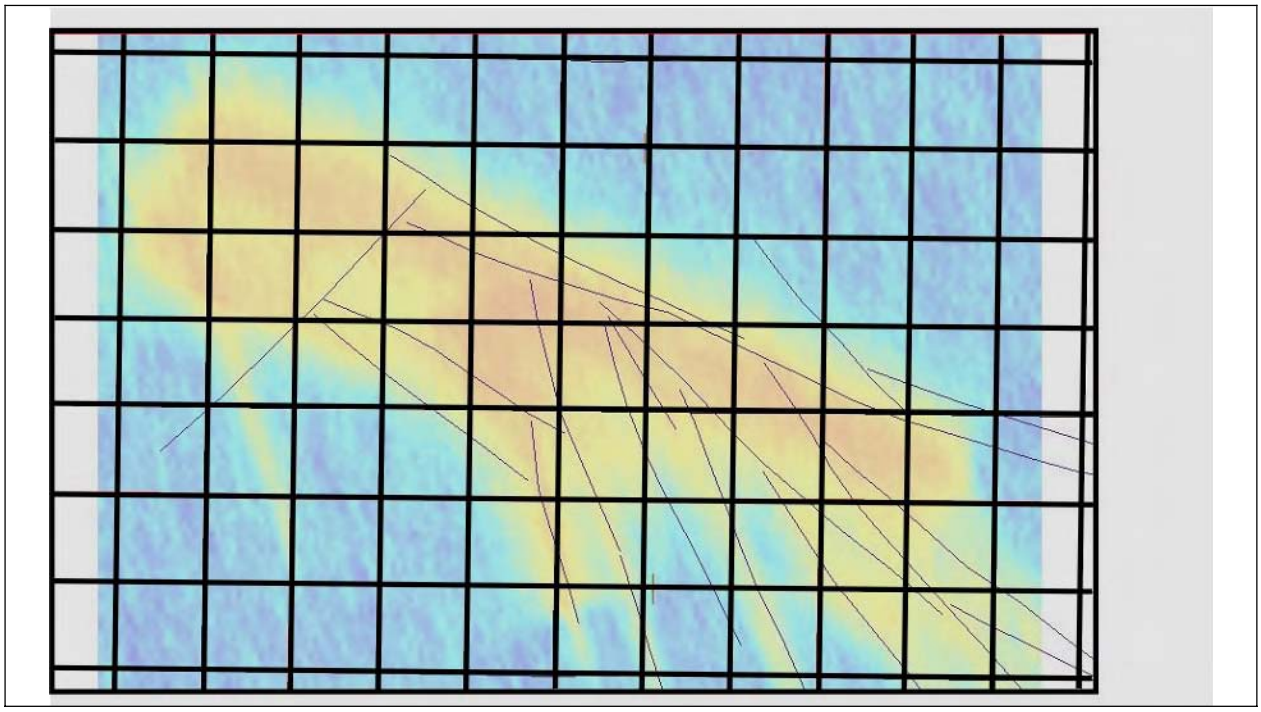

A standard cubic power law of aperture size was used to generate a “relative” fracture permeability map. No exact scaling of values. Blues are lower permeability, yellows to browns are higher. The highest permeability areas lie along the crest of the structure and where faults trend oblique to the axis.

Fig. II-27. Discrete Fracture Network (DNF) permeability from Poly3D and FracGen simulations

Calibration and Prospect Generation

The Elk City area is a highly competitive business environment. Interpretations of reservoir distribution are jealously guarded by operators. The following discussion of calibration and prospect generation will not refer to areal reservoir distribution (which was supplied by Burlington under confidentiality agreement) even though total recoverable gas is a function of both permeability and reservoir volume.

Estimated ultimate recoveries were generated through decline analysis for seven calibration wells in the project area. These values ranged from near zero to 19+ BCF. Only two wells exceeded 16 BCF recoverable and the average was slightly less than 7 BCF/well. Wells with very large (2-4 times the mean of a population) occur sporadically in this area. Often there is little else besides a large IP or near flat decline to distinguish them from their neighbors. Two such wells were present in this data set.

The operator provided average porosity and thickness values for the calibration wells. There was a poor correlation between the log derived estimates and EUR (fig. II-28).

The pseudo permeability grid was sampled at the locations of the calibration wells. The correlation between pseudo permeability and EUR was better than simple Phih and EUR. (fig. II-28). Dropping the "flyer" wells improved the correlation significantly.

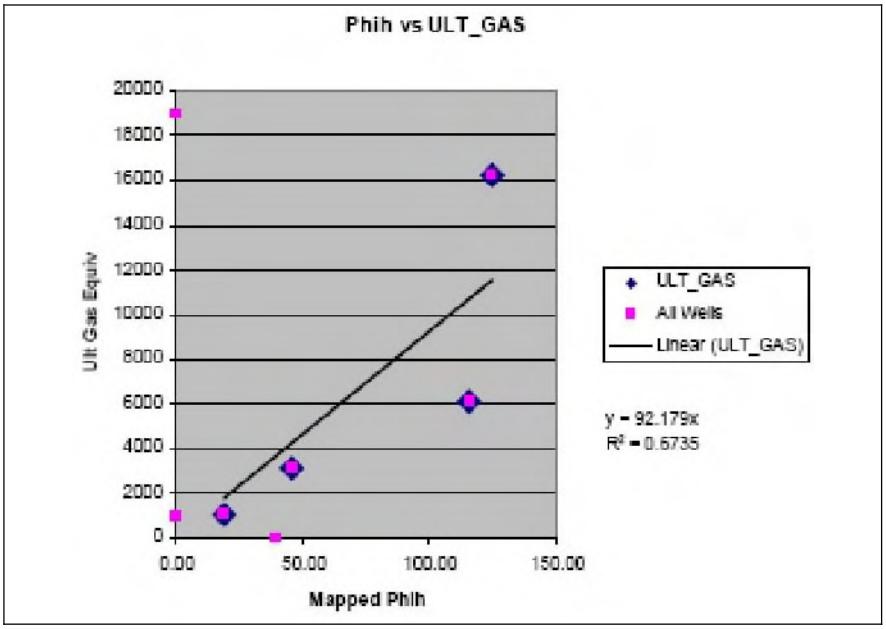

A careful log analysis was performed under difficult circumstances to quantify the Phih available in each well. Missing logs and poorly understood completion issues complicate the task. Aggressive editing of the data only yields a poor fit (blue diamonds) with a low correlation coefficient.

Fig. II-28. Phih from logs vs. EUR

Maps of average reservoir porosity and thickness were digitized and converted to porosity-height (Phih) values. The maps were multiplied (as grids) to generate a map of pseudo permeability-porosity and thickness (kPhih).

Values at the well sites were extracted and plotted against the EUR values generated previously. A graph of this data is shown in fig. II-29. The two high recovery wells show little relationship to the kPhih values. The pervasive faulting in the highly sheared Elk City structure most likely generates vertical or horizontal connectivity to reservoirs not represented (and therefore not predictable) in the logs of the calibration wells.

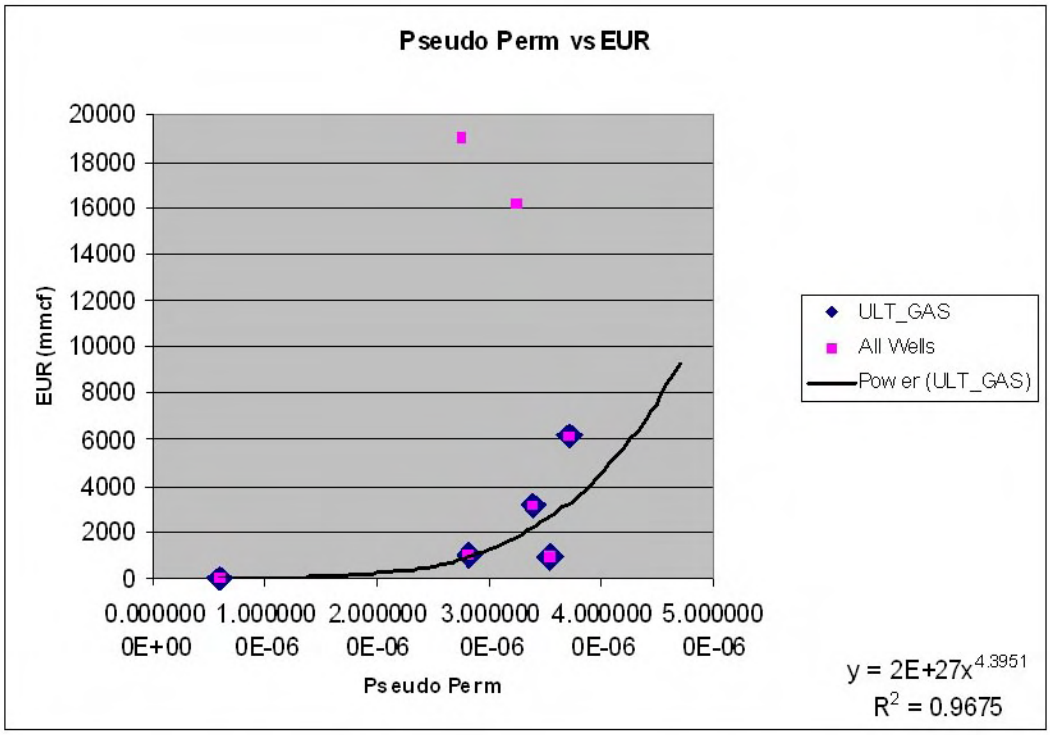

There is a good correlation between estimated pseudo permeability and EUR if the "flyers" are not included.

Fig. II-29. Pseudo Perm vs. EUR

Good estimates of minimum expected productivity can be valuable when managing drilling programs. The two "flyers" were dropped from consideration and a best fit correlation was generated to fit the remaining four wells (fig. II-30). A log fit of the data gave a R^2 value of 0.97. Four data points are hardly a true statistical sample of the potential range of outcomes but they do appear to exhibit a non-random relationship with kPhih.

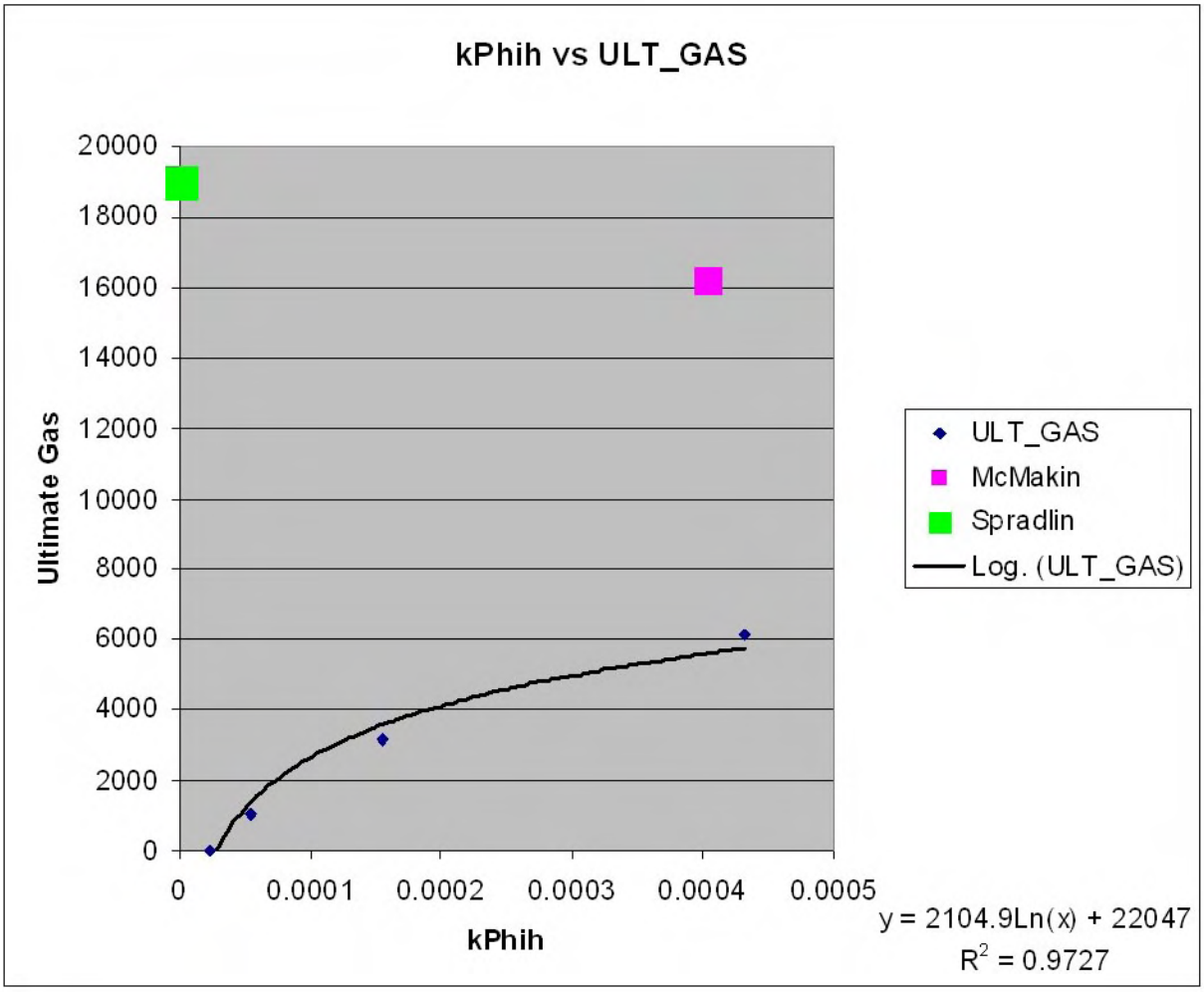

Fig. II-30. Final kPhih vs. EUR correlation

Proposed Locations

The correlation equation between EUR and kPhih was applied to the to the kPhih map to generate a recoverable gas map. The research methodology suggested a series of locations that could yield significant volumes of recoverable gas. Drilling depths to the reservoir were estimated at each location and used to further rank the locations on the basis of BCF/depth drilled.

Additionally, the recovery statistics for the wells drilled to date suggest 25-30% of the wells drilled will recover two to three times the population mean. If that relation continues to hold, three to four of the locations would yield additional reserves not predicted in this model.

Future drilling conditions and other significant risk factors need to be considered prior to pursuing these locations.

G. Well Drilling and Testing

The pace of drilling in the field area has been slow, no doubt the result of land or other negotiations. The pace of data release has been slower because of the competitive nature of Oklahoma drilling regulations.

As of this report, the operator has drilled four wells in the demonstration area deep enough to be considered valid penetrations of the reservoir. None of the wells were drilled on the exact locations recommended. The operator's acreage inventory was held confidential and not considered when the locations were selected.

Initial productivity (IP) for three of the four wells drilled range from 3.8 MMCFD to 6.7 MMCFD. One well was immediately plugged back to a shallower target and is presumed dry at the objective horizon. Typical IP's outside the prospect area are less than one MMCFD.

Log information to perform volumetrics was not available for this post appraisal. With no volumetrics and insufficient production data for type curve analysis there is little to post appraise at this time. The IP data generally fits the kPhih mapping (which remains confidential) and the fact that the aggregate IP's of the wells are higher than average suggests the acreage ranking scheme is working.

H. Key Learnings

There were three key learnings as a result of the Elk City field demonstration.

1. The presence of brittle fractures in a reservoir is not defacto evidence of material behavior that can be effectively simulated with elastic modeling tools. The total shortening in the Elk City area evidenced by the calcite twinning, deformed extensional features and cross-cutting faults made it unsuitable for elastic approaches. The simulation efforts clarified the underlying reasons for the structural complexity but the faults themselves were more reliably detected directly through the seismic. Early recognition of this situation and transition to the more suitable DFN approach would have enabled prospect generation earlier and a more favorable outcome.
2. Field demonstrations should be reserved for truly mature technology that is immediately deployable. Poly3D boundary element modeling requires supporting tools and expertise to be effective. Many of these basic support tools were developed in parallel with the field demonstration. This delayed the project and created vulnerabilities to shifting corporate goals, personnel shifts and other business issues with negative consequences.
3. Visualization tools for model construction and methods of setting appropriate boundary conditions remained significant issues with the geomechanical (BEM) technology. Efforts were undertaken to improve the visualization aspects, in particular, by evaluating and adapting potential commercial packages for geomechanical use.

Summary

1. The project targets immaturely developed Pennsylvanian-age tight gas formations in the deep Anadarko Basin, holding 16+ tcf of technically recoverable resources. Effective development of these (and deeper) formations will be essential for reversing declining natural gas production in the Mid-Continent.

2. The project area and target formation is a combination natural fracture/matrix gas play. This conclusion is supported by:
   - Direct observations of natural fractures in three cores and five FMI/EMI's.
   - Pressure transient and type-curve pressure derivative analysis showing bilinear flow.
   - Moderate correlation (r^2= 0.6) between average porosity times thickness (Phih) and EUR.
   - Excellent correlation (r^2= 0.97) between bulk permeability times porosity times thickness (kPhih) and EUR.
   - Approximately two out every six wells sees anomalous upside recoveries.

3. The research methodology suggests that a series of locations could yield significant volumes of recoverable gas. These were identified by:
   - Core and production analysis to identify key reservoir behaviors.
   - Seismic fault mapping to identify major structural elements.
   - Boundary element modeling to identify gross structural impact of faults.
   - Discrete natural fracture modeling to delineate the permeability impact of faulting and fracturing.
   - Calibration of EUR data for existing wells to Phih, permeability (k) and combined kPhih maps.
   - Delineation and ranking of undrilled areas by depth weighted recoverable gas.

III. Study Area #3: RCP Consortium Williams/Piceance Basin

A. Overview

Field Test #3 was in the Rulison area of the Southern Piceance Basin, with the RCP consortium and Williams Co. Field Test #3 is primarily in Sec. 16, 17, 20 and 21 of T6S R94W.The Piceance basin area is an active, resource rich play focused on the late Cretaceous Mesaverde group sands. There are nearly 1,200 wells between the three major fields: Grand Valley, Rulison, and Mamm Creek (fig. III-1).

The 1992 NPC resource study estimated that the Mesaverde intervals in the Piceance Basin 27.9-tcf of recoverable tight gas in the Williams Fork/Iles Fms. More recent estimates postulate nearly 100 bcf of recoverable reserves in the survey area using advanced high-density development methods.

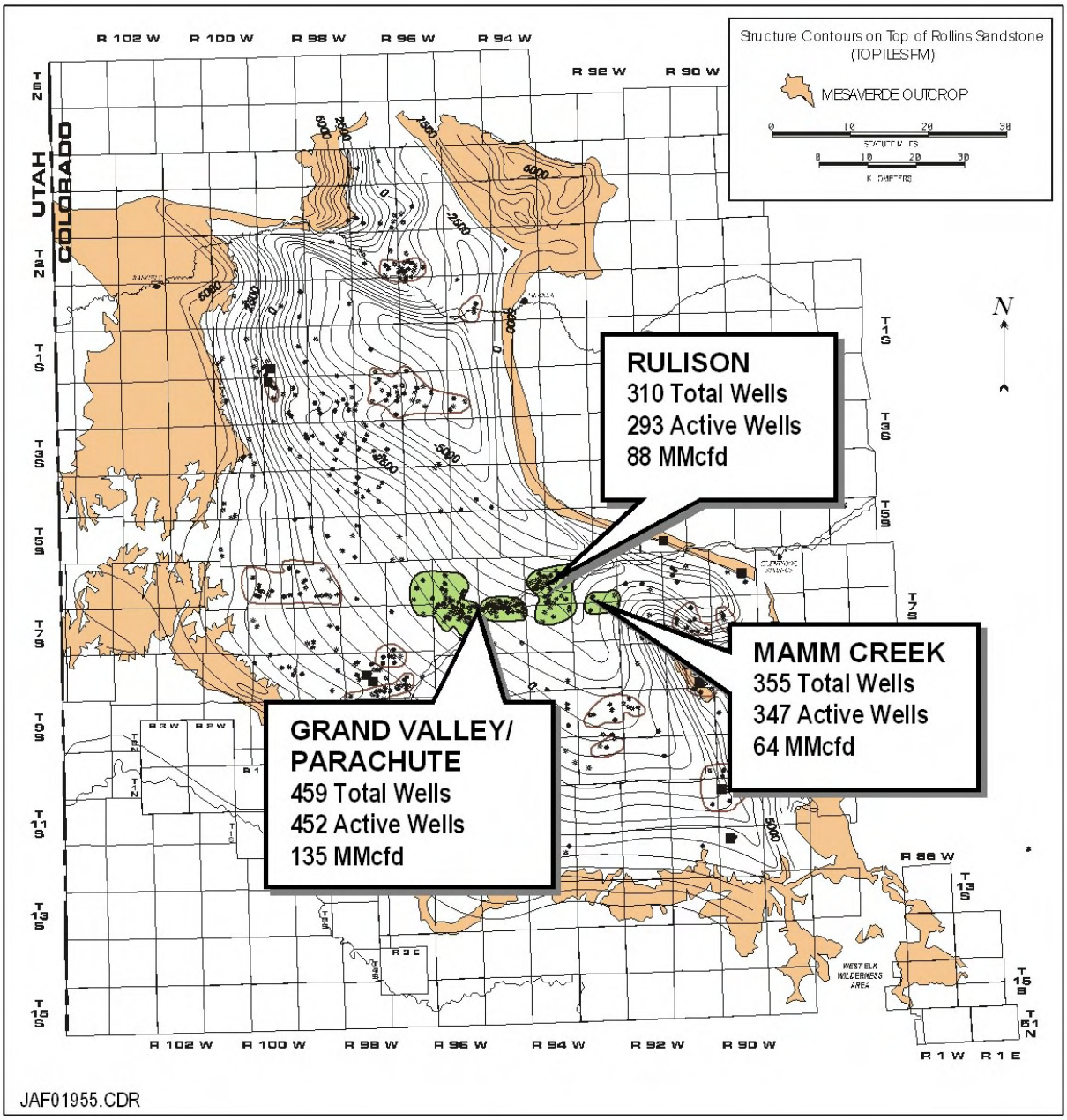

Fig. III-1. Piceance Basin regional structure contour and index map

The play targets discontinuous gas bearing lenticular sands of the Williams Fork fm (Mesaverde group) along the updip flanks of the NW-SE trending synclinal basin axis. (fig. III-2). Updip, sands are water productive and considered wet whereas the downdip sands, although individually discontinuous, yield relatively dry gas. Well spacing in the area ranges from 20 down to 10 acres. Historically the area has been considered a prime example of the basin-centered gas concept.

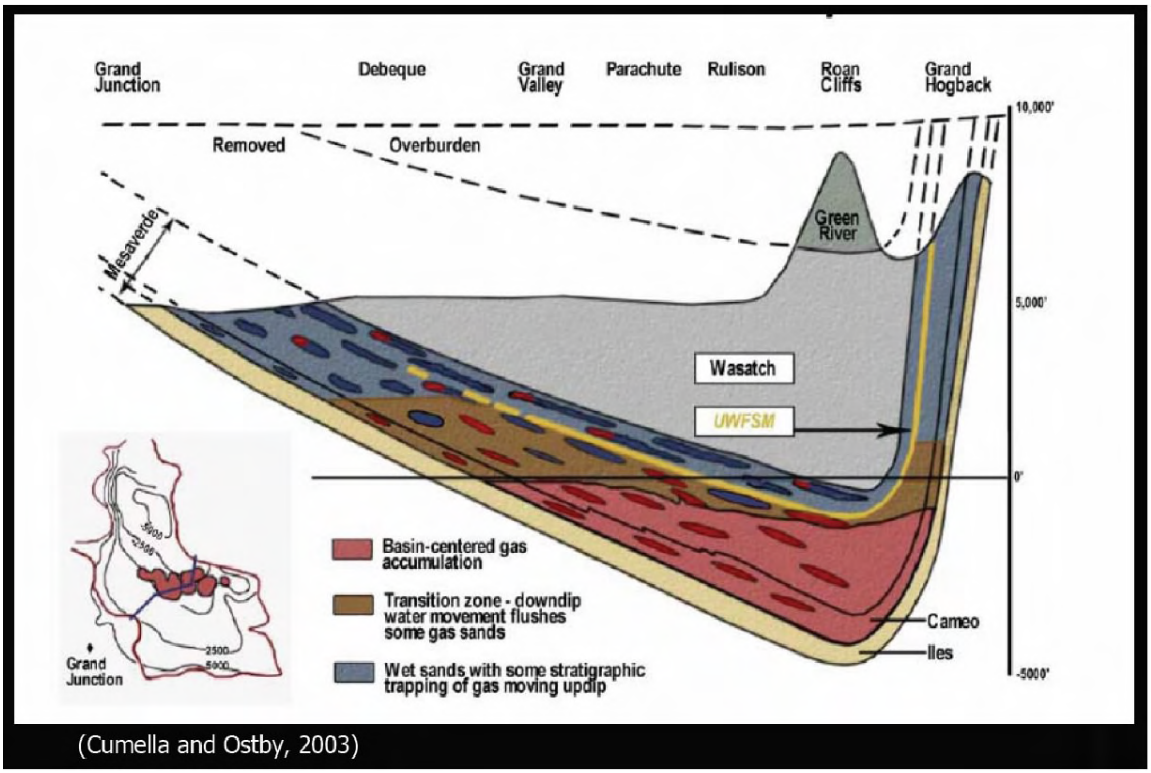

Fig. III-2. Regional cross section

Table III-1. Rulison Reservoir Properties

Data from RCP

Average drilling depth to top of Rollins	8,500 feet
Average thickness of gas saturated section	1,700-2,400 feet
Pore pressure gradient	0.44-0.66 psi/ft
Log porosity	6-14%
Frac gradient	0.6-0.9 psi/ft
Matrix permeability	0.1-2.0 microd
Effective permeability	10-50 microd
Reserves (RCP survey area)	135 bcf
Average EUR/well	1.65 bf
Well spacing	10 acres

B. Purpose

The Williams Fork Fm is a thick sequence of discontinuous, lenticular nonmarine stream deposits that ranges from 3600–5200+ feet thick which overlies the Cameo coals. The Williams Fork Fm is truncated at the top by a regional unconformity. The gas charged portion in the RCP area is approximately 1,700-2,400 feet thick (RCP studies, pers. comm.).

General reservoir properties for the area are cataloged in Table III-1 (RCP). The reservoir is generally overpressured, exhibits low permeability and consequently small drainage areas. Measured core permeability ranges from 0.1-2.0 microdarcies. Bulk production permeabilities at the wellbore scale are usually many times greater. This difference underscores the significant role of natural fractures in reservoir permeability enhancement. Predicting the distribution of the greatest concentrations of natural fracturing is the goal of the demonstration.

C. Site Selection

Three major reasons drove the decision to locate the final field demonstration in the Rulison area:

1) The up tick in natural gas prices created intense competition in the gas industry, especially in exploratory plays. Operators were reluctant to participate in joint research where results would be made public with potentially significant competitive consequences. Exploitation activities in the Rulison area were less vulnerable to confidentiality issues. The active RCP program at Colorado School of Mines offered strong technology transfer potential.

2) The Rulison area had been extensively studied for decades and yet remained the focus of intense natural gas development efforts. Decades of study ensured a large amount of supporting background data (missing in the previous two demonstration sites) and surging gas prices stimulated continuous drilling programs to test the geomechanical technology.

3) Regionally developed joint systems, believed to be so important to gas productivity at Rulison, were absent or ineffective in the two initial field demonstrations. Advancements in application of the technology and availability of high quality seismic in the demonstration area opened the opportunity to test and demonstrate the original concept with significantly improved data and tools.

D. Regional Geologic and Tectonic Setting

Fig. III-3 shows the vertical succession of lithologies in more detail. The area is underlain by the thick, marine Mancos shale. The Isles Fm is an initial marine shoreface sand influx overlain by a coastal plain coal sequence known as the Cameo coals.

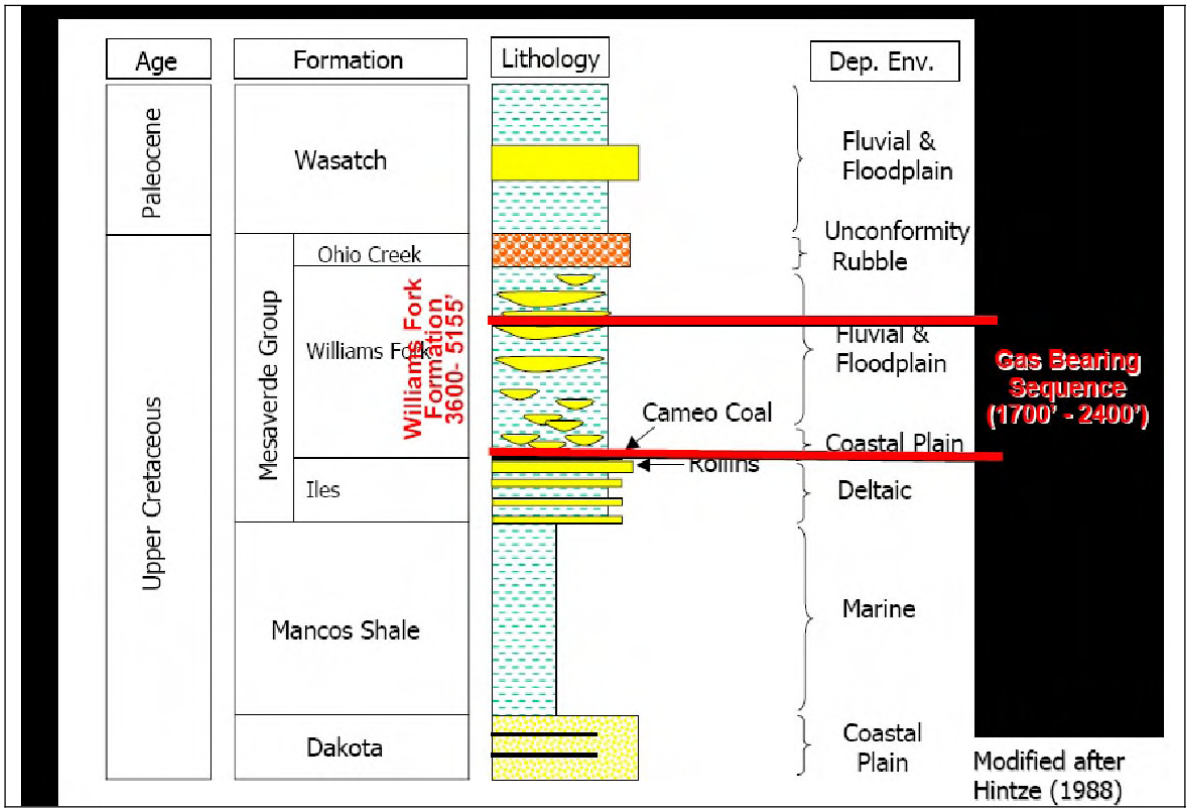

Fig. III-3. Rulison stratigraphic column section

The tectonics and structure of the general MWX/RCP area was studied in depth and described extensively as part of the MWX program (Lorenz and Finley 1991 and Lorenz, Teufel and Warpinski 1991). The regional geology was updated with additional information in 2003 when the Rocky Mountain Association of Geologists (RMAG) devoted an entire guidebook volume to the Piceance basin (Peterson, Olson and Anderson 2001). The boundary conditions for the local geomechanical modeling were determined after review of existing literature, MWX core interpretations and proprietary seismic made available as a result of participation in the RCP program.

The Piceance basin is underlain by gently warped pre-Cambrian aged rocks of the North American craton. The deepest portions of the present day basin lie to the northeast along the White River uplift. Isopach mapping shows the Williams Fork Fm thickens to the north and east across the basin reaching a maximum thickness of over 4,500 feet along the northeastern margin immediately adjacent to the late Paleocene White River uplift. (Johnson and Flores 2003).

The degree of subsidence and uplift varies across the basin from north to south. The southern area around the MWX site is more mature for its depth than the northern areas near White River Dome (Yurewicz et al 2003). The basin axis trends generally northwest (fig. III-4) and gives the impression of northeast to southwest shortening.

Macro folds in the basin generally trend NW-SE except for a few in the southwest, which appear to refract towards an eastward trend. Thrust faults and the pre-Cambrian outcrop belt along the White River uplift display a composite NW-SE trend made up of NNW and SSE segments (Lorenz and Finley 1991). Taken as a whole, the macro structural fabric suggests the paleo maximum horizontal stress lies in a northeast quadrant orientation (varying locally from north to east).

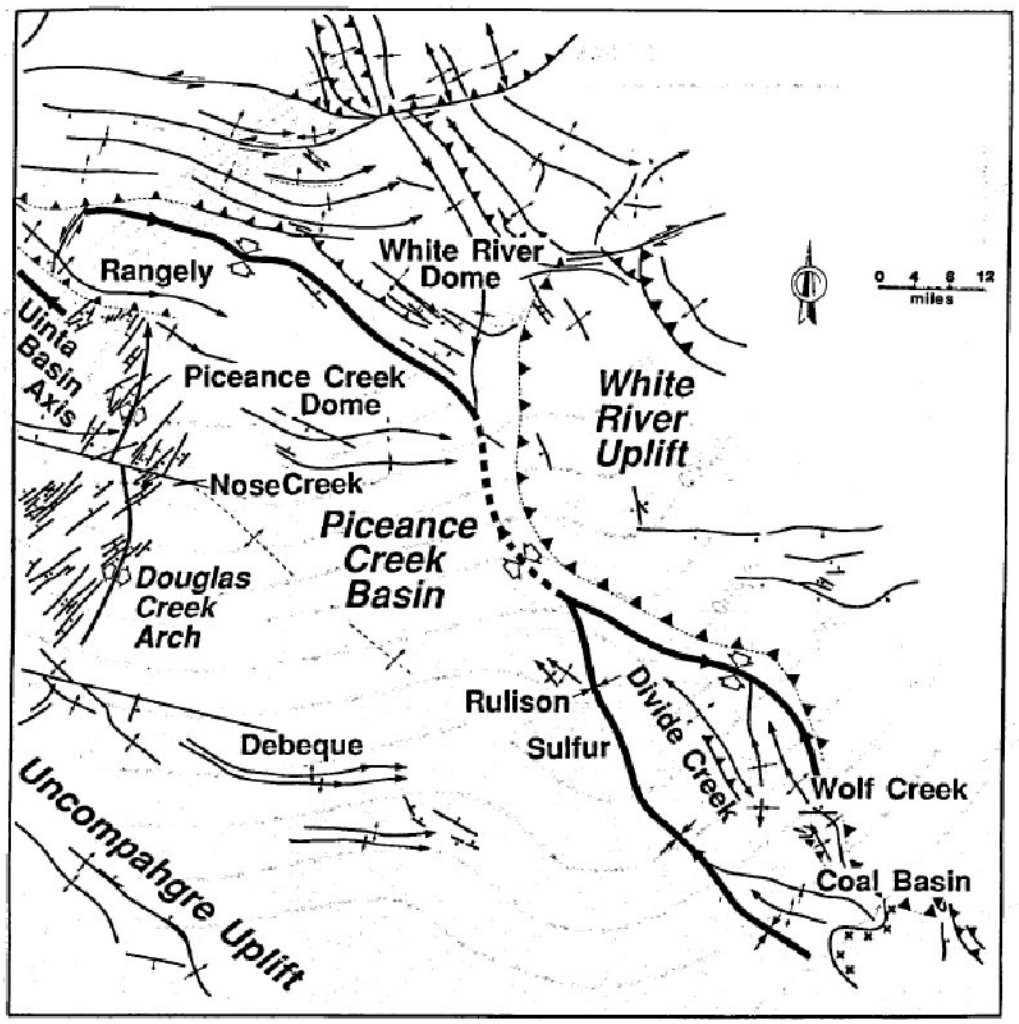

After Myal, et al, 1989

Fig. III-4. Generalized tectonic features of the Piceance basin

From oriented hydraulic fractures and core relaxation studies, we can infer that present-day maximum-horizontal principal-stress lies in a general WNW-ESE orientation across the basin. The dominant orientation of opening mode extension fractures is aligned along the same axis. When there are two directions of opening mode fractures, they are oriented near perpendicular to each other in plan view. Stress directions inferred from opening mode fracture orientation are often at odds with those derived from macro structures such as anticlines (Lorenz and Finley 1991).

Detailed determination of insitu minimum stress from injection tests indicates the stress anisotropy is confined to the more brittle lithologies such as sands and silts. Insitu stresses in the mudstones and shales approach lithostatic gradients with little to no anisotropy. From this it can be inferred that the basin is not under active tectonic stresses (neither compression nor extension) and that the stress anisotropy presently observed in the sands is a remnant or locked-in stress from a previous compressional episode (Lorenz and Finley 1991).

Additional regional seismic data indicates the area surrounding the MWX site and the RCP survey is more complex structurally than previously recognized. At the time of the MWX project, workers held the general belief that the area had been subjected only to mild far field tectonic stresses insufficient to cause the formation of significant anticlines or thrust faulting.

Fig. III-5 is a partial time slice of inferred faulting present in the local area around the RCP site. This data indicates small scale faulting is quite dense, locally exceeding four faults per mile on a linear transect. Northwest trending faults are present in a complex ladder-like pattern developed between two ENE trending less-well-developed fault zones.

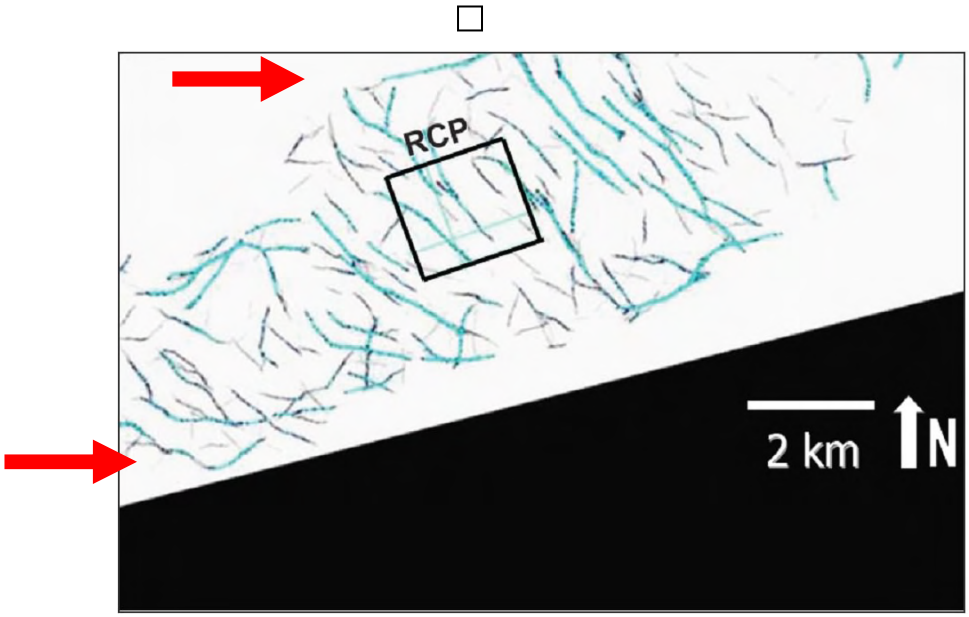

Grey and blue lines represent discontinuities, inferred to represent faults. The ant tracker slice reveals the ladder-like development of NNW trending faults between two ENE trending fault systems (red arrows)outside the RCP survey (box).

Fig. III-5. Partial Ant Tracker time slice of Seitel regional survey, Piceance basin area

Core study at the MWX site and observed offsets on seismic indicates the faults in this area are dominantly reverse in nature. This observation lays a foundation to hypothesize that the RCP survey lies in a broad stepover motion transfer zone between two right en echelon, left lateral strike slip faults. This general geologic fabric is consistent with the significant lateral inelastic strains determined from calcite twin lamellae (reported by Teufel 1991, and Lorenz and Finley 1991) and the eastward refraction of anticlinal trends south and east of the MWX site.

In general, the RCP survey lies in an area of diffuse shortening localized between two right en echelon left lateral strike slip faults. The shortening presents as grain scale deformation, mild warping of the sedimentary layers and subtle northwest trending reverse faults. Vitrinite reflectance indicates a strong degree of burial and later uplift, in comparison to other parts of the basin.

MWX Fractures and Stresses

The comprehensive data set collected during the MWX program remains a valuable integrated resource for tight-gas reservoir characterization research. This important data point was re-examined in light of the more extensive local 3D seismic data available for the Multi-site project. Of particular interest are the relationships in fracturing—its style, its geologic habitat, and insitu stress. All of which were investigated extensively during the MWX program through the use of core, strain relief, and well test data.

Fractures in whole core recovered during the MMX program were described, classified and exhaustively documented in tabular format. The information in the data tables was converted to spreadsheet format. Following digitization, the fracture data was expanded into a pseudo log format. Log data format placed the fracture information into an evenly sampled vertical depth sequence. This enabled calculation of sums or averages of attributes per foot of wellbore, which was helpful for identifying internal trends and/or relationships with other depth-controlled data.

Fig. III-6 displays logs of running average fracture width per 200 wellbore feet and fracture density per foot of wellbore. A prominent breccia zone was cored over a 400-foot interval starting just below 6,000 feet MD. Fractures characterized as shears were encountered in three intervals between 4,800’MD and 6,800 feet MD.

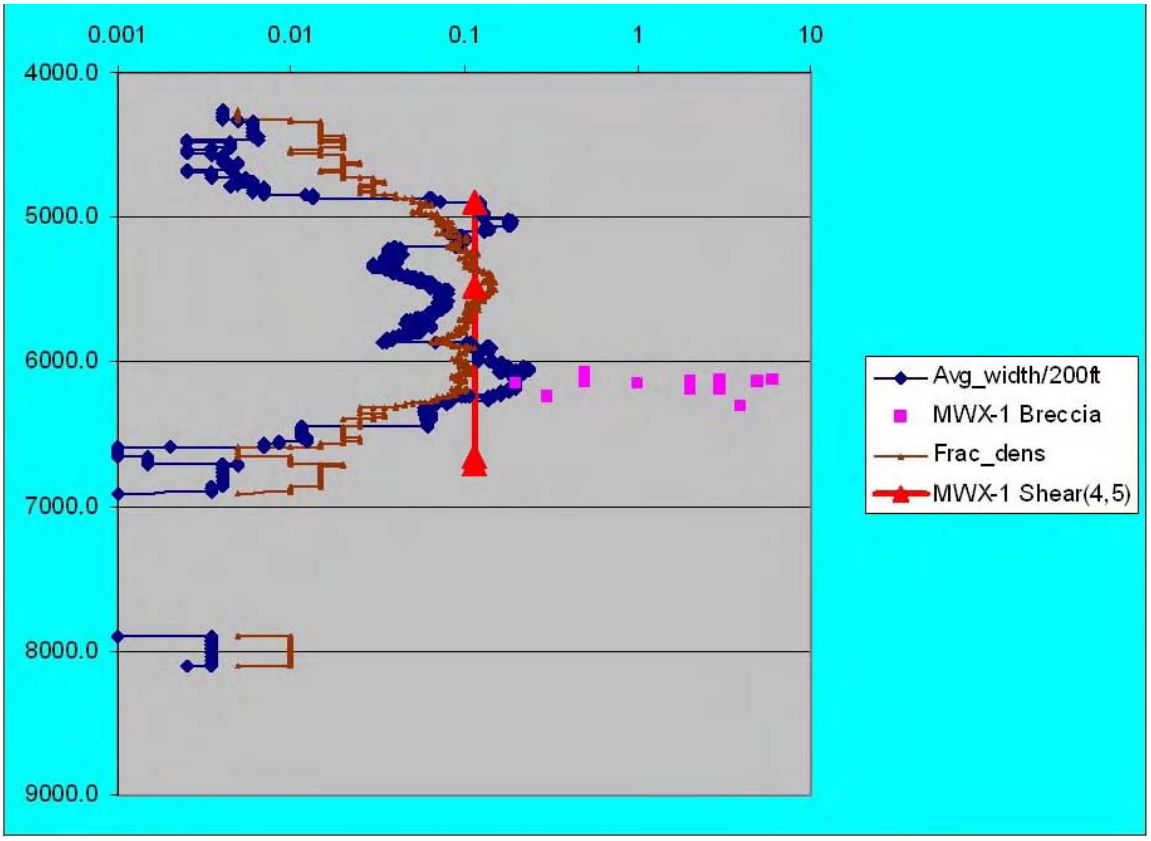

Fig. III-6. MWX fracture "logs" section

The small faults were classified as reverse. The greatest average width and fracture density occur within the interval containing the shear fractures and the breccia. Both attributes increased suddenly with the first occurrence of a shear fracture and declined noticeably near the breccia and before the last described shear fracture. *An apparent relationship of predictability exists between the density and apertures of the opening mode fractures and the observed shears.*

Extensive insitu stress and pressure data were also collected during the MWX project. This data is shown with respect to depth and fracture style in fig. III-7. The pressure gradient shows a low rate of increase shallow in the well, increases significantly across the 5,000-7,000 foot MD interval and shows relatively little increase below 7,000 feet MD.

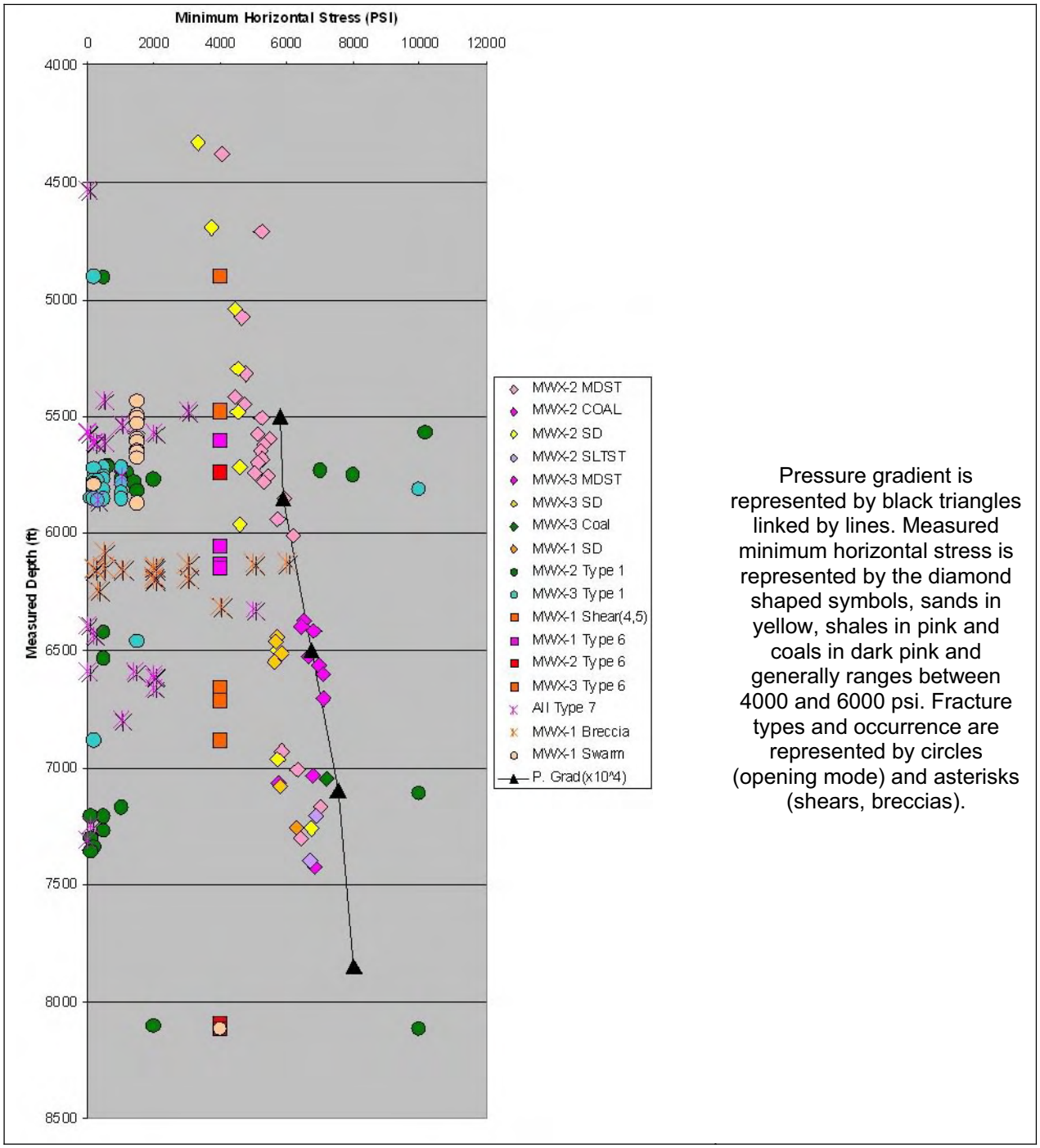

Fig. III-7. MWX fracture types and pressure gradients section

Minimum horizontal stress measured in the sands (diamond symbols) diverges from the shale trend below 5,500 feet MD, shifts with the pressure gradient around 6,500 feet MD, and appears to merge again with the shale values below 7,000 feet MD. Dickite mineralization occurs in the fractures at 6,200 feet MD (majority) and again (minor) around 6,700 feet MD (Lorenz and Finley 1991).

Given the reverse nature of the minor shear fractures observed in the wells, the pressure gradient change, the downward increase in differential stress between the sands and shale and localized Dickite mineralization, a minor reverse fault(s) is interpreted to intersect the well between 6,000 and 6,400 feet MD.

Boundary element modeling performed during this project indicates the upthrown (hanging wall) side of a reverse fault is typically the volume of greatest compressive stress concentration. In this well, it is interesting to note the downward divergence of minimum horizontal stress values measured in the sands and shales approaching the interpreted fault. This coincides with the greatest average fracture width observed in the well and very nearly the greatest fracture density.

Together these attributes indicate a relatively large volume of void space in the fractures immediately above the fault. The measured minimum horizontal stress gradient is very low through this interval. *The localized development of extension fractures in the hanging wall of reverse faults is counter intuitive to the original project hypothesis and suggests the fractures are related to unloading rather than the direct result of extensional stress distribution around the fault during its active displacement*.

The MWX area has been uplifted and cooled since its time of maximum burial. Lorenz and Finley (1991) estimated the Mesaverde reached its maximum depth of burial between 36 and 40 millions of years before present (MYBP). They estimate 1,000-2,000 feet of unroofing since then. They project maximum paleo temperatures to be on the order of 150-200 degrees C with a tendency towards the higher values.

A temperature log from the MWX-I indicates a present-day bottom hole temperature of approximately 116 degrees C (Sandia MWX I Final Report 1987). Yurewicz (2003) suggest heat flow is higher in the southern portions of the basin where MWX was drilled because of geothermal activity. Exact estimates may vary but there has been significant uplift and cooling in the MWX area during the past 10 million years (MY).

E. Site Characterization

The Reservoir Characterization Project (RCP) of the Colorado School of Mines (CSM) is an industry/academic research consortium focused on advancing geophysical technologies used for subsurface reservoir characterization. The consortium is headed by Dr. Thomas Davis of CSM. Phase X of the consortium has investigated the utility of 4D seismic methods for improving reservoir management of a naturally fractured tight gas reservoir located in western Colorado. Williams Production Company is the operator of the field area.

4D seismic methods involve collecting seismic data during reservoir depletion. Ideally this is accomplished by repetitively occupying the same shot/receiver stations using similar acquisition parameters over several years. The RCP consortium is performing such a seismic

production monitoring project approximately two miles north of the original MWX field site in the Piceance basin. The survey partially overlaps an older DOE seismic survey that serves as an early development baseline (fig. III-8).

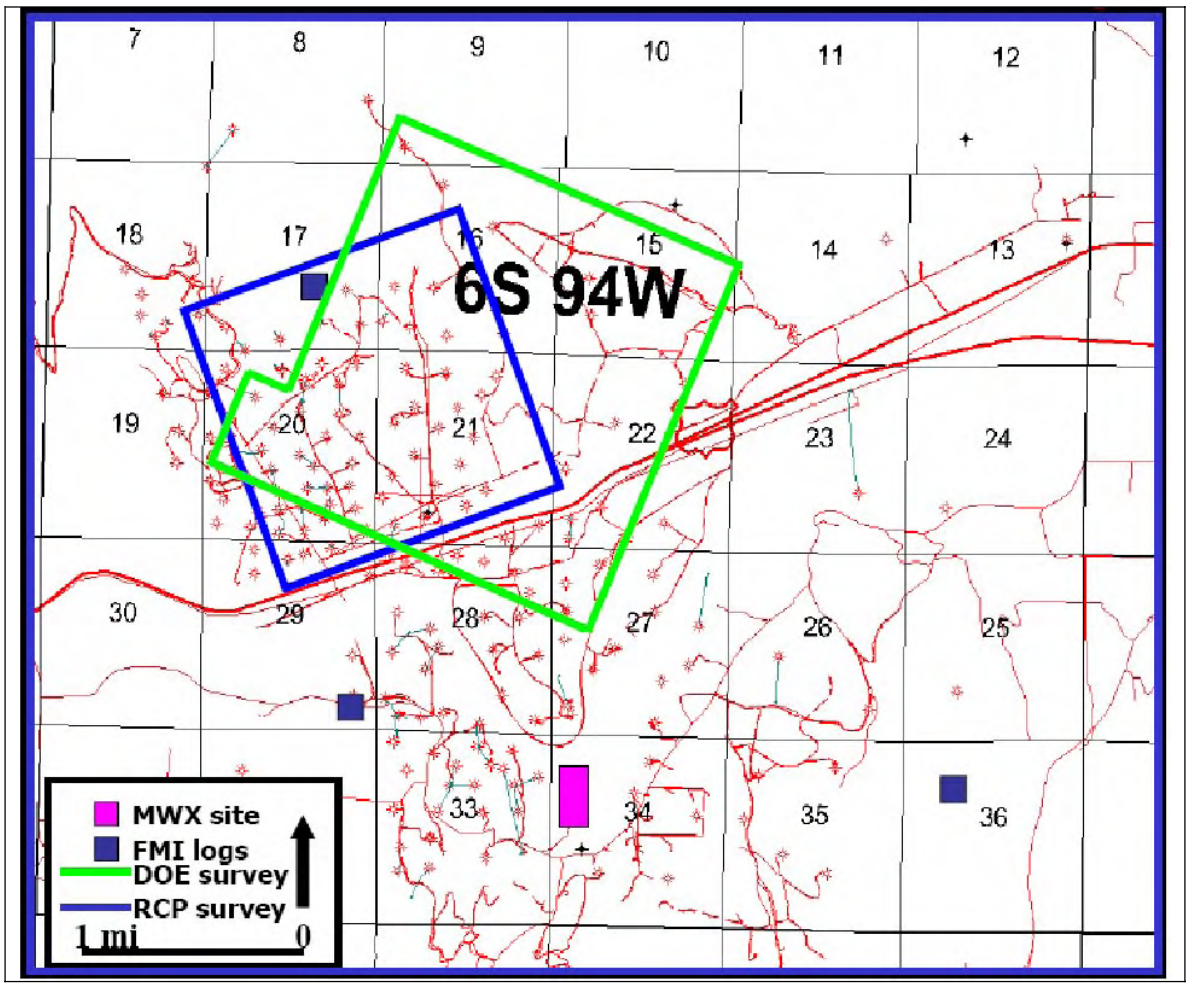

Fig. III-8. RCP survey location section

The RCP 9-component 3D seismic survey extends over approximately four square miles of the field. Full fold coverage in the survey is somewhat less. Extensive processing and reprocessing has been done to yield a research quality 4D seismic data survey.

The objective of the field project was to demonstrate the utility of geomechanical simulation of stress fields around faults in predicting well bore productivity in the fractured reservoir prior to drilling. Of specific interest was using the simulation results to high grade a tight gas development program and improve overall productivity during the development program.

As previously discussed, the area is more highly faulted than previously recognized. Researchers and students used advanced methods to define and map the faulting in far greater detail than possible in the earlier DOE survey. The improved resolution of the RCP survey and improved interpretational tools reveal complexities in the local geology not previously recognized.

The detailed fault interpretation was done by Kjetil Jansen (2003) using the Ant tracker algorithm embedded in Schlumberger's Petrel™ software package. He identified over 500 individual faults (each defined by 10's to 100's of small patches) in the four square mile 3D seismic volume. Displacements on many (perhaps most) were very close to the limits of seismic resolution. Fig. III-9 is a perspective view of the raw patch volume in depth.

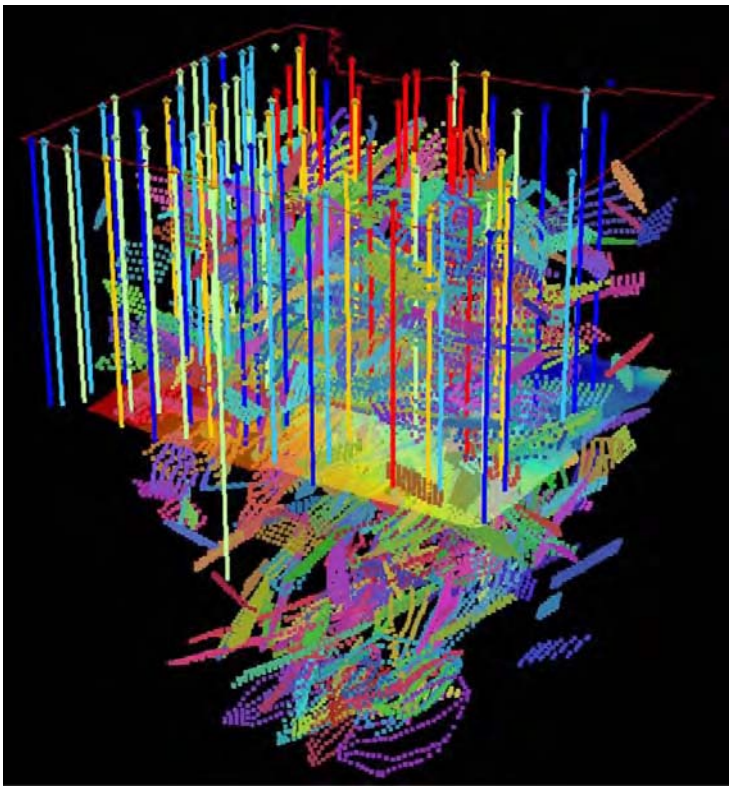

Raw "patch" volume as received from K. Jansen. Dots are fault "patches", one per discontinuity point, each color a different fault. Wells appear as vertical lines; survey boundary as red outline.

Fig. III-9. Raw "patch" volume as received from K. Jansen

The fault patches were received in Petrel™ ASCII text format output. The data set was reformatted to fault name, x, y, z (time) and converted to depth using a time-depth relation supplied by Veritas, Inc. The data set consisted of 45,500 discontinuity points from 553 faults. The largest fault had 280 points and the smallest 15; the mean was 80 points. The faults ranged in depth between –4,792 and –15,626 feet below the datum.

Due to computational and processing time considerations, we reduced the number of faults to be modeled. We used two basic decimation/modeling approaches. Initially, we used the largest faults, at depth, below the reservoir. This approach overly simplified the problem and provided diffuse, inconclusive maps at the reservoir level. The fault volume was re-evaluated to identify the faults with the most pillars that cut the reservoir interval (fig. III-10). This approach resulted in a more credible number of faults and effectively filtered the majority of false picks from consideration.

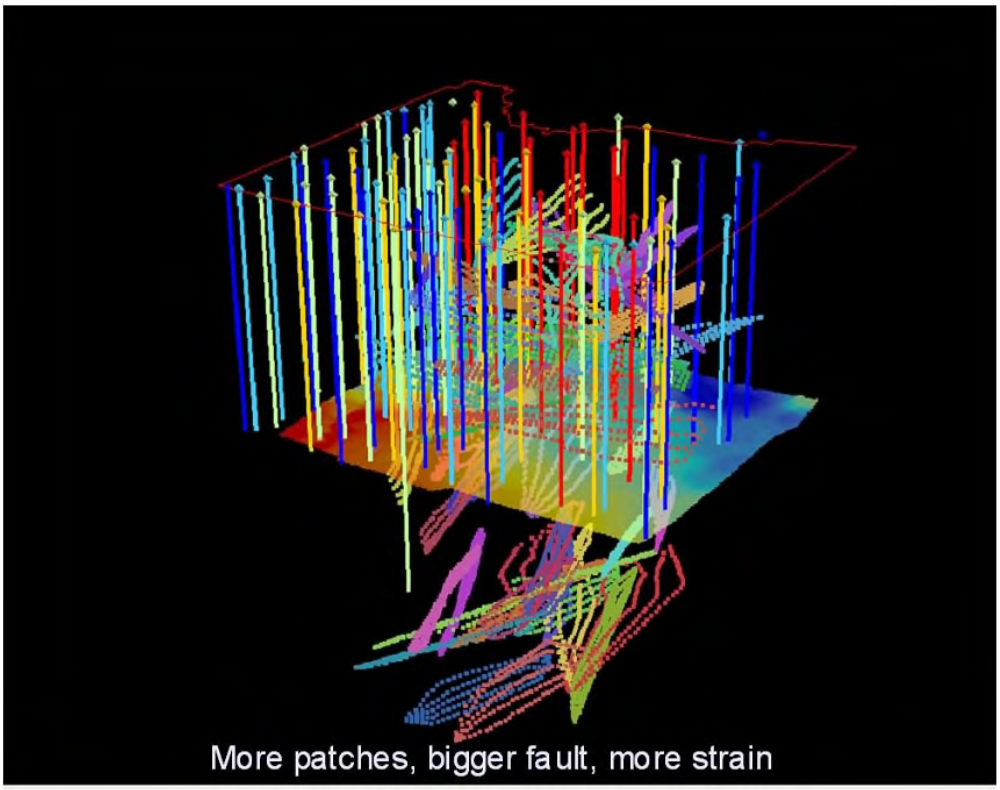

The fault swarm is funnel-like in shape, concave upward, slightly elongate along a NW-SE axis. colored points are the raw fault pillars with greater than 130 points by count. Faults are differentiated by color.

Fig. III-10. Faults with GT 130 patches

Each set of fault pillars was individually edited in a 3D visualization package to remove anomalous points and simplify the faults for simulation. The ant tracker software had captured a very high degree of structural detail, often imaging individual fault segments, many of which we simplified for simulation purposes. The final fault set (fig. III-11) used for geomechanical simulation included only the 26 largest faults that actually cut the section above the Cameo (approximately 5% of the total originally identified in the volume).

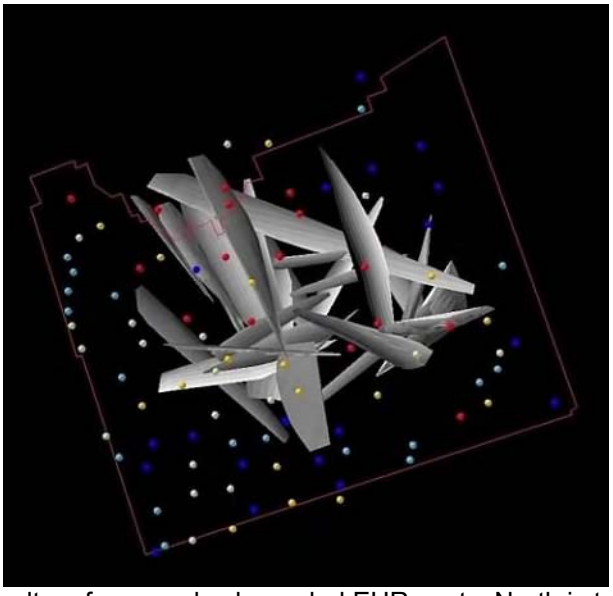

Plan view of survey with fault surfaces and color coded EUR spots. North is to top. This view shows the rough NW-SE orientation of the fault system. The faults show reverse motion in section view on the seismic and will have reverse-oblique slip displacement when “stressed” from N50E.

Fig. III-11. Poly3D model fault cluster

Poly3D is a linear elastic model and the horizontal patterns of the stress (and strain) field are the same regardless of the absolute values input as boundary conditions. When we ran the Poly3D model using stress boundary conditions we used a Poisson’s ratio of 0.2 and a Young’s modulus of 40,000 as mechanical properties for the reservoir. The boundary conditions were set at –4,000 psi stress from N50E.

This would come closest to yielding a pure shear stress along the ENE trending strike slip fault system identified on the regional survey (fig. III-5). There was no reliable way to estimate the magnitude of the original paleo horizontal stress. Therefore, we chose a value of –4,000 psi—a reasonable if not absolutely correct approximation. Fig. III-12 shows the base well control, survey outline and Cameo structure in 3D.

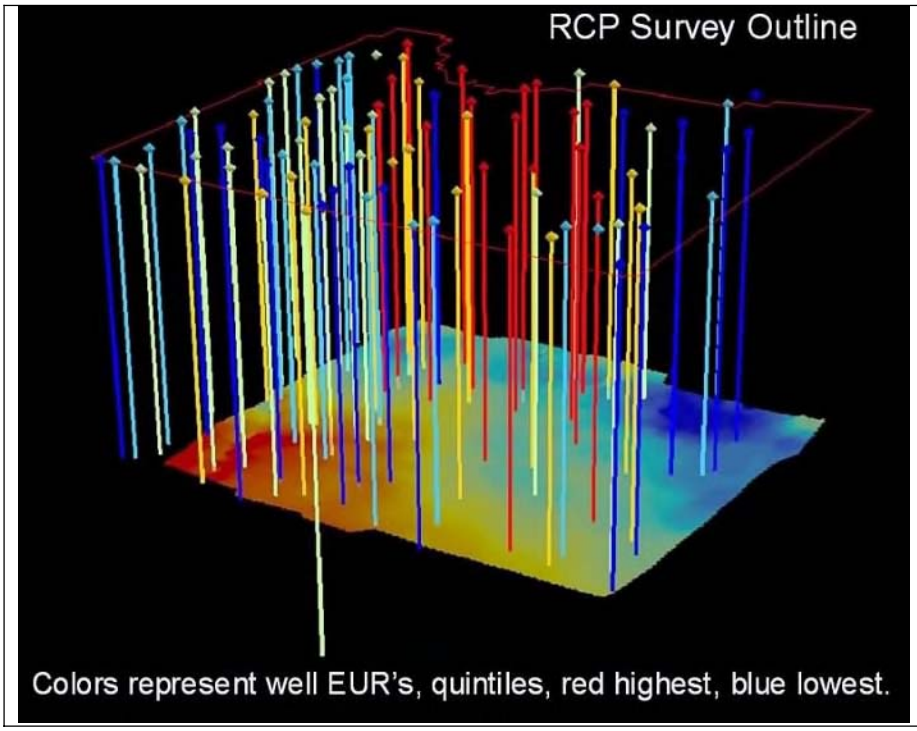

The population of EUR data was sorted into quintiles and assigned a color from blue (lowest) to red (highest). The sphere at the top of each well and the color of the path follow this scheme. The seismic survey outline is represented by the red outline at the top of the view. A gridded Cameo coal surface is shown at depth for reference.

Fig. III-12. Base well control

The Poly3D simulation was performed on a three dimensional volume of observation points. Figures III-13 through III-15 illustrate the model and two cross sections through the simulation volume. The calculated compressional strain values are shown as cubes in the cross sections. They have been color coded by quintile, red being the highest, blue the lowest.

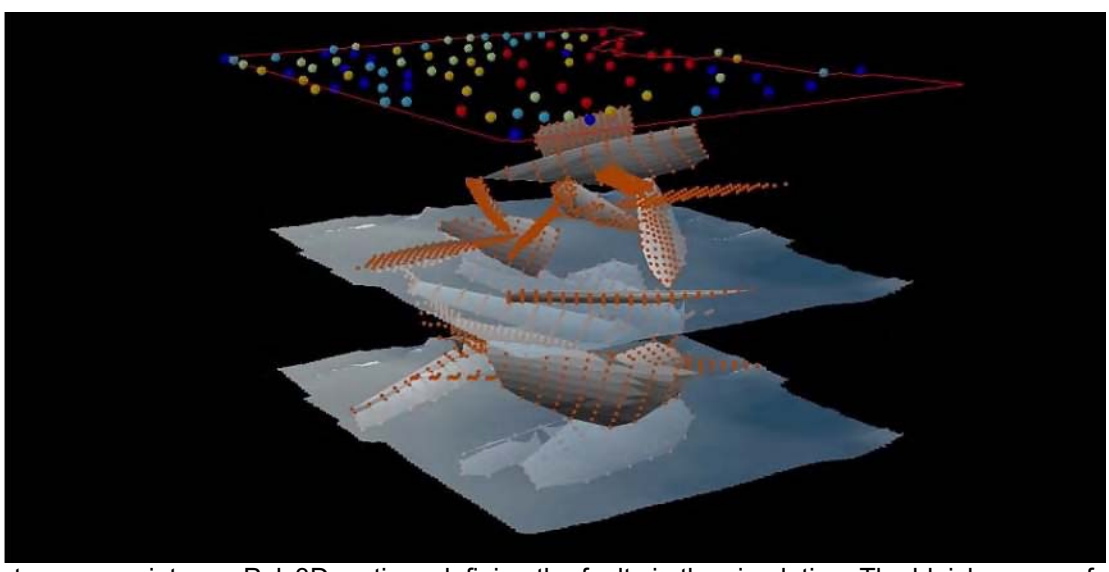

Burnt orange points are Poly3D vertices defining the faults in the simulation. The bluish grey surfaces approximate the top and bottom of the reservoir interval.

Fig. III-13. Perspective view northwest along the major fault trend

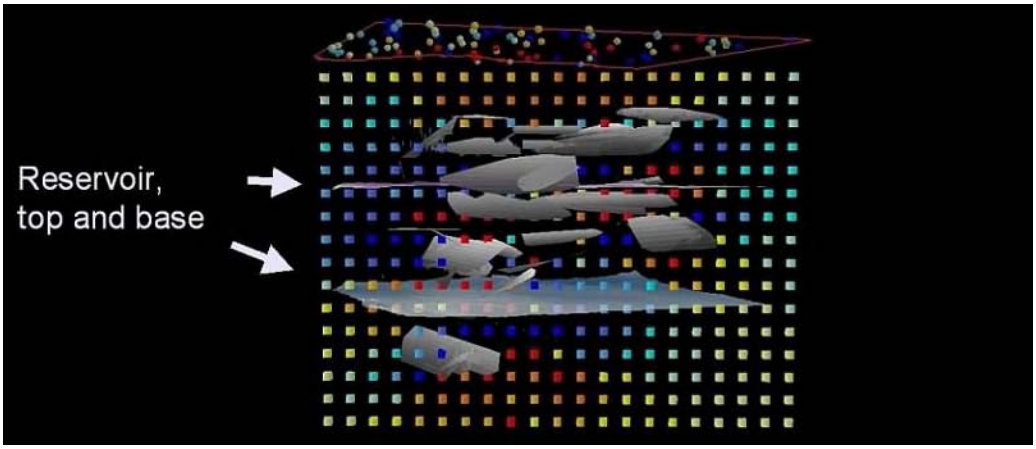

E-W section view of model looking to north. Cubes are sorted and coded by quintiles, red highest principal compressive stress, blue lowest stress. The estimated top and base of the reservoir are indicated by arrows and surfaces for reference. Note the vertical and horizontal variability of the principal compressional stress field across the model. Almost no column of cubes is orange and red from top to bottom. This means no vertical well will see a uniform amount of unloading fractures as it traverses the reservoir section; this may be one significant reason for the high degree of variability in the production data.

Fig. III-14. EW section Poly3D model

On fig. III-15 note the finite extent of most faults. The blue cubes representing lower compressive stresses are located in the volumes of relative extension that form on the upthrown sides of the faults at the lower tips and downthrown sides near the upper tips. Theoretically, it makes a difference *where* the well bore intersects the fault. When there is significant sand variability in an area, the best productivity is found where good sands are coincident with the higher fault strain volumes. If faults are penetrated near their midpoint, away from the higher strain concentrations along their tips, the results may be disappointing.

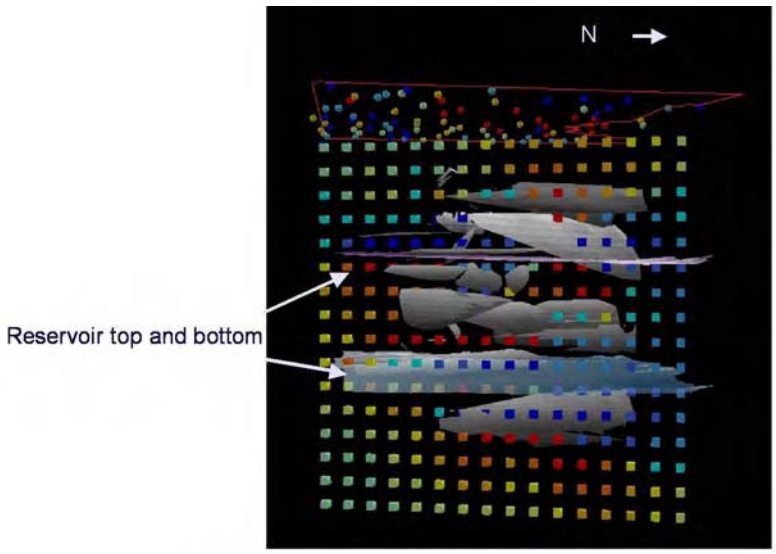

N-S cross-section of the modeled volume, same color scheme as previous figure. Red cubes are high-modeled strain, blues are low.

Fig. III-15. NS cross section Poly3D model

Figure III-16 is a perspective view of the most intensely strained (red cubes) volume of the model. Not only are there concentrations of strain around the faults, but interference between the faults generates volumes of high strain "connecting" the faults. This simulation suggests there may be significant vertical connectivity within the reservoir between the faults. Thus even though the reservoir sands themselves may be of limited extent, interfering strain fields (volumes of more intense fractures) between the faults may affect observed hydrocarbon column heights and drainage volumes.

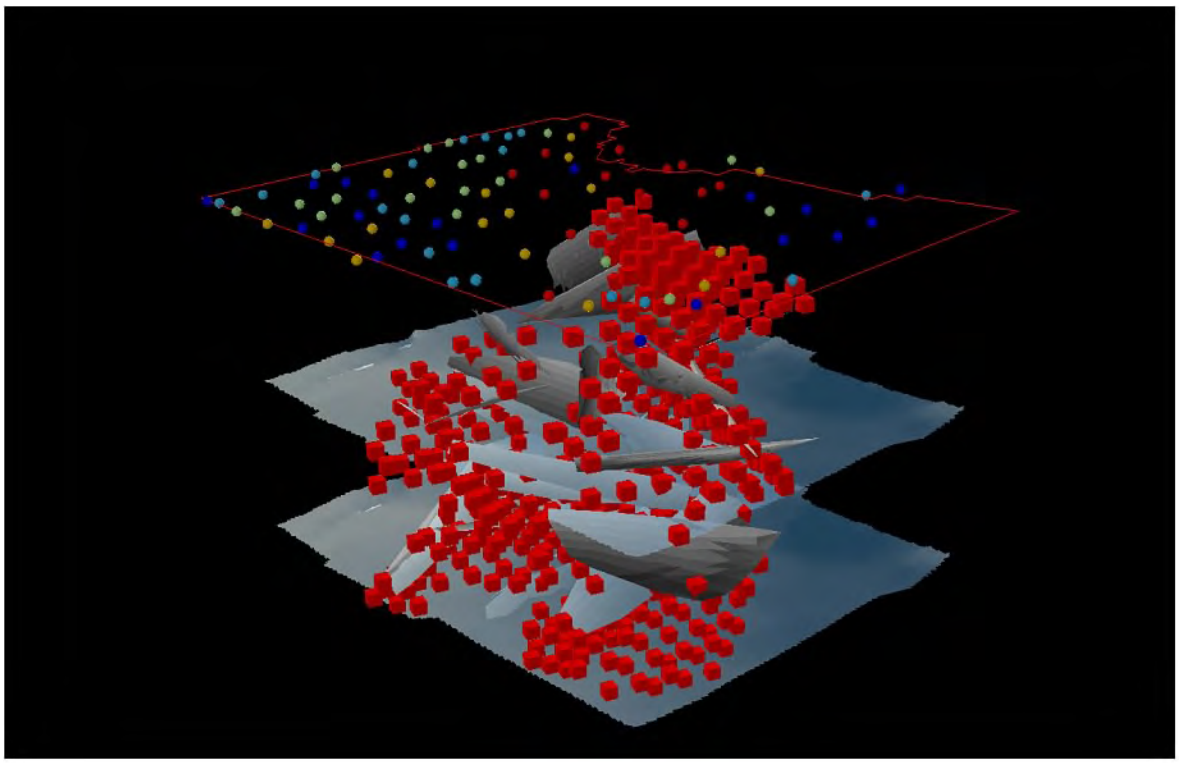

This illustration shows the 5% of the model volume with the greatest simulated strain. The red cubes outline an irregular volume of space around and between the faults where simulated fault displacements would have caused concentrations of shortening in the reservoir. It is likely the volume is interconnected by the network of small faults identified by the ant tracker software.

Fig. III-16. 3D view greatest strain

Interpreting the simulation volume and relating it to well bore productivity was a challenge. Well bores are evaluated on the basis of volume/location (EUR/well location). The Williams Fork reservoir interval is approximately 2000 ft thick in the RCP area. No single horizon based simulation will reflect the potential within the section as a whole. To resolve this issue and make the simulation results more comparable to the drilling results, the simulated stress values for single x, y points (multiple depths) in the volume were averaged across the depths to represent the vertical volume at a planar single point(average strain/point). The resulting map is shown in figure III-17 and forms the basis for evaluating the effectiveness of the simulation and projecting future results.

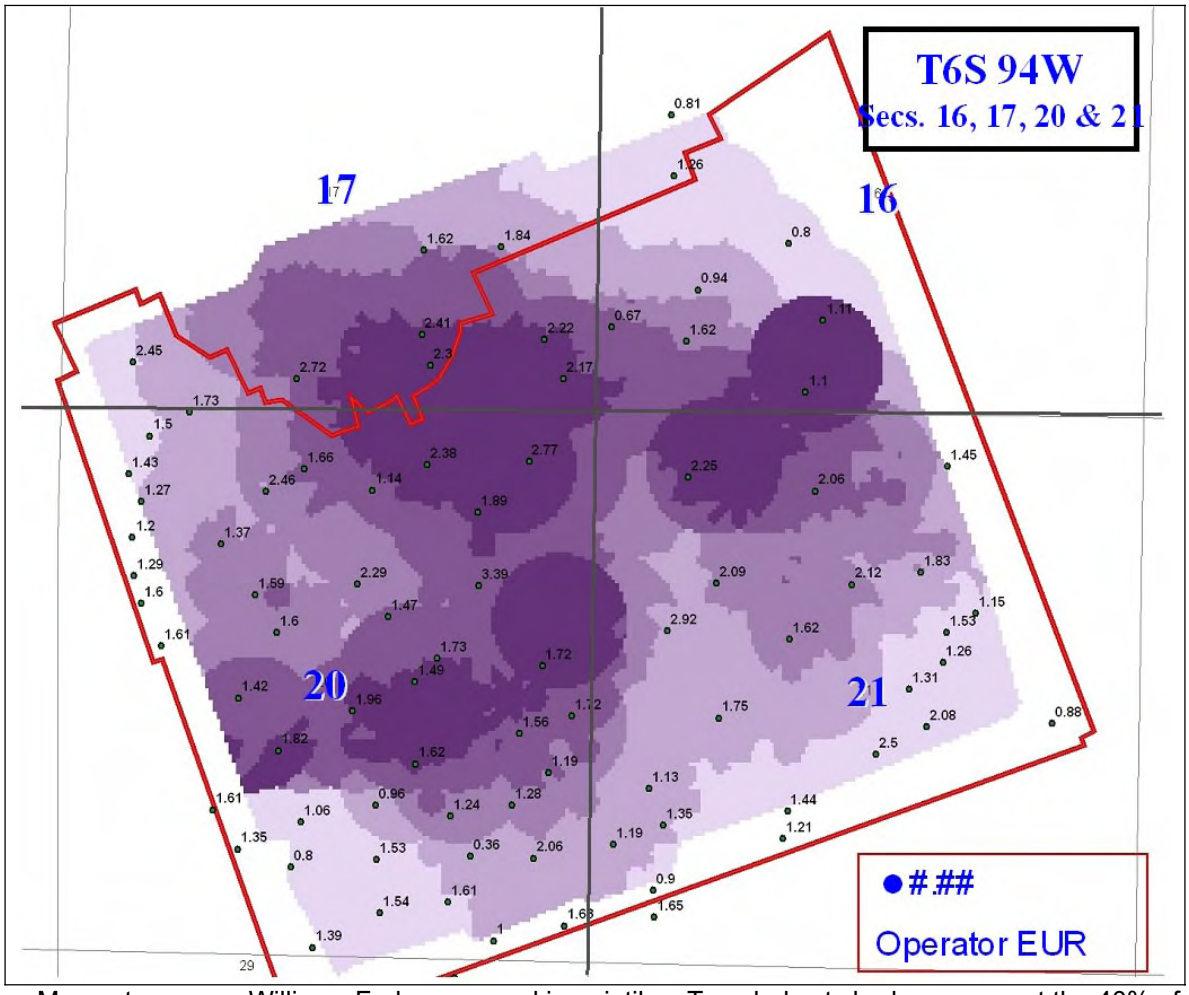

Mean stress over Williams Fork expressed in quintiles. Two darkest shades represent the 40% of the reservoir with the greatest compressional strain.

Fig. III-17. Geomechanical model results

F. Post-Simulation Appraisal and Impact Assessment

Geomechanical Simulation Results

The Multisite program prior to field demonstration #3 indicated three styles of fracturing to be considered as part of the evaluation:

1. shear fractures—directly related to faults
2. unloading extension fractures—related to burial/uplift cycles
3. unloading extension fractures—related to tectonic relaxation

The complex nature of the faulting present within the field area precluded attempts to model shear stresses in any detail. Thus, the density of faulting identified by the ant tracker became a defacto shear stress map. The RCP area is small with little structural relief at the reservoir horizon.

As a result, visco-elastic modeling efforts across the area would yield little variability upon which to base a high grading scheme. A complex three dimensional strain field reflecting the faults and their interference with each other seemed to best fit the sporadic nature of production and held the most promise of providing a useable map.

The objective of the structural modeling effort was to predict the reservoir volume with the greatest fault related strain. And by extension, the greatest concentration of opening mode fractures. The MWX well control and the location of high productivity sweetspots with respect to macrostructural elements indicate that the greatest concentrations of extension fractures occur in volumes of rock where the fault related compressional strain has been the greatest.

The seismic and geomechanical model covered an area of eight quarter sections (each 160 acres; 1,280 acres total):

- Three of the quarter sections (SE Sec. 17; NE Sec. 20; and NW Sec. 21) are in areas of interpreted high-enhanced permeability.
- Five of the quarter sections (SW Sec. 16; NW Sec. 20; SE Sec. 20; NW Sec. 21; and SW Sec. 21) are in areas of low or no enhanced permeability.

Examination of well performance (EUR) in these eight quarter-sections was used to test the geomechanical model results.

The mean stress map was scaled in quintiles, dark purple the highest average stress (used here interchangeably with strain because Poly3D is linear elastic) and the light lavender the lowest quintile. To simplify the evaluation, the top two quintiles (most strained areas) were considered potential high permeability areas. The lower 3 quintiles less permeable.

The wells were cataloged by location against the strain map and the results are tabulated in Tables III-2 and III-3. Wells within the mapped high strain areas, on average, were nearly 50% more productive than the wells falling in the lower three quintiles of the average simulated strain map.

Table III-2. Well productivity in high enhanced perm areas

	SE Sec. 17	NE Sec. 20	NW Sec. 21	TOTAL
No. Wells	6	10	6	22
EUR (Bcf)	12.6	20.3	13.1	46.0
EUR/Well (Bcf)				
• Average	2.1	2.0	2.2	2.1
• Range	1.6 to 2.3	1.1 to 3.4	1.6 to 2.9	1.1 to 3.4

Table III-3. Well productivity in low/no enhanced perm areas

	SW Sec. 16	NW Sec. 20	SW Sec. 21	SE Sec. 20	NW Sec.21	TOTAL
No. Wells	6	13	8	15	6	48
EUR (Bcf)	6.2	20.3	10.6	21.3	8.5	67.0
EUR/Well (Bcf)						
• Average	1.0	1.6	1.3	1.4	1.4	1.4
• Range	0.7 to 1.6	1.2 to 2.5	0.9 to 1.7	0.4 to 2.1	1.1 to 1.8	0.4 to 2.5

The economic benefit of this productivity improvement has been estimated and is tabulated in Table III-4. When evaluated using modest gas prices and operating costs, wells in the higher average strain areas show 20-fold improvement in net profit. These results indicate that successful natural fracture-based "sweet spot" detection through geomechanical methods should improve profits in good areas and may transform an economically marginal tight gas area into a viable development project.

Table III-4. Comparative economics provide additional insights on the value of the geomechanical technology

	Low/No Enhanced Perm Area		High Enhanced Perm Area	
Gas Price ($/Mcf)		$5.00		$5.00
Basis Diff. ($/Mcf)		(0.75)		(0.75)
Prod. Tax (@ 5%)		(0.21)		(0.21)
O&M/G&A ($/Mcf)		(0.84)		(0.84)
Op. Revenues ($/Mcf)		$3.20		$3.20
D&C Costs (M$)	$1,250		$1,250	
Gross EUR (Bcf)	1.4		2.1	
Net EUR (@ 0.85 NRI)	1.19		1.79	
D&C Costs ($/Mcf)		(1.05)		(0.70)
Return on Cap. (2x D&C)		(2.10)		(1.40)
Net Profits ($/Mcf)		**$0.05**		**$1.10**

Results from the most recent drilling in the area was not available at the time of this evaluation. Fig. III-18 shows the projected drilling locations for 2005 and 2006. A further post appraisal of the geomechanical simulation after those drilling results are available would be appropriate.

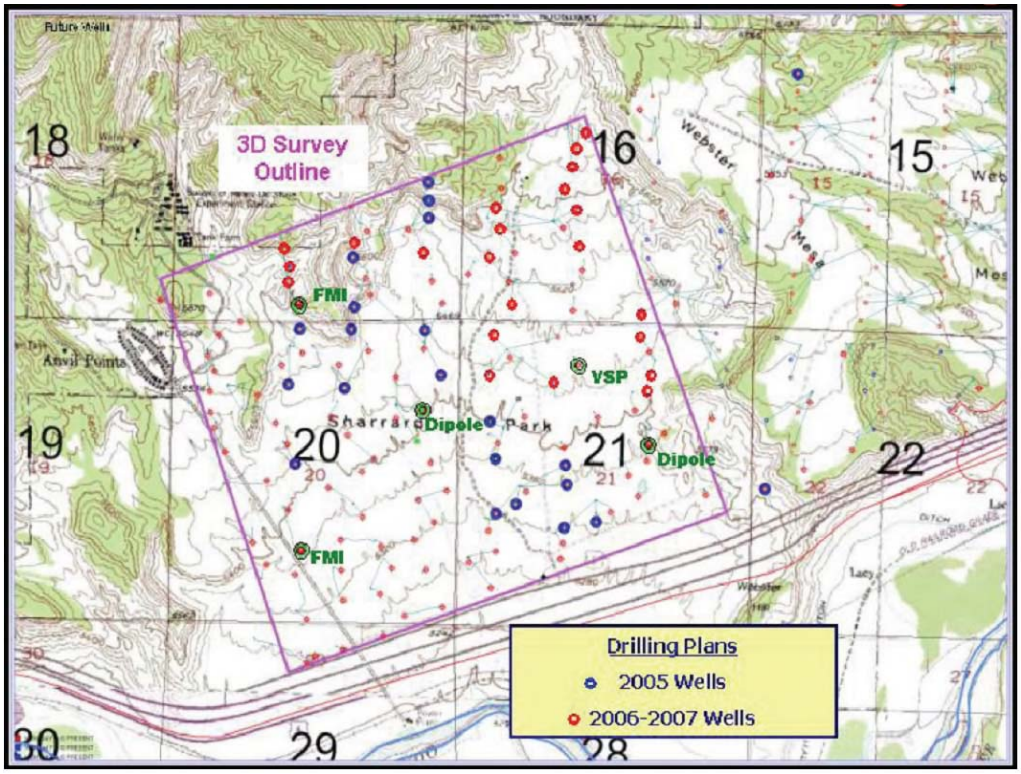

Fig. III-18. Future activity

The RCP survey was conducted over a tight gas sweetspot localized in a small compressional pop-up or "flower" structure formed along an intermediate scale strike-slip fault. Permeability is enhanced with small scale faulting that occurred during its formation, as well as extension fractures at both matrix and bed scale during the relaxation of stress associated with uplift. *There is potential for a 20 fold increase in profit near term and improved prioritization of drill sites during longer term development operations by taking these three steps:*

1. *Correctly identifying the subtle structure*
2. *Geomechanically simulating the tectonic strain fields*
3. *Targeting the most strained volumes of reservoir during development operations*

IV. Evolution of Project Premise

A. Original Project Premise

The Multi Well Experiment program focused attention on naturally fractured reservoir prediction as an essential technology to increase production of natural gas from large volumes of identified low permeability reservoirs in the United States. Extensive reservoir characterization studies performed and documented during the program indicated low permeability reservoirs would require natural fractures to produce commercial volumes of gas. These low permeability gas resources would be required to meet projected domestic demand for gas and if these resources were deemed essential so too would the technologies needed for their extraction.

Development of natural fracture prediction technologies was pursued simultaneously using several approaches. One of these approaches utilized geomechanics in an endeavor to predict the distribution of brittle natural fractures in a reservoir. Predictions of natural fracture distribution would be made by simulating the distribution of stresses around subtle structures and delineating envelopes where failure criteria had been met and the reservoir fractured as a consequence. The Multisite Field demonstration program was intended to demonstrate this practical application of rock mechanics.

Individual fractures described in the low permeability reservoirs were observed to be evidence of brittle material failure. Brittle failure occurs when strain from imposed stress exceeds the capacity of the rock to deform elastically. Generally accepted elastic methods were to be employed to predict reservoir failure. Input fault geometries, reservoir horizons and other attributes were to be derived from seismic mapping of the prospect. Brittle fractures are a short term phenomenon, so fewer long term geologic assumptions (a common source of error in earth science modeling) were required. The method would use accepted principals of material failure, directly mapped geometries and simple assumptions to generate reliable maps of enhanced reservoir permeability and increase gas production from complex, difficult reservoirs.

Successfully demonstrating the methodology across several resource rich basins would validate the approach and lead to its widespread industry acceptance. A group of well regarded, technically astute companies recruited to participate in a field demonstration program would spread application of the technology even further.

B. Changes to Original Project Premise

Simultaneous demonstration of an unproven low-permeability gas exploration technology across three different basins is an aggressive goal. Demonstrations in different basins and different settings were intended to highlight the broad applicability of the approach and widen the potential industry audience. Instead, the demonstrations served to highlight the

complexities of different fractured reservoir settings and the difficulties of using a single approach to reservoir characterization problems.

The original premises of the field demonstration project were modified as a result of the cumulative experience in different basins and settings. Among the modifications were:

1. Faults and fault tip related fracture systems were found to be extremely high permeability conduits in some settings.
    - Water, an undesired product, was a frequent occurrence. Thus there could be some situations where the permeability enhancement associated with natural fracturing allowed gravity segregation of gas and water in the low permeability reservoirs contrary to the premise of basin centered gas.
    - Extensional fractures whose origins were closely associated with the compressional fault systems did not appear to effectively enhance the permeability of the reservoirs examined in this study. Subsequent deformation and cementation associated with continuing tectonic activity negated their effectiveness.
2. Regional joint systems, when present, provided significant permeability enhancement to the tight gas reservoirs. Their distribution is not uniform and less well understood than originally believed.
    - It is more effective to conceptualize the reservoirs as a power law distribution of fractures from grain scale (micro) to joint scale (macro) than as “matrix” and “fractures” as popularized in engineering oriented reservoir simulators.
    - Griffith material concepts are effective because they more closely approximate the structure and behavior of the reservoirs during development.
        - Griffith failure criteria are more easily visualized and implemented than the Coulomb criteria originally proposed for the project.
    - The origin of the regional joint systems is complex, related to both regional and local geologic events.
        - Co-located and coplanar compressional and extensional fabrics are common and appear paradoxical in their origins.
        - The brittle joints observed in the reservoirs (reflecting elastic failure) are most likely the consequence of long term (geologic time scale) inelastic and visco elastic material behaviors.
        - Long-term cycles of burial and uplift together with lateral compression and relaxation are important elements of matrix permeability and brittle joint development.
3. Geomechanics, as an overall framework for conceptualizing natural fracture development, is effective for understanding and predicting natural fracture permeability in tight gas reservoirs.

- An effective geomechanical approach may involve a variety of tools and techniques (simulation or statistical) depending on the nature of the fractures and available data. Geomechanical simulations are valuable tools for validating structural interpretations.
- Geomechanics requires far more detailed information about the reservoir across a geologic time frame than originally believed. This requirement reduces the practical level of precision achievable.
- Most geomechanical tools provide non-unique solutions. All information pertaining to the reservoir permeability should be incorporated to reduce the uncertainty of the resulting interpretation.

Prediction of natural fracture distribution in low permeability reservoirs is not a simple problem in elastic rock mechanics. Experience gained during this project indicates the distribution of joints in low permeability reservoirs is a complex, indirect function of lithology and release of inelastic and viscoelastic strains accumulated through the life of the reservoir through brittle failure. Fault propagation zones can be predicted based on seismically resolvable faults at lower amounts of strain if accurate rock property information is available. Additional tools such as discrete fracture networks or geostatistics may be more appropriate in areas of highly strained rock.

C. Key Learnings

Effective exploration for naturally fractured reservoirs using a geomechanical approach is accomplished through a systematic process that incorporates a thorough understanding of basin scale geologic history, and detailed interpretations of local geology with sound principals of rock mechanics. Simulations are used to validate the geologic interpretations and extrapolate areas of greater or lesser potential.

Gas and water in highly faulted volumes of low permeability gas reservoir have often segregated and taken on a more conventional arrangement of gas over water. The faults themselves and their propagation zones may be extremely permeable and either highly gas or water productive depending on their location within the hydrocarbon column.

Most of the features referred to as “fractures” in the subsurface are strain relaxation joints. These joints result from cycles of burial and uplift or lateral compression and relaxation singly or in combination. The joints occur in power law distribution from grain to joint scales. Lithology plays a role in the nature and degree of jointing; determining whether the reservoir simply develops increased permeability from grain bounding micro fractures or actually develops a systematic rectilinear joint system. Increased jointing can be predicted by identification of areas where regional inversion or lateral compression have been above average in magnitude.

Successful natural fracture prediction efforts during development drilling operations can increase production profits significantly over statistical drilling practices

D. Thoughts for the Future

Geomechanical simulation has an important role to play in validating geologic interpretations and identification of subtle deformation. Actions that make such tools more easily utilized in exploration programs would be beneficial.

Cyclic loading and unloading is known to impact reservoir quality in gas storage facilities. Data presented here suggests the natural cyclic loading and unloading of burial and uplift or tectonic compression could be used to quantitatively predict matrix permeability in lesser-explored areas.

Well bore radii (and thus bulk permeability) are increased during cavitation completions in coalbed methane production. Under some conditions, similar results might be achieved in low permeability gas reservoirs. Determination of the appropriate conditions and procedures could unlock significant resources as valuable new completion technology.

REFERENCES

Abbaszadeh, M. and H. Cinco-Ley. 1995. Pressure transient behavior in a reservoir with a finite conductivity fault. *SPEFE*. March 1995:26.

Aguilera, Roberto. 1995. *Naturally Fractured Reservoirs*. PenWell Books, Tulsa, Oklahoma.

Ball, M.M., M.E. Henry and S.E. Frezon. 1991. Petroleum geology of the Anadarko basin region, Province (115), Kansas, Oklahoma, and Texas. *U.S. Geological Survey, Open-File Report:* 88-450W.

Barrett, Fred. 1999. personal communication with R. L. Billingsley

Billingsley, Randal L. and L. W. Evans. 1995. Old wells, new concepts and a fractured reservoir: the Amoco, Champlin 242d #1, Echo Springs Area, GGRB, Wyoming. Paper presented at AAPG Rocky Mountain Section Meeting, April, at Reno, NV: vol. 79, no. 6:915.

Bourne, Stephen J. and E. J.M. Willemse. 2001. Elastic stress control on the pattern of tensile fracturing around a small fault network at Nash Point, UK. *Journal of Structural Geology* 23:1753-1770.

Bourne, Stephen J. et al. 2000. Predictive modeling of naturally fractured reservoirs using geomechanics and flow simulation. *9th ADIPEC* paper no. 0911: 1-10.

Brevetti, Joseph C. 1985. Evaluation of fractured carbonates in the mid-continent region. *SPWLA Annual Logging Symposium*, June 1985

Dart, R.L. 1990. In situ stress analysis of wellbore breakouts from Oklahoma and the Texas Panhandle. *U.S. Geological Survey, Bulletin*1866-F:28.

Donovan, R.N. 1995. The Slick Hills of Oklahoma and their regional tectonic setting. In Structural Styles in the Southern Midcontinent, 1992 Symposium, Ed. K.S. Johnson, K.S. *Oklahoma Geological Survey*, Circular 97:178-186.

Donovan, R.N., Morgan, K.M., Wilhelm, S., Marchini, W., and Bridges, S., 1987. Lineaments in the Slick Hills, southwestern Oklahoma -- An application of remote sensing technology*: Transactions of the Southwest Section of the American Association of Petroleum Geologists*: p. 74-79.

Engelder, T. and Mark P. Fischer. 1996. Loading configurations and driving mechanisms for joints based on the Griffith energy-balance concept. *Tectonophysics* 256:253-277.

Hentz, T.F. 1994. Depositional, structural, and sequence framework of the gas-bearing Cleveland Formation (Upper Pennsylvanian), Western Anadarko basin, Texas Panhandle. *Bureau of Economic Geology, Report of Investigation* 213:73.

Higgs, Nigel G and John S. Bradley (1993). Pers. comm. to R. Billingsley

Jansen, Kjetil. 2003. Seismic investigation of wrench faulting and fracturing at Rulison Field, Colorado. Master's thesis, Colorado School of Mines available from http://geophysics.mines.edu/rcp/theses/Jansen_2005.pdf: INTERNET

Johnson, Ronald C. and Romeo M. Flores. 2003. History of the Piceance Basin from latest Cretaceous through early Eocene and the characterization of lower tertiary sandstone reservoirs. In *Piceance Basin 2003 Guidebook*, eds K. M. Peterson, T. M. Olson and D. S. Anderson, Rocky Mountain Association of Geologists: 21-62

Jones-Cecil, M., R.N. Donovan and L. Bradley, 1995. Structural framework of the Meers Fault and Slick Hills area, southwestern Oklahoma, based on magnetic data. In Structural Styles in the Southern Midcontinent, 1992 Symposium, ed. K.S. Johnson. *Oklahoma Geological Survey, Circular* 97:187-207.

Keighin, C. William, B. E. Law and R. M. Pollastro. 1989. Petrology and reservoir characteristics of the Almond Formation, Greater Green River Basin, Wyoming. ed. Edward B. Coalson et al, pub. *The Rocky Mountain Association of Geologists* in *Petrogenesis and Petrophysics of Selected Sandstone Reservoirs of the Rocky Mountain Region*: 281-298 and 344-347.

Kennedy, C.L. 1982. The Deep Anadarko Basin. Petroleum Information Corporation: 359.

Koperna, 200. Personal communication to R. L. Billingsley.

Koepsell, Randy, Stephen P. Cummella and Mike Mullen. 2003. The practical use and application of the magnetic resonance imaging log in the Piceance basin. In *Piceance Basin 2003 Guidebook*. Pub: Rocky Mountain Association of Geologists: 13: 233-251

Lajtai, E.Z. and J.R. Alison. 1979. A study of residual stress effects in sandstone. *Canadian Journal of Earth Science* 16:1547-1557

LaPointe, Paul and J. A. Hudson. 1985. Characterization and Interpretation of Rock Joint Patterns. IN GSA's Special Paper 199: 4

Laubach, Stephen E. and J.C. Lorenz. 1992. Preliminary assessment of natural fracture patterns in Frontier formation sandstones, southwestern Wyoming. In Rediscover the Rockies, Christopher E. Mullen, ed. *Wyoming Geological Association (WGA) 43rd Field Conference Guidebook*: 87-96.

Lorenz, John C. and Sharon J. Finley. 1991. Regional fracture II: fracturing of Mesaverde reservoirs in the Piceance basin, Colorado. *AAPG Bulletin* 75-11: 1738-1757.

Lorenz, John C. et al. 1988. Results of the multiwell experiment: in situ stresses, natural fractures and other geological controls on reservoirs. *EOS* 69-35: 817, 825-826.

Lorenz, John C., Lawrence W. Teufel and Norman R. Warpinski. 1991. Regional fractures I: a mechanism for the formation of regional fractures at depth in flat-lying reservoirs. *AAPG Bulletin* 75-11: 1714-1737.

Lorenz, John C. 1989. . *AAPG Bulletin* 73-5: 704-705

Marrett, Randall 1997. Permeability, porosity, and shear-wave anisotropy from scaling of open fracture populations. *Rocky Mountain Association of Geologists Fractured Reservoirs: Characterization and Modeling*: 217-226.

McBee, W., Jr. 1995. Tectonic and stratigraphic synthesis of events in the region of the intersection of the Arbuckle and Ouachita structural systems, Oklahoma. In Structural Styles in the Southern Midcontinent, 1992 Symposium, ed. K.S. Johnson. *Geological Survey, Circular* 97:45-81.

McKoy, Mark L. and W. Neal Sams. 1997. Tight gas reservoir simulation: modeling discrete irregular strata-bound fracture networks and network flow, including dynamic recharge from the matrix. natural gas. Paper presented at DOE/MC Conference, 24-27 March, at Houston, TX. AC21-95MC31346.

McKoy, Mark L. 1996. Two-dimensional stochastic fracture porosity models and flow simulation of reservoirs in the Paludal interval of the Mesaverde group, MWX well test site, Piceance Creek Basin, Colorado. *DOE Report* No. 14CF-R96-001.

McKutcheon, A. 2001. Personal communication to F. L. Billingsley

Myal, F. R. et al. 1989. Geologic and production characteristics of the tight Mesaverde group: Piceance basin, Colorado. *DOE Report No.* DE-AC21-88MC24120.

National Petroleum Council (NPC). 1992. *The Potential for Natural Gas in the United States, Demand and Distribution*: Vols I-VI

Nelson, Ronald A. 2001. *Geologic Analysis of Naturally Fractured Reservoirs.* Pub: Gulf Professional Publishing Company: 2nd ed.

Ostensen, R.W. 1983. Microcrack permeability in tight gas sandstone. *SPE Journal (Dec)* 23-6: 919-927.

Peterson, Kristine M., Terrilyn N. Olson and Donna S. Anderson, Eds. 2001. Piceance Basin 2003 Guidebook Rocky Mountain Association of Geologists (RMAG): 194-207

Pollard, David D. and Atilla Aydin. 1988. Progress in understanding jointing over the pat century. *Geological Society of America Bulletin*: vol. no. 100-8:1181.

Price, N.J. 1966. *Fault and Joint Development in Brittle and Semi-Brittle Rock*, Pergamon Press, New York, 176 pp.

Robbins, S.L., and G.R. Keller, Jr. 1992. Complete Bouguer and isostatic residual gravity maps of the Anadarko basin, Wichita Mountains, and surrounding areas, Oklahoma, Kansas, Texas, and Colorado. *U.S. Geological Survey, Bulletin* 1866-G:11.

Roberts, Laura N. R., Michael D. Lean, and Thomas M. Finn. 2004. Timing of oil and gas generation of petroleum systems in the southwestern Wyoming province. *RMAG Mountain Geologist (July)* 41-3: 87-118.

Roux S. 2002. Personal communication with R. L. Billingsley.

Sandia National Laboratories and CER Corporation, Multiwell Experiment Project Groups. 1987. Multiwell Experiment Final Report: I. The marine interval of the Mesaverde Formation. In *Sandia Report:* SAND87-0327-UC-92a: April 1987:

Stanford Rock Fracture Project, Stanford University Structural Geology and Geomechanics. Available from http://pangea.stanford.edu/research/geomech/RFP/RFP.html: INTERNET.

Teufel, Lawrence W. 1991. Permeability of naturally fractured reservoirs. *AAPG Bulletin* 75-3: 680.

Thomas, A.L. 1993. Poly3D: a three-dimensional, polygonal element, displacement, discontinuity, boundary-element computer program with applications to fractures, faults, and cavities in the Earth's crust. Master's thesis, Stanford University, Stanford, CA.

Thomas, W.A. and D.L. Baars. 1995. The Paradox Transcontinental Fault Zone. In Structural Styles in the Southern Midcontinent, 1992 Symposium, ed. K.S. Johnson. *Oklahoma Geological Survey, Circular* 97:3-12.

van der Pluijm, Ben A., et al. 1997. Paleostress in Cratonic North America: Implications for deformation of continental interiors. In Science: 277:794-795.

Warpinski, Norman R. 1989. Elastic and viscoelastic calculations of stresses in sedimentary basins. *SPE Formation Evaluation* 4:522-530.

Webb, et al. 2004. Petrology and petrophysics of the Lance formation (upper Cretaceous), American Hunter, Old Road Unit 1, Sublette County, Wyoming. In *Johan Field: Case Study of a Tight-Gas Fluvial Reservoir*. Ed. J. W. Robinson and K. W. Shanley. Rocky Mountain Association of Geologists: no. 52:183-213.

Winkler, J.E., S.A Kelley and S.C. Bergman. 1999. Cenozoic denudation of the Wichita Mountains, Oklahoma, and southern mid-continent: apatite fission-track and thermochronology restraints *Tectonophysics* 305:339-353.

Yurewicz, D.A., et al. 2003. Source Rock Analysis and Hydrocarbon Generation, Mesaverde group and Mancos shale, Northern Piceance Basin, Colorado. In *Piceance Basin 2003 Guidebook*, eds K. M. Peterson, T. M. Olson and D. S. Anderson, Rocky Mountain Association of Geologists: 130-154

ACRONYMS AND ABBREVIATIONS

2D..... two-dimensional

3D..... three-dimensional

AAPG ..... American Association of Petroleum Geologists

ARI ..... Advanced Resources Inc.

AVO..... amplitude variations with offset (technology)

Bbl ..... barrel

bcf ..... billion cubic feet

BEM ..... boundary element model

BHP/z ..... bottomhole pressure/gas deviation factor

BO ..... barrels of oil

boe ..... barrels of oil equivalent

BTU ..... British thermal unit

C..... centigrade

CAOF ..... calculated absolute open flow

COCORP ..... Consortium for Continental Reflection Profiling

CSM ..... Colorado School of Mines

CTE ..... coefficient of thermal expansion

DFN..... discrete fracture network

DOE ..... U.S. Department of Energy

EUR..... estimated ultimate recovery

E&P ..... exploration and production

FERC ..... Federal Energy Regulatory Commission

FETC..... Federal Energy Technology Center

Fm ..... formation

FMI ..... formation micro-imaging

FMS..... formation micro-scanner

FTP ..... flowing tubing pressure

GGRB..... Greater Green River basin

GRI..... Gas Research Institute

IP..... Initial productivity

k ..... permeability

kgal..... thousands of gallons

klbs..... thousands of pounds

kPhih ..... bulk permeability times porosity times thickness

kpsi..... thousands of pounds per square inch

Mcfd ..... thousands of cubic feet per day

MD..... measured depth

μd ..... microdarcies

md ..... millidarcies

md/pu ..... millidarcies/porosity unit

MMcfd ..... millions of cubic feet per day

MOL ..... master orientation line

MPa..... megapascals

MWX ..... multi-well experiment

MY..... millions of years

MYBP..... millions of years before present

NETL..... National Energy Technology Laboratory

NPC..... National Petroleum Council

P&A..... plugged and abandoned

PDS..... Proprietary Schlumberger Format

PE ..... photoelectric effect

phi ..... porosity

Phih ..... average porosity times thickness

Poly3D..... three-dimensional, polygonal element, displacement discontinuity boundary element computer program

PRDA ..... Program Research and Development Announcement

psi..... pounds per square inch

PTA ..... pressure transient analysis

R&D..... research & development

RCP..... Reservoir Characterization Project

RMAG ..... Rocky Mountain Association of Geologists

Ro..... vitrinite reflectance in oil

Sc..... Coulomb stress

SEG..... Society of Exploration Geophysicists

SEM ..... scanning electronic microscope

sp ..... spontaneous potential (log)

tcf ..... trillion cubic feet

TD ..... total depth

UPRC ..... Union Pacific Railroad Corporation

USGS ..... United States Geological Survey

Vr..... vitrinite reflectance

WRB..... Wind River basin

WOGCC ..... Wyoming Oil and Gas Conservation Commission

APPENDICES

A. Bullfrog 5-12 Core Report

B. Natural Fracture Supporting Documentation